SELF-ORGANIZATION AND CHARACTERIZATION OF PORPHYRINIC NANOPARTICLES AND NEW CATALYTIC OXIDATION BY NANOPARTICLES OF IRON TETRA-PENTAFLUOROPHENYLPORPHYRIN

by

GABRIELA MARIA SMEUREANU

A dissertation submitted to the Graduate Faculty in Chemistry in partial fulfillment of the requirements for the degree of Doctor in Philosophy, The City University of New York

2007

ProQuest Information and Learning Company
300 North Zeeb Road
P.O. Box 1346
Ann Arbor, MI 48106-1346

This manuscript has been read and accepted for the Graduate Faculty in Chemistry in satisfaction of the dissertation requirements for the degree of Doctor in Philosophy.

04/16/2007

_____ _____

Date Prof. Charles Michael Drain
Chair of Examining Committee

04/16/2007

_____ _____

Date Prof. Gerald Koeppl
Executive Officer

Prof. James D. Batteas
_____

Prof. Hiroshi Matsui
_____

Prof. Lynn Francesconi
_____

Supervisory Committee

THE CITY UNIVERISTY OF NEW YORK

ABSTRACT

SELF-ORGANIZATION AND CHARACTERIZATION OF PORPHYRINIC NANOPARTICLES AND NEW CATALYTIC OXIDATION BY NANOPARTICLES OF IRON TETRA-PENTAFLUOROPHENYLPORPHYRIN

by

Gabriela Maria Smeureanu

Adviser: Professor Charles Michael Drain

Certain applications of supramolecular porphyrinic systems, such as molecular sieves and photonics, rely on precise nanoarchitectural control of the molecules and/or atoms; therefore they require self-assembled systems of discrete arrays and highly ordered crystals.

In this work we investigate functional materials wherein the function derives from the assembly —electron and energy transfer are examples. Recognition groups based on hydrogen bonding are generally designed to efficiently form intermolecular interactions between two or more molecules. The two complementary recognition groups used here are: uracyl (U) and 2,6-diacetaminopyridine (P) derivatives. Attaching two copies of these recognition motifs to the opposite sides of meso aryl porphyrins (free base and metallo) allow these to self-assemble or self-organize via triple hydrogen bonds. These structural and functional studies may serve as a basis for understanding the photo physical properties of the self-organized aggregates.

The use of porphyrins for self-assembly and self-organization of molecules and ions to create functional photonic materials has been cornerstone of much research because of their structural rigidity, chemical stability and rich photo and electro chemical properties. Herein we report the self-assembly of squares formed from four 5,15-bis- (4-pyridyl)-10,20-bis-(4-dodecyloxyphenyl) porphyrin linked together by coordination to cis-platinum (II) dichloride.

Colloidal porphyrin nanoparticles can be considered self-organized systems that are governed by the principles of supramolecular chemistry. Nanoparticles, a unique subset of the broad field of nanotechnology, play an important role in a wide variety of fields including advanced materials, pharmaceuticals, and environmental detection and monitoring. Porphyrin and metalloporphyrin nanoparticles are promising components for advanced material chemistry because of the rich photochemistry, stability, and catalytic activity. The formation and characterization of these nanoparticles are discussed using different techniques (e.g. UV-Vis, Fluorescence, DLS and AFM). These nanoparticles on hydrophilic surfaces de-aggregate into 10-300 nm particles and we observed that different hydrocarbon substituents and metals affect particle size. These systems can serve as sensors and other photonic devices, but my particular focus is on the catalytic properties of nanoparticles of an iron porphyrin. Using gas chromatography coupled with mass spectrometry and hydrogen and oxygen isotope experiments we discovered that these systems have different reactivity than the same porphyrin in solution and that the turnovers are more than 10-fold greater.

Acknowledgments

I would like first of all to thank to my mentor Dr. Charles Michael Drain for his help, patience, mentoring, guidance and support during my doctoral graduate studies. In professor Drain's laboratory I was involve in a multidisciplinary research which combined the talents and skills of a variety or researchers, that help me to be adept at viewing technical and scientific problems from several vantage points and allowed me to grow as a scientist. He is such a wonderful mentor.

I would like also to thank to my committee members Prof. James D. Batteas from Texas A&M University and Prof. Lynn Francesconi and Prof. Hiroshi Matsui from Hunter College for their suggestions, expertise and help during my thesis work.

Thanks to Prof. Klaus Grohmann for his help as a graduate student advisor during my graduate study at CUNY.

I am very grateful to Dr. Cliff Soll for his help with GC-MS studies and for answering all my questions.

My warmest thanks to my friends and lab-mates Dr. Diana Samaroo, Giorgio Bazzan and Ivana Radivojevic for their help during my research and for made my years at Hunter College great and enjoyable.

Thanks also to my co-workers Dr. Mikki Vinnodu, Jacopo Samson, Sebastian Thompson and Alessandro Varotto.

Special thanks to my parents Ligia and Vasile Smeureanu for their unconditional love, patience, encouragement and support without which this work would have not been completed and I would not be here today.

My deepest gratitude to my boyfriend Stelian Dubei for his love and encouragement over these past years and to my Romanian friends Iulian and Nicole Popa, Gabriela and George Solotchi, Rodica Nyerges, Mirela Settenhofer and my old friend Doina Mihai for their love and continuous support during the years I spent in the doctoral program at Hunter College.

Dedicated to my mother and the memory of my father

for their caring, encouragement and love

Mama si Tata

Multumesc pentru incurajare si suport

Table of Contents

RESEARCH OUTLINE 1

1. SELF-ASSEMBLED MULTIPORPHYRIN ARRAYS WITH HYDROGEN BONDING RECOGNITION GROUPS

1.1. Introduction 5
1.2. Self-assembled multi-porphyrin systems: Experimental and Characterization 10
1.2.1. Experimental Methods 10
1.2.2. Results and discussion 11
1.3. Conclusions 24

2. SELF-ASSEMBLED AND SELF-ORGANIZATION OF PORPHYRIN MATERIALS ON SURFACES

2.1. Introduction 29
2.2. Porphyrinoids definition and scope 31
2.3. Supramolecular chemistry 34
2.4. Self-organized porphyrins on surfaces 35
2.4.1. Surfaces 35
2.4.2. Applications 37
2.4.3. Self-Organization on Surfaces 39
2.5. Self-assembled porphyrinic materials on surfaces 40
2.6. Liquid Crystalline porphyrinic arrays 45
2.7. Conclusions 48

3. COLLOIDAL PORPHYRIN NANOPARTICLES AS SUPRAMOLECULAR SYSTEMS

3.1. Introduction 57
3.2. Applications of Porphyrin Nanoparticles 60
3.3. Preparation of Porphyrin Nanoparticles 62
3.4. Characterization of Porphyrin Nanoparticles 66
3.4.1. Structure 66
3.4.2. Optical Properties 67
3.5. Particles Stability and Dynamics 68

3.6. Characterization and Preparation of $TPPF_{20}$ colloids 70
3.6.1. Stabilizer 71
3.6.2. Temperature 73
3.6.3. Concentration 73
3.6.4. Host/guest solvent ratio and intermolecular forces 75
3.6.5. Mixing 77
3.6.6. Surfaces 78
3.7. Conclusions 79
3.8. Appendix 81

4. NEW CATALYTIC OXIDATION OF CYCLOHEXENE BY NANOPARTICLES OF 5, 10, 15, 20-TETRAKIS-(2,3,4,5,6-PENTAFLUOROPHENYL) PORPHYRIN IRON (III)

4.1. Introduction 107
4.2. Experimental 111
4.3. Results and discussion 114
4.4. Mechanism Insights 116
4.5. Conclusions 119
4.6. Appendix 131

BIBLIOGRAPHY 139

Research outline 139
Chapter 1 140
Chapter 2 143
Chapter 3 150
Chapter 4 154

List of Tables

Table 3. 1.	Stabilizer effects on nanoparticle size	71
Table 3. 2.	Effects of host solvent on the size of $TPPF_{20}$ nanoparticles	76
Table 3. 3.	Average AFM heights of $TPPF_{20}$ colloids deposited onto hydrophilic glass surfaces	79
Table 3. 4.	TPP nanoparticles characterization	82
Table 3. 5.	TtolylPP nanoparticles characterization	83
Table 3. 6.	TtbutylPP nanoparticles characterization	84
Table 3. 7.	$TPPF_{20}$ nanoparticles characterization	85
Table 3. 8.	TCPP Me nanoparticles characterization	86
Table 3. 9.	TmethoxyPP nanoparticles characterization	87
Table 3. 10.	ToctyloxyPP nanoparticles characterization	88
Table 3. 11.	OEPP nanoparticles characterization	89
Table 3. 12.	Summary of free bases porphyrin nanoparticles characterization data	90
Table 3. 13.	CoTPP nanoparticles characterization	91
Table 3. 14.	ZnTPP nanoparticles characterization	92
Table 3. 15.	FeTPP nanoparticles characterization	93
Table 3. 16.	CoTTbutylPP nanoparticles characterization	94
Table 3. 17.	ZnTTbutylPP nanoparticles characterization	95
Table 3. 18.	ZnTCPP Me nanoparticles characterization	96
Table 3. 19.	ZnOEPP nanoparticles characterization	97
Table 3. 20.	MgOEPP nanoparticles characterization	98
Table 3. 21.	$FeTPPF_{20}$ nanoparticles characterization	99
Table 3. 22.	Summary of metal porphyrin nanoparticles characterization data	100
Table 4. 1.	Fe (III) $TPPF_{20}$ nanoparticles: a green catalysis of cyclohexene oxidation	120
Table 4. 2.	Fe (III) $TPPF_{20}$ nanoparticles: Control reactions	121
Table 4. 3.	Fe(III)$TPPF_{20}$ nanoparticles catalyst experiments Control reactions (temperature and mixing method)	122
Table 4. 4.	The standard response of GC area for each component	131

List of Figures

Figure 1. 1.	Discrete hydrogen bonding arrays	7
Figure 1. 2.	Porphyrins bearing complementary hydrogen bonding motifs with flexible linkers	9
Figure 1. 3.	Heterocomplementary U≡P; homocomplementary U=U; homocomplementary P≡P hydrogen bonding	13
Figure 1. 4.	Possible configurations of free base and metallo-porphyrins assemblies	14
Figure 1. 5.	Contact mode atomic force microscopy (AFM) studies of the individual porphyrinic compounds PCP, UC(Zn)U and the self- organized aggregates PCP+ UC(Zn)U drop cast onto glass and mica surfaces	16
Figure 1. 6.	Contact mode atomic force microscopy (AFM) studies of the individual porphyrinic compounds UCU, PC(Zn)P and the self-organized aggregates UCU+ PC(Zn)P drop cast onto glass and mica surfaces	17
Figure 1. 7.	Contact mode atomic force microscopy (AFM) histograms of the individual porphyrinic compounds and the self-organized aggregates on glass. (PCP, UC(Zn)U, PCP+UC(Zn)U)	18
Figure 1. 8.	Contact mode atomic force microscopy (AFM) histograms of the individual porphyrinic compounds and the self-organized aggregates on glass. (UCU, PC(Zn)P, UCU+PC(Zn)P)	19
Figure 1. 9.	Contact mode atomic force microscopy (AFM) histograms of the individual porphyrinic compounds and the self-organized aggregates on mica. (PCP, UC(Zn)U, PCP+UC(Zn)U)	20
Figure 1. 10.	Contact mode atomic force microscopy (AFM) histograms of the individual porphyrinic compounds and the self-organized aggregates on mica. (UCU, PC(Zn)P, UCU+PC(Zn)P)	21
Figure 1. 11.	Dynamic Light Scattering (DLS) histograms of the each individual porphyrinic compound and the hetero complementary compounds. (PCP, UC(Zn)U, PCP+UC(Zn)U)	22

Figure 1. 12.	Dynamic Light Scattering (DLS) histograms of the each individual porphyrinic compound and the hetero complementary compounds. (UCU, PC(Zn)P, UCU+PC(Zn)P)	23
Figure 2. 1.	The three basic porphyrinoids pigments	31
Figure 2. 2.	(A) square results from the 90° topology of the pyridyl groups and (B) cube results from the 180°topology of the pyridyl groups on the isomeric porphyrins	41
Figure 2. 3.	Molecular model of the *cis*-Pt(II) porphyrin assembly based on MM-2 energy minimization using Chem 3D	42
Figure 2. 4.	Two possible conformations of the square and possible interactions between the supramolecular squares	43
Figure 2. 5.	AFM image of the dodecyloxyphenyl film on glass 50 uL drop-dried on glass (2.63×10^{-4} M)	44
Figure 2. 6.	Adsorption of porphyrins bearing long-chain hydrocarbons that serves as liquid crystal-forming motifs	47
Figure 2. 7.	AFM image (7.0x7.0 μm^2) of several nanocrystalline domains of supramolecular porphyrin array formed on glass by depositing solution of ~10-fold-higher concentration	48
Figure 3. 1.	The fluorescence intensity of a 1:1 mixture of free base TPP and Fe(III)tetratolylporphyrin nanoparticles	70
Figure 3. 2.	DLS reveals the slight dependence of the size of $TPPF_{20}$ nanoparticles on TetraEGME stabilizer concentration	72
Figure 3. 3.	The temperature during nanoparticle preparation affects the particle size	74
Figure 3. 4.	The concentration of $TPPF_{20}$ in the DMSO host solvent strongly affects nanoparticle size as measured by DLS	75
Figure 3. 5.	The volume ratio of host solvent to guest solvent	76
Figure 4. 1.	Typical dynamic light scattering data indicating the diameter of the catalytic nanoparticles	123
Figure 4. 2.	Typical UV-Vis spectrum for $FeTPPF_{20}$ in THF and correspondent nanoparticles in water	123
Figure 4. 3.	Typical AFM of the nanoparticles	124

Figure 4. 4.	GC of a standard, solution phase reaction as reported previously	125
Figure 4. 5.	Typical UV-visible spectra of the solvated Fe(III)TPPF$_{20}$ in CH_3CN/CH_3OH after 30 min reaction, and 10 ± 5 nm nanoparticles of the complex in water after 20 hours reaction	125
Figure 4. 6.	GC of a typical nanoparticle catalyst reaction. (With H_2O_2)	126
Figure 4. 7.	GC of a typical nanoparticle catalyst reaction. (With O_2)	126
Figure 4. 8.	Mass Spectra profile when using nanoparticles in 10% H_2O^{18} showing ~ 10% ^{18}O incorporation into ketone	127
Figure 4. 9.	Mass Spectra profile when using nanoparticles in 10% H_2O^{18} showing ~ 0% ^{18}O incorporation into alcohol	128
Figure 4. 10.	Mass Spectra profile when using nanoparticles in H_2O with 97% ^{18}O added showing ~ 95% ^{18}O incorporation into alcohol	129
Figure 4. 11.	Mass Spectra profile when using nanoparticles in H_2O with 97% ^{18}O added showing ~ 10% ^{18}O incorporation into ketone	130

List of Schemes

Scheme 3. 1. Preparation of porphyrin nanoparticles 62
Scheme 4. 1. Catalytic oxidation reaction of cyclohexene by $FeTPPF_{20}$ 109
Scheme 4. 2. Preparation of 10 nm $FeTPPF_{20}$ nanoparticles in water 110

Abbreviations

AFM	Atomic Force Microscopy
DLS	Dynamic Light Scattering
ESI-MS	Electrospray Mass Spectrometry
GC-MS	Gas Chromatography - Mass Spectrometry
NMR	Nuclear Magnetic Resonance
UV-Vis	Ultraviolet-visible spectroscopy
M	Metal
FB	Free base porphyrin
SAM's	Self assembly monolayers
LED's	Light emitting diode
MCM-41	Mobile crystalline material
a.u.	Intensity in arbitrary units
PEG	Polyethylene glycol
THF	Tetrahydrofuran
DMF	Dimethylformamide
DMSO	Dimethyl sulfoxide
C	Porphyrin core
UCU	Uracyl Porphyrin
UC(Zn)U	Zinc Uracyl Porphyrin
PCP	2,6-diacetaminopyridylporphyrin
PC(Zn)P	Zinc 2,6-diacetaminopyridylporphyrin
Rec	Recognition groups
TPP	5,10,15,20-tetraphenylporphyrin
TtolylPP	5,10,15,20-tetratolylphenylporphyrin
TtbutylPP	5,10,15,20-tetratbutylphenylporphyrin
TmethoxyPP	5,10,15,20-tetramethoxyphenylporphyrin
TCPP-ME	5,10,15,20-tetracarboxyphenylporphyrinmethylether
ToctyloxiPP	5,10,15,20-tetraoctyloxyphenylporphyrin
OEP	2,3,7,8,12,13,17,18-octaethylporphyrin
$TPPF_{20}$	5,10,15,20-Tetrakis (pentafluorophenyl) porphyrin

Research outline

Porphyrins are a class of organic molecules with a macrocyclic tetrapyrrole core and different substituents. Porphyrins have remarkable photo-, catalytic-, electro-, and biochemical properties.[1] They are extensively used in self-assembling processes to prepare monolayers and thin films.[2, 3] Multiporphyrin arrays are prepared both by organic synthesis and self-assembling techniques,[1-4] and self-organized nanomaterials composed of porphyrins have also been prepared.[4] Porphyrin nanoparticles are promising components of advanced materials because of the rich photochemistry, stability, and proven catalytic activity.[5]

The supramolecular chemistry of porphyrin systems is extraordinary diverse because the rigid macrocycles offer a variety of topologies that can be match with the topologies of hydrogen bonding moieties and metal ion coordination geometries. Supramolecular chemistry depends on the pre-organization of complementary molecular receptors on component molecules. [2, 6]

The spontaneous association into organized systems can be categorized as self-assembly and self-organization. Self-assembly [2, 6-9] results in the formation of a discrete supramolecular entities. On the other hand, self-organization of ions or molecules results in non-discrete systems where at least one dimension is variable (linear polymer or two dimensional arrays), and these systems tend to be more dynamic and tolerant of defects. Together, self-assembled and self-organized systems are expected to make important contribution in some electronic applications.[7, 10-12]

Other applications include molecular sieves that are specific for a given molecule or sets of molecules,[13] non-linear optical materials,[14] nano-crystalline and nano-aggregated materials[15]. Self-assembled systems are used as catalysts or design to recognize target analyte with increased specificity over simple chromophoric systems. Also, redox and and photo-physical properties of the materials make them suitable for applications in sensors, electronic devices and electroluminescent materials. More recently supramolecular chemistry has been used in the formation of high-spin materials[16] with design spin properties that may be used in a variety devices such as sensors, actuators or magnetic storage devices.

This thesis focuses on the supramolecular chemistry – self-assembled and self-organized – porphyrin materials and demonstrates some of the properties and applications. The intermolecular interactions use hydrogen bonding, metal ion coordination, and dispersion forces for the preparation and characterization of aggregates and nanoparticles.

Much of the rich supramolecular chemistry of porphyrinoids, and the potential applications of porphyrinoid materials, have been pioneered by Drain and coworkers, and this thesis constitutes the latest chapter in the story.

References:

1. Chambron, J.-C.; Heitz, V.; Sauvage, J.-P., *In The Porphyrin Handbook*, Kadish, K. M.; Smith, K. M.; Guilard, R., Eds. Academic Press: New York, **2000**; Vol. 6, 1-42.
2. Lehn, J.-M., *Pure Appl. Chem.* **1994,** 66, (10/11), 1961-1966.
3. Belanger, S.; Hupp, J. T., *Angew. Chem., Int .Ed.* **1999,** 38, 2222 - 2224.
4. Drain, C. M.; Nifiatis, F.; Vasenko, A.; Batteas, J., *Angew. Chem., Int. Ed* **1998,** 37, 2344-2347.
5. Kosal, M. E.; Chou, J.-H.; Nalwa, H. S.; Rakow, N. A.; Suslick, K. S., Academic Press: New York, **2000**; Vol. 6, p 43-131.
6. Lehn, J.-M., *Angew. Chem. Int. Ed. Engl.* **1990,** 29, 1304-1319.
7. Drain, C. M., *Proc. Natl. Acad. Sci., USA* **2002,** 99, 5178.
8. Drain, C. M.; Batteas, J. D.; Flynn, G. W.; Milic, T.; Chi, N.; Yablon, D. G.; Sommers, H., *Proc. Natl. Acad. Sci., USA* **2002,** 99, 6498-6502.
9. Milic, T. N.; Chi, N.; Yablon, D. G.; Flynn, G. W.; Batteas, J. D.; Drain, C. M., *Angew. Chem. Int. Ed.* **2002,** 41, (12), 2117-2119.
10. Drain, C. M.; Mauzerall, D. C., *Biophysic. Journal.* **1992,** 63, 1544-1555.
11. Drain, C. M.; Mauzerall D. C, *Biochemistry and Bioenergetics.* **1990,** 24, 263-268.
12. Drain, C. M.; Christensen, B.; Mauzerall, D.C., *Proc. Natl. Acad. Sci., USA* **1989,** 86, 6959-6962.

13. Drain, C. M.; Hupp, J. T.; Suslick, K. S.; Wasielewski, M. R.; Chen, X., *Journal of Porphyrins and Phthalocyanines* **2002,** 6, (4), 243-258.

14. Ogawa, K.; Zhang, T.; Yoshihara, K.; Kobuke, Y., *J. Am. Chem. Soc.* **2002,** 124, 23.

15. Alivisatos, A. P.; Barbara, P. F.; Castleman, A. W.; Chang, J.; Dixon, D. A.; Klein, M. L.; McLendon, G. L.; Miller, J. S.; Ratner, M. A.; Rossky, P. J.; Stupp, S. I.; Thompson, M. E., *Adv. Mater.* **1998,** 10, (16), 1297-1336.

16. Epstein, A. J., *MRS Bulletin* **2000**, Vol.25, 11, 33-40.

1.

SELF-ASSEMBLED MULTIPORPHYRIN ARRAYS WITH HYDROGEN BONDING RECOGNITION GROUPS

1. 1. Introduction

Life on Earth depends on efficient solar energy conversion mediated by photosynthesis. Light harvesting by pigments such as chlorophylls is the first step in photosynthesis. In plants, algae, and purple photosynthetic bacteria the protein-pigment antenna complexes capture solar energy, and efficiently funnel this energy to an energetic sink referred to as the reaction center. The first photosynthetic organisms appeared about 4.5 billion years ago, and evolution has optimized the process such that photosynthetic "devices" have reached over 90% efficiency in the transformation of light energy into biochemical energy.[1, 2] Any effort to mimic or indeed improve upon photosynthesis to create solar energy converting devices must maximize the light-harvesting process and efficiently couple this to the electron transfer process that results in the production of a useful chemical or electrical potential.

Silicon based solar cells represent a functioning technology but mass production has not led to the expected drop in manufacturing price so that solar energy production still is about ten times more expensive than conventionally produced electrical energy.[3] During the last decade, in spite of considerable effort, non-silicon based artificial systems still remain at about 10% efficiency.[3] Organic, or plastic solar cells have the potential to be mass produced at much lower costs using continuous processing, and proof-of-principle devices have been demonstrated,[4-6] but the efficiency is still well below the commercialization value of about 6%.[3] Inspired by natural photosynthesis, our initial focus is to construct light-harvesting systems with increased photon capture cross sections that enables hybrid solar cells to function even under low light illumination conditions.[7] For light-harvesting purposes, an assembly of excitonically-coupled chromophores acting as the antenna system must ensure that the exciton energy transfers to the trap with high efficiency.[8-10]

Recently, a variety of covalent multichromophoric arrays[11-13] and dendrimers have been elegantly synthesized as antennas and their photophysics was investigated.[14-16] However, complex multistep syntheses generally render the covalent systems prohibitively expensive for practical, commercially viable applications. The alternative, noncovalent approach, in which appropiately designed cromophores self-assemble into functional antenna systems obviates much of the synthetic efforts and costs. However, self-assembled systems necessitate careful consideration of organizational robustness under the application conditions since only weak intermolecular forces such as metal ligation, hydrogen bonds, π–π interactions and dispersion forces hold these structures together.[17-20]

The architecture of the chromophores should maximize energy transfer and be stable for use in potential devices. Once the self-assembly algorithm has been programmed into a molecule by equipping it with groups suitable for specific intermolecular interactions, the outcome of the process is dictated by a fine balance between kinetics and thermodynamics. Since the thermodynamic structure is usually the product, the components can reassemble thus affording an autorepair mechanism for this component of the device. Self-assembly is also a functional principle for natural light-harvesting antennae, as illustrated by numerous studies of the antenna chlorosomes of green photosynthetic bacteria.[21-25]

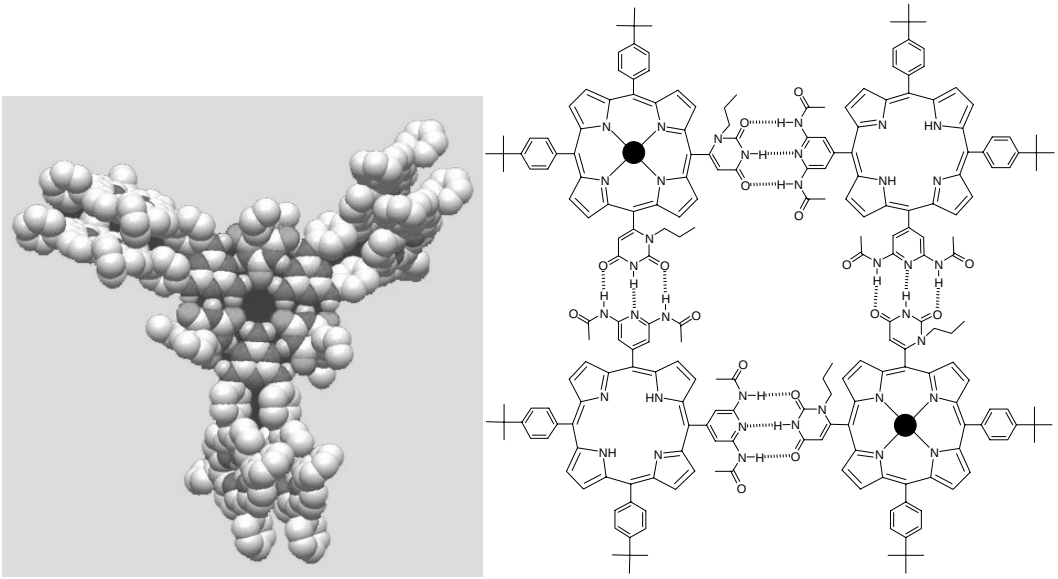

Figure 1. 1. Discrete hydrogen bonding arrays.

Because such self-assembled antenna architectures can lead to functional light-harvesting nanostructures,[26, 27] a deeper understanding of their energy transfer capabilities is required in order to optimize their use in efficient hybrid solar cells.

Self-assembly of discrete porphyrin arrays mediated by hydrogen bonding into cage-like dimers and rosettes[28, 29] were the earliest systems, and these were followed by assemblies of squares and nonameric arrays.[30, 31] (Figure 1. 1.) Florescence depolarization studies indicated good energy transfer among the porphyrin dimers in the rosettes, and excitation of a zinc porphyrin in the heterocomplementary squares resulted in fluorescence predominantly from the free bases.

Balaban *et al.* later made a series of compounds of free bases and Zn porphyrins with similar uracyl and diacetamidopyridyl complementary recognition groups capable of forming triple hydrogen bounding, but with flexible linkers between the porphyrins and the self-assembly motifs. Steady state and transient fluorescence studies of the electron transfer (from the Zn to free base) were done to asses the efficiency of these self-organized materials. The questions remained however, about the extent of aggregation of these systems. Thus, I did the work related to the aggregation and self-organization of these porphyrins with complementary hydrogen bonding motifs. Figure 1. 2. shows the structures of the porphyrinic systems: **UCU, UC(Zn)U, PCP, PC(Zn)P** where P=2,6 diacetaminopyridine, U=uracyl and C=porphyrin core.

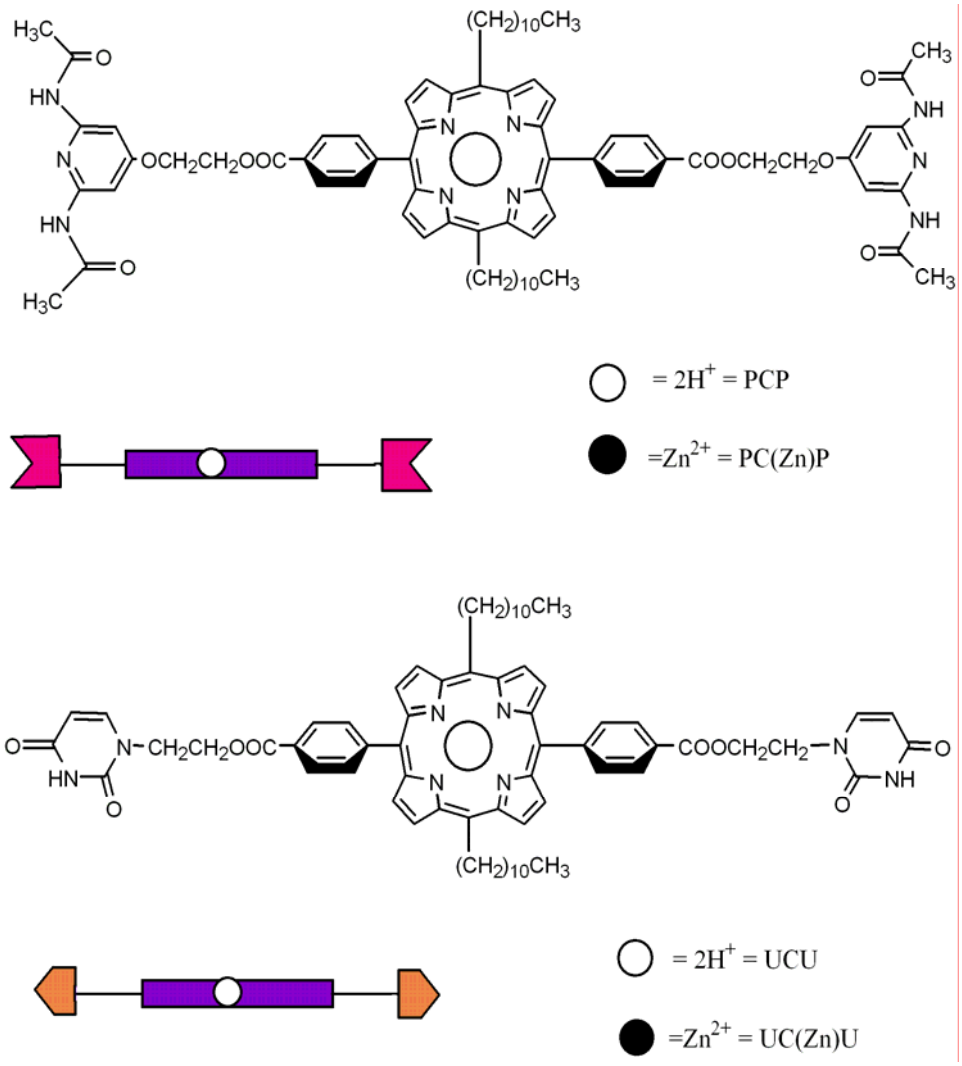

Figure 1. 2. Porphyrins bearing complementary hydrogen bonding motifs with flexible linkers.

1. 2. Self-assembled multi-porphyrin systems: Experimental and Characterization

1. 2. 1. Experimental Methods

AFM Investigations and Dynamic Light Scattering Experiments

Dynamic light scattering (DLS) measurements were recorded using the PD2000DLS (PDDLS/Cool Batch 90T from Precision Detectors) instrument and 0.5 × 0.5 mm glass cuvette, for each individual porphyrin and for the 1:1 mixtures (UCU+PC(Zn)P and PCP+UC(Zn)U) at 25μM solution concentrations in chloroform. Solutions were filtered through a 0.2 μm syringe filter.

Atomic force microscopy (AFM) images were recorded using a Veco Nanoscope III instrument using contact mode on glass coverslips cleaned using H_2O : NH_4OH : H_2O_2 (4:1:1) followed by several rinses with distilled water and drying in an oven at 100 °C. The 25 μM solution of each individual compound and the 1:1 combinations were drop cast using a 0.2 μm syringe filter onto the clean glass or freshly cleaved mica surface and allowed to dry in the air in a capped cell culture dish. The silicon cantilever (CSC21) contact mode tip had a nominal convolution of 10 nm. Images were taken in several places of the sample where a high, medium, and low density of particles were observed, where the latter two likely are more representative of the aggregates found in solution. Each of the porphyrins and the self-organized aggregates were deposited on at least five different cover slips on different occasions. Several areas of each sample were analyzed by AFM; the histograms represent the particle distribution for the given AFM, but are representative of the other samples.

1. 2. 2. Results and discussion

The focus of our research is to investigate the aggregation of each individual porphyrin system **UCU, UC(Zn)U, PCP, PC(Zn)P** and each complementary combination **UCU + PC(Zn)P, PCP + UC(Zn)U.** Complementary recognition groups (**Rec**) capable of triple hydrogen bonding such as 2,6-diacetamidopyridine (**P**) and uracyl (**U**) have been shown to induce self-organization into large chiral suprastructures when flexible tartaric esters are used as the core.[32, 33] With rigid groups such as anthracene, polymeric materials with adaptive properties may be obtained.[34] These hydrogen bonding motifs allow the self-assembly of a large variety of architectures[35] depending on the topologies of the component molecules. Here free base or Zn(II) porphyrins serve as the core functional entity. The photophysical properties of both the free base and the zinc porphyrins are well established, and zinc metalloporphyrins can serve as energy donors to free bases (**FB**) energy acceptors if the molecular or supramolecular structure is appropriate.

The design of these second generation of porphyrin assemblies which have several advantages over the previous systems: (*i*) the synthetic methods are direct and readily scalable; (*ii*) increased solubility by placement of long alkyl groups at the *meso* positions of the porphyrins (*iii*) the ester linkages are inert to redox processes, wherein it has been observed that the amido linkages used previously have a propensity to quench the fluorescence of the energy donors by competing electron transfer reactions, thus shortening the lifetimes and reducing the energy transfer rate and its efficiency;

(*iv*) the present design strategy allows for a modular self-organization of components in a variety of architectures. The primary disadvantage of these porphyrins is that the flexible linkers allow a large variety of conformations and relative macrocycle orientations, so that the nanoarchitectures of the self-organized products are not well defined and considerably more dynamic. Figure 1. 2. presents the porphyrins used in this work for the noncovalent assembly of functional units.

The main reasons the linker are used to append the uracyl (U) and 2,6-diacetaminopyridine (P) recognition groups to the porphyrins are: 1) ease of synthesis and therefore scale-up; 2) increased solubility and 3) the possibility for a modular assembly of components in a variety of architectures by self-assembly. The energetics of the triple hydrogen bound motifs have been calculated [30, 31] (hetero complementary U≡P, E ~ 8 kcal/mol, double hydrogen bounds between homo complementary U=U, E ~ 3 kcal/mol, and the 2-4 possible hydrogen bonds between homocomplementary P≡P, E ~ 5 kcal/mol) (Figure 1. 3.). These compounds allow a modular assembly of Zn(II) donor porphyrins with free base acceptor porphyrins in predefined architectures that allow the study of energy transfer in noncovalent supramolecular assemblies.

Figure 1. 4. presents some of the possible architectures of these ditopic arrays in terms of metallation state. Note that the length of these arrays in solution is dictated by thermodynamics of the intermolecular interactions, thus the conditions used (concentration, solvent, temperature, water content in the solvent, etc.) The degree of pi-stacking, which is maximally about 5 kcal/mol per pi-pi interaction, is dependent on the concentration as well.

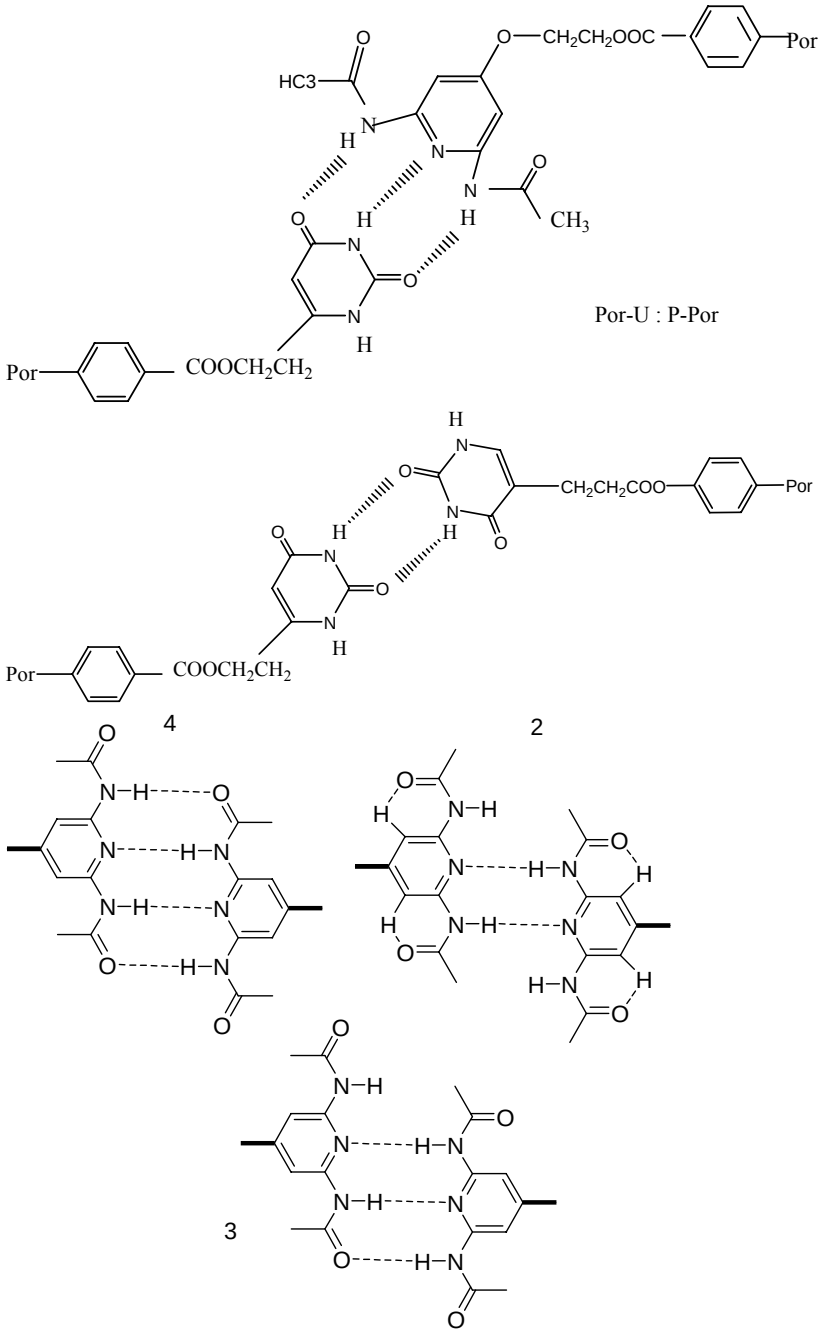

Figure 1. 3. (Top) hetero complementary U≡P hydrogen bonding; (center) homocomplementary U=U hydrogen bonding; and (bottom) homocomplementary P≡P showing the three possible hydrogen bonding interactions where the structure with two hydrogen bond also shows the hydrogen bond between the carbonyl and the aromatic proton observed in NMR spectra.

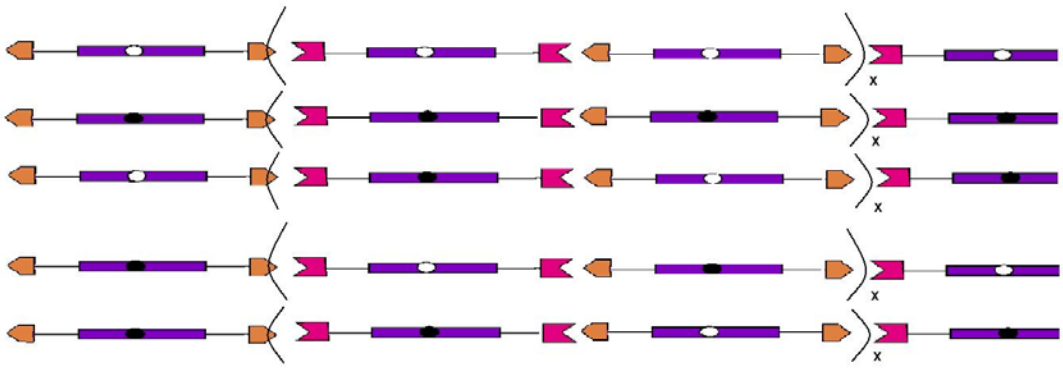

Figure 1. 4. Possible configurations of free base and metallo-porphyrins assemblies, from top to bottom: all free base porphyrins, all metalloporphyrins, Zn(II) pyridylporphyrins with free base uracyl porphyrins, free base pyridyl porphyrins with Zn(II) uracyl porphyrins, and an array with a percentage of the free base. The zinc systems serve as energy donors and the free base as energy acceptors.

Ultimately, utilization of these, or similar, systems in solar energy harvesting devices will require deposition onto surfaces. Thus we examined the self-organization of these molecules and various mixtures of them drop cast onto clean glass and freshly cleaved mica. Several key conclusions can be made. The association of molecules by homo-complementary hydrogen bonding motifs, in this case uracyl–uracyl interactions and diacetamidopyridyl – diacetamidopyridyl interactions, is known to occur in solution. The specific single and double H-bonding interactions between uracyls (and there are four possible H-bonding interactions between the pyridyl moieties with varying degrees of stability) are a few kJ mol^{-1} less than the hetero-complementary triple H-bonding interactions.[31, 36] The homo-complementary interactions become increasingly important as concentration increases, as do non-specific interactions such as π−stacking. These intermolecular interactions lead to aggregation of the individual component molecules as the solutions are concentrated.

As expected, dynamic light scattering (DLS) of 25 μM solutions in dry $CHCl_3$ at 25 °C of the individual porphyrins (**UCU, PCP, PC(Zn)P, UC(Zn)U**) reveals that a small quantity of the compounds aggregate to form particles with similar diameters of ~ 200 nm but with varying dispersities. Contact mode atomic force microscopy (AFM) studies of these individual porphyrinic compounds drop or spin cast onto glass surfaces from 25 μM solutions in $CHCl_3$ show a small surface density of particles that are 15 ± 5 nm high by 210 ± 30 nm in diameter, while on mica surfaces the heights are somewhat smaller. Again the dispersities are different for each compound.

Because of the greater intermolecular interactions by the complementary H-bonding motifs, it is expected and observed that 1:1 ratios of these compounds form larger aggregates at the same 25 μM concentrations in $CHCl_3$ at 25 °C as the components. Thus DLS indicates large amounts of 380 nm ± 20 nm diameter particles for **PCP ≡ UC(Zn)U**, and a bimodal distribution of 50 nm and 380 nm diameter particles of **UCU ≡ PC(Zn)P**. Contact mode AFM studies on glass and mica show a much higher surface density of the target assemblies compared to the individual compounds, with ~ 20 nm heights and ~300 nm diameters. In solution the nanoscaled aggregates of both the compounds and the mixtures likely contain a large amount of solvent, and are composed of numerous sub-domains, as has been shown with other porphyrinic nanoparticles.[37] Thus, upon deposition and solvent evaporation the nanoparticles collapse and can break apart into the subdomains. Fluid dynamics as the solvent evaporates also contributes to the observed morphologies. Thus, the AFM data and particles distribution histograms (Figure 1. 5. , 1. 6. , 1. 7. , 1. 8. , 1. 9. , 1. 10.) are generally consistent with the DLS data (Figure 1. 11., 1. 12.).

Compounds	AFM (on glass)	AFM (mica)
PCP	3x3 micron 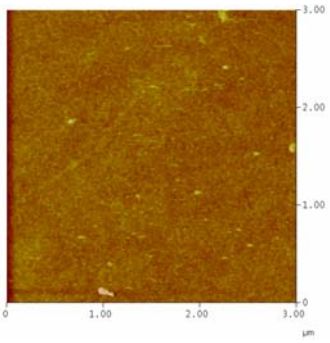	1.5x1.5 micron 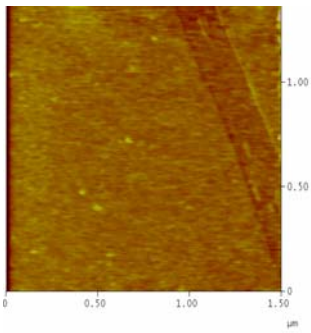
UC(Zn)U	3x3 micron 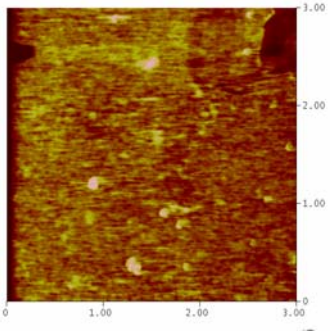	2x2 micron 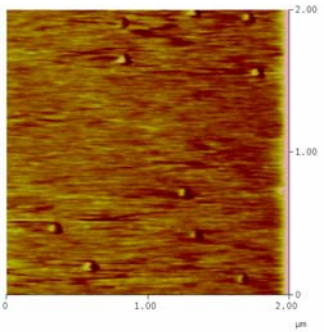
PCP+UC(Zn)U	5x5 micron 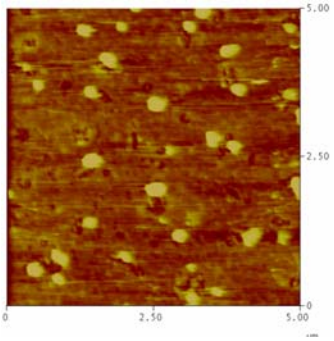	5x5 micron 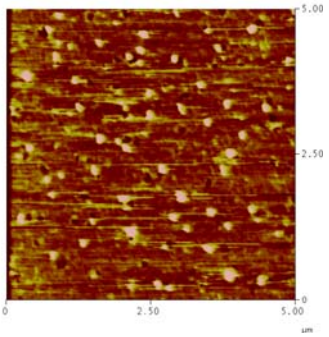

Figure 1. 5. Contact mode atomic force microscopy (AFM) studies of the individual porphyrinic compounds and the self-organized aggregates drop cast onto glass and mica surfaces from 25 μM solutions in $CHCl_3$. The contact mode silicon cantilever (CSC21) tip has a nominal convolution of 10nm

Compounds	AFM (on glass)	AFM (mica)
UCU	5x5 micron 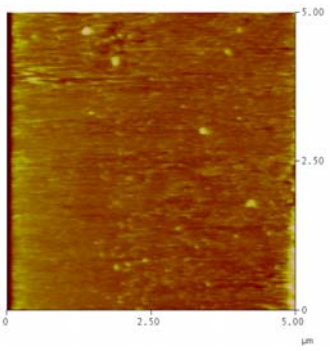	5x5 micron 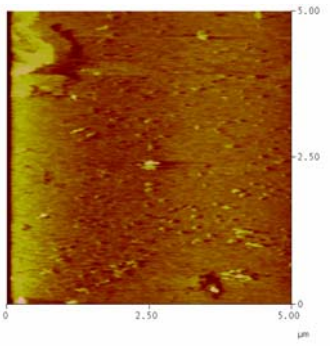
PC(Zn)P	1.5x1.5 micron 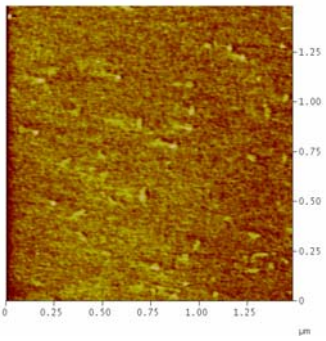	1.5x1.5 micron 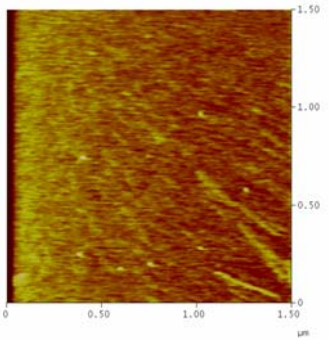
UCU+PC(Zn)P	3x3 micron 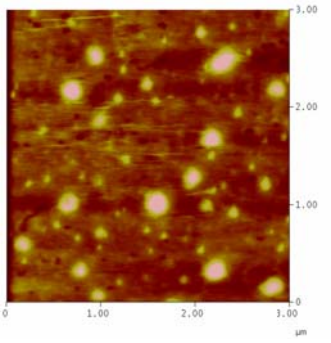	5x5 micron 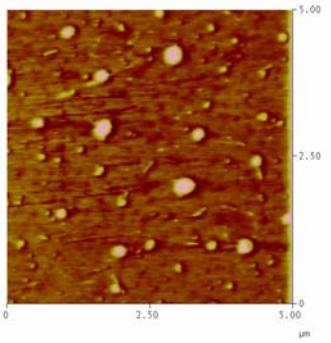

Figure 1. 6. Contact mode atomic force microscopy (AFM) studies of the individual porphyrinic compounds and the self-organized aggregates drop cast onto glass and mica surfaces from 25 μM solutions in $CHCl_3$. The contact mode silicon cantilever (CSC21) tip has a nominal convolution of 10nm.

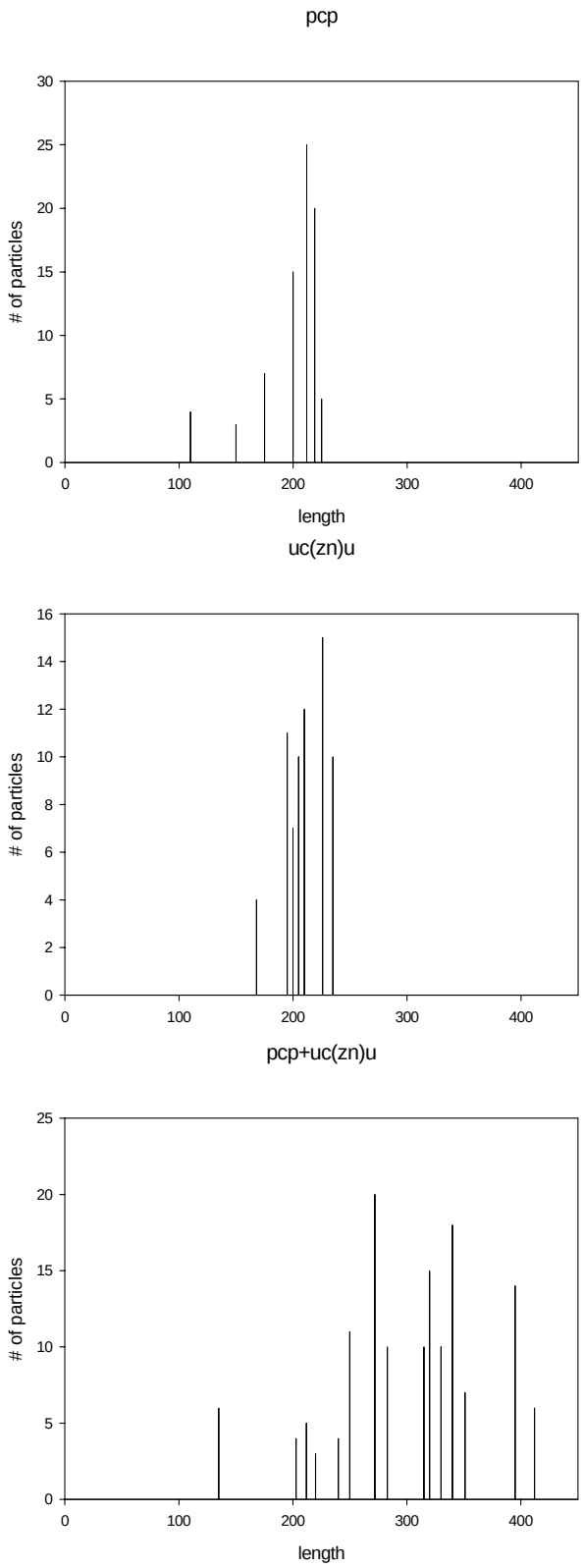

Figure 1. 7. Contact mode atomic force microscopy (AFM) histograms of the individual porphyrinic compounds and the self-organized aggregates on glass. (PCP, UC(Zn)U, PCP+UC(Zn)U)

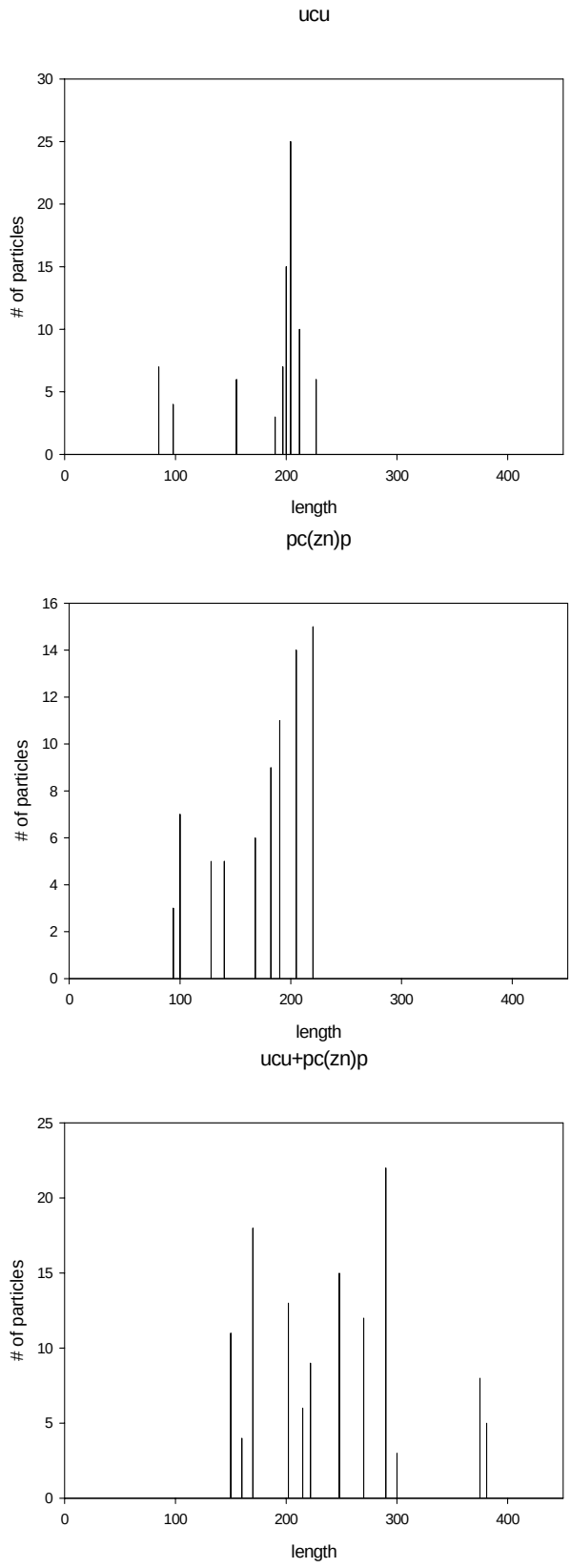

Figure 1. 8. Contact mode atomic force microscopy (AFM) histograms of the individual porphyrinic compounds and the self-organized aggregates on glass. (UCU, PC(Zn)P, UCU+PC(Zn)P)

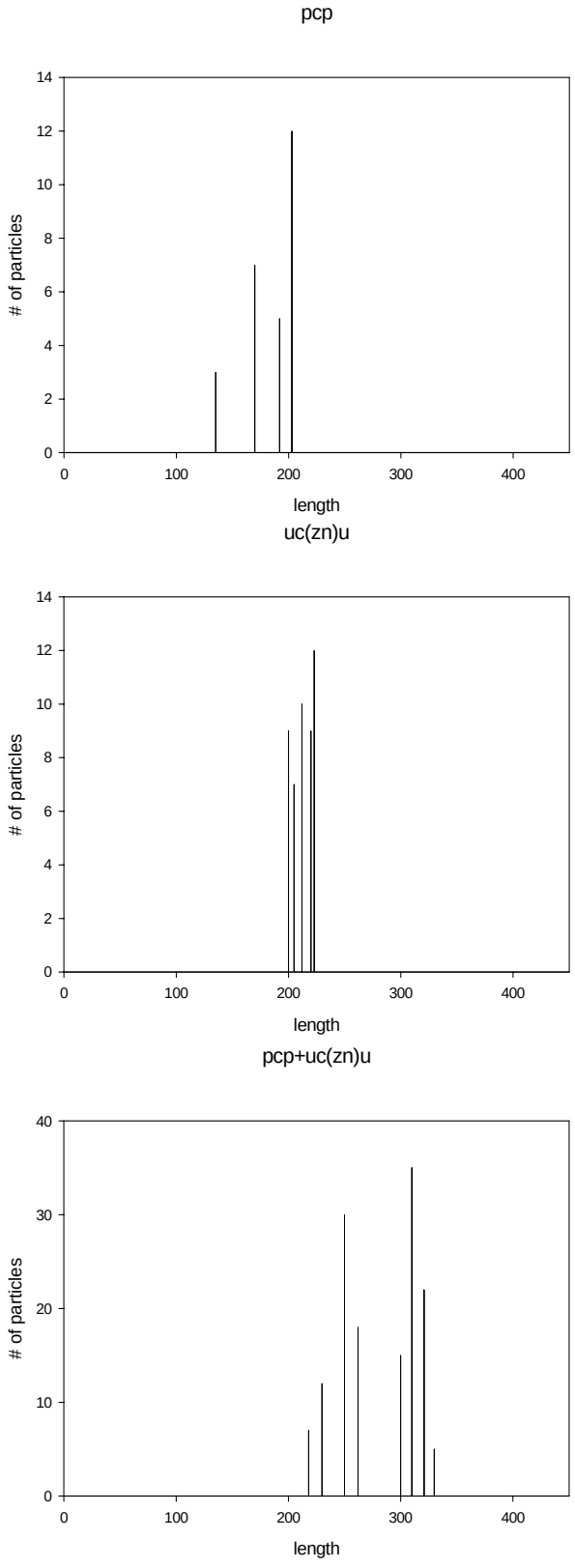

Figure 1. 9. Contact mode atomic force microscopy (AFM) histograms of the individual porphyrinic compounds and the self-organized aggregates on mica. (PCP, UC(Zn)U, PCP+UC(Zn)U)

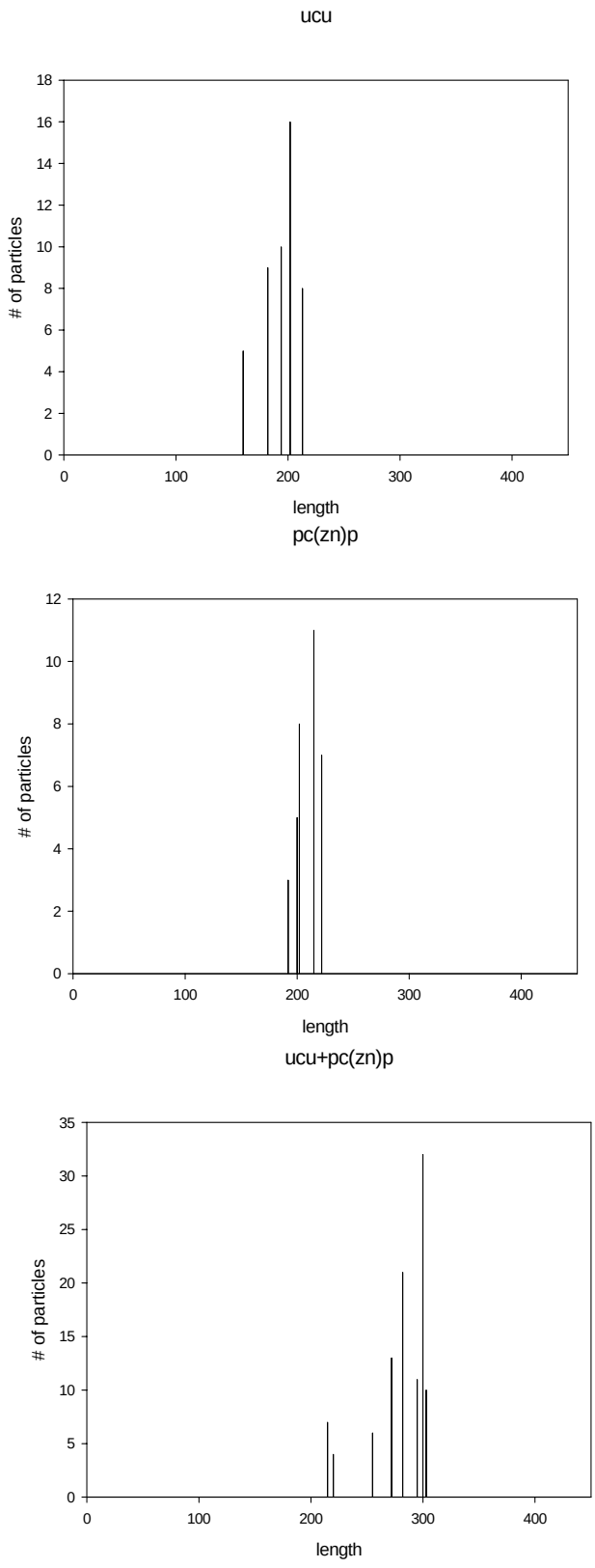

Figure 1. 10. Contact mode atomic force microscopy (AFM) histograms of the individual porphyrinic compounds and the self-organized aggregates on mica. (UCU, PC(Zn)P, UCU+PC(Zn)P)

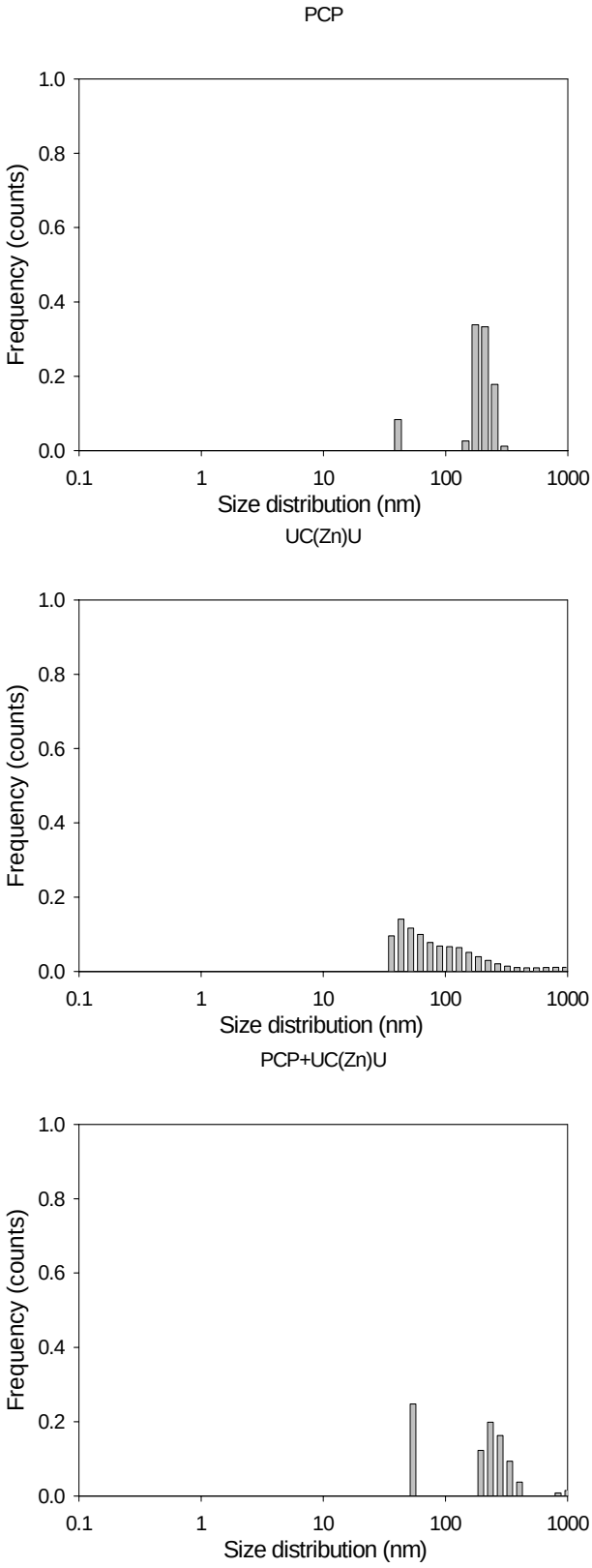

Figure 1. 11. Dynamic Light Scattering (DLS) histograms (diameter) of the each individual porphyrinic compound and the hetero complementary compounds. (PCP, UC(Zn)U, PCP+UC(Zn)U)

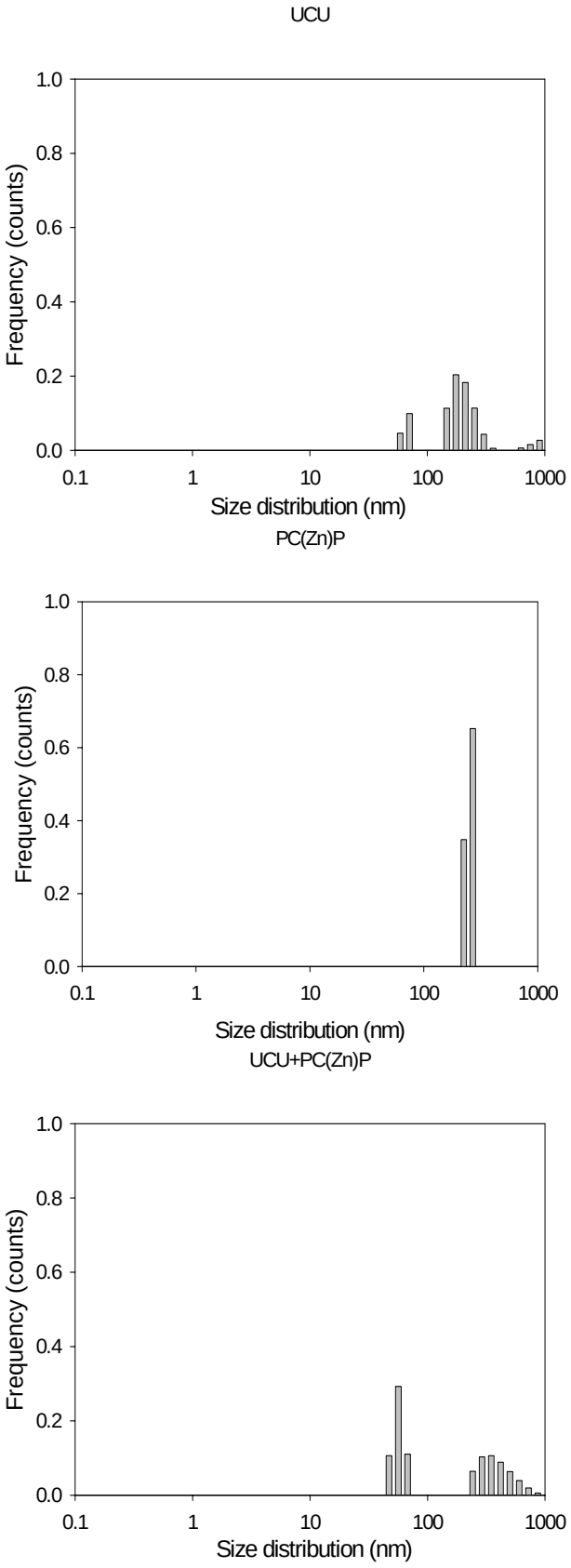

Figure 1. 12. Dynamic Light Scattering (DLS) histograms (diameter) of the each individual porphyrinic compound and the hetero complementary compounds. (UCU, PC(Zn)P, UCU+PC(Zn)P)

1. 3. Conclusions

Our conclusion based on DLS and AFM measurements are that the individual compounds, both the free base porphyrins and the zinc metallated porphyrins, are less aggregated in solution, and result in smaller particles on the surface with much smaller surface densities compared to the heterocomplementary assemblies. The two heterocomplementary combinations (UCU+PC(Zn)P and PCP+UC(Zn)U) are more aggregated in solution, albeit with a greater size distribution and result in large patches on both glass and mica surfaces in much greater surface densities. These results are consistent with the experimentally determined intermolecular interaction energies for triple hydrogen bond motifs. The DLS for individual porphyrins (free base and metallated) at 25μM concentration show a distribution of globular particles about 200-250nm in length, and this correlates well with the AFM data after drop casting the solution on glass or mica surface. DLS and AFM indicate that 25μM solutions of the complementary pairs (PCP+UC(Zn)U and UCU+PC(Zn)P) tend to aggregate into somewhat larger globular structures. DLS data fits better to a cylindrical geometry (length 300-350 nm, diameter 25-30 nm) and this is confirmed by the AFM data (glass and mica). There is higher surface density for the assemblies than for individuals components. The cylindrical geometry is consistent with the topology of the intermolecular interactions in that the assembly of individual chains occurs in one direction and then the chains aggregate, largely due to pi-pi interactions, to result in nanorods with a small aspect ratio.

As expected, the 2,6-diacetamidopyridyl – uracyl moieties afford complementary hydrogen bonding motifs that promote the association of the donor and acceptor molecules in moderately polar and non-polar solvents. Since these are thermodynamic products at least initially, it is reasonable to expect that different solvent conditions, temperatures, and method to deposit onto the surfaces can result in different particle sizes, particle distributions, particle morphologies, and surface coverage. From one standpoint, this parameter can be exploited to tune the self-organization of these materials into hierarchical structures and sizes. Since porphyrins and phthalocyanines are excellent candidates for the formation of photonic materials such as solar energy antennas, and since they are significantly more robust chromophores than the photosynthetic pigments, these easy to synthesize arrays will be incorporated into proof-of-principle devices in the future.

References:

1. Blankenship, R. E., *Molecular Mechanisms of Photosynthesis* **2002**.

2. Mauzerall, D. C., *Clinics Derm.* **1998,** 16, 195-201.

3. Jacoby, M., *Chem. Engineering News* **2004**, 29-32.

4. Brabec, C. J.; Sariciftci, N. S.; Hummelen, J. C., *Adv. Funct. Mater.* **2001,** 11, 15- 26.

5. Shaheen, S. E.; Brabec, C. J.; Sariciftci, N. S.; Padinger, F.; Fromherz, T.; Hummelen, J. C., *Appl. Phys .Lett.* **2001,** 78, 841-843.

6. Hoppe, H.; Sariciftci, N. S., *J. Mater. Res.* **2004,** 19, 1924-1945.

7. Linke-Schaetzel, M.; Bhise, A. D.; Gliemann, H.; Koch, T.; Schimmel, T.; Balaban, T. S., *Thin Solid Films* **2004,** 451-452, 16-21

8. van Grondelle, R.; Dekker, J. P.; Gillbro, T.; Sundstrom, V., *Biochim. Biophys. Acta* **1994,** 1187, 1-65.

9. Andrizhiyevskaya, E. G.; Frolov, D.; van Grondelle, R.; Dekker, J. P., *Biochim.Biophys. Acta* **2004**.

10. Bahatyrova, S.; Frese, R. N.; Siebert, C. A.; Olsen, J. D.; van der Werf, K.; van Grondelle, R.; Niederman, R. A.; Bullough, P. A.; Otto, C.; Hunter, C. N., *Nature* **2004,** 430, 1058-1062.

11. Brookfield, R. L.; Ellul, H.; Harriman, A.; Porter, G., *J. Chem. Soc.* **1986,** 82, 219-233.

12. Davila, J.; Harriman, A.; Milgrom, L. R., *Chem. Phys. Lett.* **1987,** 136, 427-430.

13. Gust, D.; Moore, T. A.; Moore, A. L.; Gao, F.; Luttrull, D.; DeGraziano, J. M.; Ma, X. C.; Makings, L. R.; Lee, S. -J.; Trier, T. T.; Bittersmann, E.; Seely, G. R.; Woodward, S.; Bensasson, R. V.; Rougée, M.; De Schryver, F. C.; Van der Auweraer, M., *J. Am. Chem. Soc.* **1991,** 113, 3638-3649.

14. Gensch, T.; Hofkens, J.; Herrmann, A.; Tsuda, K.; Verheijen, W.; Vosch, T.; Christ, T.; Basché, T.; Müllen, K.; De Schryver, F. C., *Angew. Chem. Int. Ed.* **1999,** 38, 3752-3756.

15. Hofkens, J.; Maus, M.; Gensch, T.; Vosch, T.; Cotlet, M.; Köhn, F.; Herrmann, A.; Müllen, K.; De Schryver, F., *J. Am. Chem. Soc.* **2000,** 122, 9278-9288.

16. Adronov, A.; Fréchet, J. M., *J. Chem. Commun.* **2000**, 1701-1710.

17. Fleischer, E. B.; Shachter, A. M., *Inorg. Chem.* **1991,** 30, 3763-3769.

18. Drain, C. M.; Lehn, J.-M., *Chem. Commun.* **1994**, 2313-2315.

19. Drain, C. M.; Bazzan, G.; Milić, T.; Vinodu, M.; Goeltz, J. C., *Israel J. Chem* **2005,** 45, 255-269.

20. Balaban, T. S.; Eichhöfer, A.; Prische, M. J.; Lehn, J.-M., *Helv. Chim. Acta* **2006,** 89, 333-351

21. Blankenship, R. E.; Olson, J. M.; Miller, M., *Kluwer Academic Publishers: Dordrecht, The Netherlands,* **1995**, 399-435.

22. Blankenship, R. E.; Brune, D. C.; Wittmershaus, B. P., *Kluwer Academic Publishers: Dordrecht, The Netherlands,* **1998**, 32-46.

23. Frigaard, N. U.; Bryant, D. A., *Microbiol. Monogr. Springer-Verlag: Berlin* **2006**.

24. Balaban, T. S.; Holzwarth, A. R.; Schaffner, K.; Boender, G.-J.; de Groot, H. J.

M., *Biochemistry* **1995,** 34, 15259-15266.

25. Balaban, T. S.; Tamiaki, H.; Holzwarth, A. R.; Würthner, F., *Ed. Topics Curr. Chem. Springer Verlag: Heidelberg* **2005**.

26. Balaban, T. S., *Encyclopedia of Nanoscience and Nanotechnology* **2004,** 4, 505- 559.

27. Harvey, P. D., *In The Porphyrin Handbook,* **2003,** 18, 63-250.

28. Drain, C.; Fischer, R.; Nolen, E.; Lehn, J., *Chem. Commun.* **1993**, 243-245.

29. Drain, C.; Russel, K.; Lehn, J.-M., *Chem. Commun.* **1996**, 337-338.

30. Drain, C. M.; Goldberg, I.; Sylvain, I.; Falber, A., *Top Curr Chem* **2005,** 245, 55- 88.

31. Shi, X.; Barkigia, K. M.; Fajer, J.; Drain, C. M., *J. Org. Chem.* **2001,** 66, 6513-6522.

32. Fouquey, C.; Lehn, J.-M.; Levelut, A.-M., *Adv. Mater* **1990,** 2, 254-257.

33. Gulik-Krzywicki, T.; Fouquey, C.; Lehn, J.-M., *Proc. Natl. Acad. Sci .USA* **1993,** 90, 163-167.

34. Berl, V.; Schmutz, M.; Krische, M. J.; Khoury, R.G.; Lehn, J.-M.,*Chem. Eur.J* **2002,** 8, 1227-1244.

35. Lehn, J.-M., *Supramolecular Chemistry. Concepts and Perspectives* **1995**.

36. Drain, C. M.; Shi, X.; Milić, T.; Nifiatis, F., *Chem. Commun.* **2004**, 287-288.

37. Gong, X.; Milić, T.; Xu, C.; Batteas, J. D.; Drain, C. M., *J. Am. Chem. Soc.* **2002,** 124, 14290- 14291.

2 .

SELF-ASSEMBLED AND SELF-ORGANIZATION OF PORPHYRIN MATERIALS ON SURFACES

2. 1. Introduction

For the foreseeable future, the vast majority of commercial electronics, photonics, and other devices will be in the solid state and incorporated onto or into a substrate. The formation of organic light-emitting diodes (OLEDs), for example, generally requires the careful deposition of several to several tens of layers of various organic and inorganic materials, and the thickness of each must be precisely controlled. An alternative ‘‘bottom–up’’ approach exploits knowledge of intermolecular interactions to self-assemble molecules into supramolecular structures, self-organize molecules into monolayers, or electrostatically deposit films layer by layer.[1-5]

The degree of predictable and long-range molecular order decreases from self-assembly to self-organization to layer by layer. Notable applications of the second mode of bottom–up assembly are the deposition of thin films of liquid crystals for various display applications.

Because exact alignment of molecules is not usually possible with the layer-by-layer approach, applications of this method to date have focused on modifications of large surface areas. This chapter focuses on the methods and applications of self-assembled and self-organized porphyrinic materials on surfaces; however, many of the themes and methods discussed are applicable to a variety of other chromophores and other organic molecules. Porphyrinoids are tetrapyrrolic macrocycles that are excellent molecules for various commercial applications because of their remarkable stability, considering their rich photonic properties. A crucial step toward the application of nanoscaled photonic devices is the ability to design and create increasingly larger architectures of interactive molecules and to incorporate these entities into device components.[2-5]

The efficiency of electronic and energy transfer in organic-based materials depends on both the molecule and the architecture of these molecules in the device. Other major considerations include the interconnections between the organic material and inorganic components as well as environmental factors. In addition to increasing the performance and efficiency of devices, the components of devices that are molecule-based will be more environmentally benign than much of the inorganic materials they replace. These studies show that there is a correlation between the device's physical properties and the morphology of the self-organized, photoactive, organic layer.

2. 2. Porphyrinoids definition and scope

Porphyrins are tetrapyrrolic macrocycles (Figure 2. 1) found in nature in systems such as hemoglobin, myoglobin, various cytochromes (C, P450, etc.), chlorophylls, methyl-Co-M reductase in methanogenic bacteria, and a plethora of other biological systems.[6] They function as transporters of small molecules such as dioxygen, mediators of electron transport, oxidation catalysts, light-harvesting and energy transport conduits, and catalysts for the reduction of a methyl thioether, respectively. Although porphyrins can bind virtually every metal in the periodic table (and a few nonmetals), in biological systems, these metals are usually Mg, Fe, Co, and Ni—where the redox chemistry of the latter three provides the function.

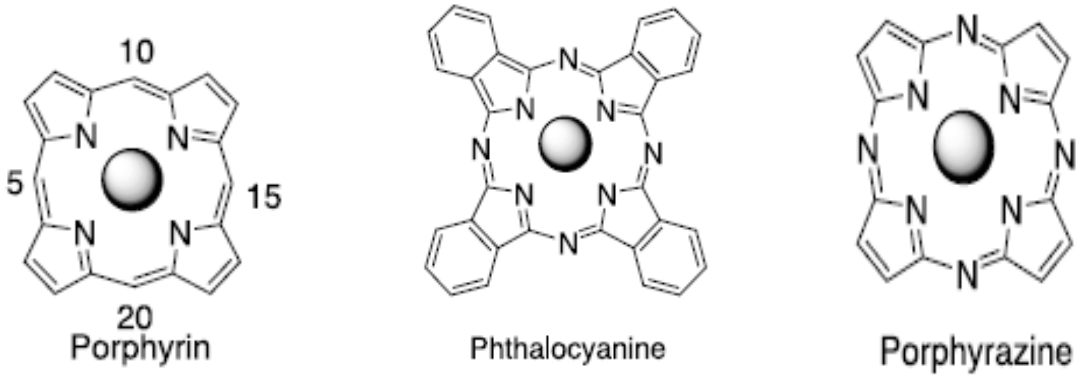

Figure 2. 1. The three basic porphyrinoids pigments

The limited flexibility and restricted aperture of the square planar ligand modulate both the redox potential and the coordination geometry of bound metals, which in turn modulate the redox and photophysical properties of the macrocycle. The remarkable stability of the macrocycle and the wide distribution in nature have indicated to some researchers that porphyrins may be prebiotic.[6] Because of their biological relevance and diverse functions, a large number of porphyrin derivatives have been synthesized in the laboratory in the last decades using the methods of Adler et al.[7] and Lindsey[8] and, more recently, a solventless ‘‘green’’ synthesis.[9] These methods have allowed commercial applications of porphyrin derivatives that include oxidation catalysts, blood substitutes, therapeutics, sensors/actuators, photonic materials, dyes, and various forms of ‘‘toners’’ in photolithography. In the past decade, there has been substantial effort to create and characterize the properties of multiporphyrinic systems for materials applications.[10-12]

Two related macrocycles—phthalocyanines and porphyrazines— (Figure 2. 1) have also been the subject of much research for similar applications, but multichromophoric systems of these dyes are less well developed at present.[13-16] Although all three types of macrocycles have related photophysical properties, the porphyrins have been the primary focus of research because of synthetic accessibility and greater solubility in organic solvents. In the context of nanotechnology and materials chemistry, the aforementioned properties of porphyrinoids can be exploited for a variety of applications that include: (1) molecular electronics [4, 17-19] (2) components of nanoscaled sensors, actuators [20-22] and photonics [23, 24] (3) both

structural and chemically active elements in molecule-constructed molecular sieves [25-28] (4) catalysts [29] and (5) part of biomolecular encapsulating systems.[30, 31]

For many of these applications, the precise geometric alignment of the chromophores in the materials is essential for function. The problem, then, is how to make nanomaterials of organic compounds wherein a few to a few hundred molecules are brought together in a predefined or predictable geometry—as opposed to aggregates, colloids, and gels (all of which have important applications in nanotechnology as well).

The remarkable progress in organic chemistry has provided many elegant molecular systems with more than one porphyrin linked by covalent bonds.[8, 19] These include acetylene, phenylacetylene, bridged, fused, and other linkages. For many of these molecular systems, the interspatial relationships of the macrocycle are well defined. However, the significant limitation of these molecular systems is that the product yield drops precipitously as the number of chromophores increases. There are varieties of polymeric systems bearing porphyrins or with porphyrins as part of the polymeric chain where the dispersity varies from system to system, but the yields are generally better than for the above molecular system. Both the molecular and polymeric systems have provided a wealth of information of the nature of energy and electron transport mediated by the porphyrins and the various linkers, as well as the means to gate these processes. Several functional materials have also been reported, vide supra. The focus of this chapter is on self-assembled and self- organized porphyrinic systems on surfaces.

2. 3. Supramolecular chemistry

Self-assembly and self-organization are spontaneous processes that allow simple components to form more complex and more ordered systems.[32-39] In terms of molecules, the spontaneous self-assembly of a given set of molecules results in a discrete supramolecular entity or three-dimensional lattice, whereas the spontaneous self- organization of a set of molecules results in systems that are usually not discrete and ordered in only one or two dimensions. The former is usually less tolerant of defects or errors in structure than the latter. Much of the initial inspiration and concept for both self-processes comes from the study and observation of biological systems. For example, the self-assembly of a set of helical proteins into a discrete ion channel relies on the complex intermolecular interactions between the component molecules. One may observe the opening and closing of a single ion channel that gates ionic currents across a lipid membrane (which is an example of a self-organizing system). The intermolecular interactions are governed by the electron distributions in molecular orbital and by complementary shapes or structures. For purposes of discussion, the intermolecular interactions are heuristically classified and include hydrogen bonding, electrostatic interactions, coordination chemistry, and van der Waals forces acting in concert. The ‘‘lock-and-key’’ concept for shape complementarity has a long history.[32, 33] Thus nature provides a plethora of examples, which demonstrate that self-assembly and self-organization are effective means to build complex, functional structures in good yields.

The self-assembly of discrete supramolecular systems generally relies on the use of component molecules designed with specific intermolecular interactions such as H-bonds, metal ion coordination, and sometimes electrostatics because these noncovalent bonds are directional and stronger than other intermolecular forces.[1] However, the self-organization of materials generally relies on a greater number of weaker, nonspecific interactions such as dipolar, van der Waals, and hydrophobic/hydrophilic forces. Crystals of supramolecular systems are an example of structures that arise from both directional and nondirectional intermolecular interactions.[36, 38, 40, 41] In most cases, the architectures of molecules arising from both self-processes are the thermodynamic products.

2. 4. Self-organized porphyrins on surfaces

2. 4. 1. Surfaces

The advantages of using supramolecular chemistry to construct materials that can serve as components of nanoscaled devices include the ability to construct complex structures efficiently, but there are several significant technical challenges. The reversibility of the intermolecular interactions that allow self-assembly and self-organization to result in thermodynamic products in high yields also means that the structure of the system is sensitive to environmental factors such as concentration, temperature, ionic strength, etc. [11, 42-44]

Because the formation of the desired nanoarchitectures of organic molecules generally proceeds in solutions and these are to be incorporated onto surfaces as components of devices, the first challenge is to deposit the self-assembled or self-organized system onto an appropriate substrate. The inherent concentration changes during deposition and solvent evaporation may significantly alter the supramolecular structure, or result in undesirable aggregates.

Other factors such as surface chemistry and surface energetics may also affect the structure of self-assembled or self- organized systems. The second challenge is to design supramolecular systems on surfaces that are stable to the operating conditions of the device. Device stability to thermal fluctuations, redox chemistry, environmental changes such as humidity, and dioxygen is crucial. But all of these factors can affect the equilibrium of self- assembled systems, thus also the structure and function. There are numerous examples of porphyrin-containing self-organized monolayers[45, 46] thin films[47, 48] and polymeric materials [49]on surfaces; however, there are only a few examples of self-assembled (discrete, mono-dispersed) systems that can be deposited onto surfaces with high structural fidelity that are stable at room temperature. These last constructs are the primary subject of this chapter. An important aspect of all types of nanoscaled materials on surfaces is the role of surface chemistry and surface energetics in determining the final structure/orientation of the molecules. This is especially true of self-assembled and self-organized systems because the surface properties may induce unanticipated structural changes, or may be exploited as a further means of dictating the final structure.[43, 44]

A host of surface chemical preparations can be utilized to modify the surface chemistry, and hence the surface energetics of the substrate to impact the structure of adsorbing materials. For example, Au surfaces can be modified by self-assembly of alkanethiol-based compounds. The chemistry of glass or mica surfaces can be readily changed by organosilanes, allowing for the generation of hydrophobic or hydrophilic surfaces. Chemical modification of the surface can even allow the direct assembly of species on surfaces by providing the appropriate anchor groups on which to build. Weakly bound aggregates, such as those organized by π-stacking, can be made to either retain or lose their initial solution structure depending on the competition between the interaggregate interactions, the interactions of the component molecules, and the interactions of the aggregates with the surface. This has been readily demonstrated by the adsorption of porphyrinic nanoparticles on surfaces.[43, 44, 50, 51]

2. 4. 2. Applications

Some of the applications of these porphyrinic materials are envisioned to be in the areas of molecular electronics[5, 52] and photonic materials.[2, 3, 17] The latter applications exploit both the functionality and the rigid structure of porphyrins to make materials such as molecular sieves,[25, 28] catalysts,[53] sensors,[54] actuators,[18] and nonlinear optics.[55] Elegant synthetic organic work has yielded discrete multiporphyrinic systems held together by covalent bonds using a variety of linkers,[19] or by direct fusion of the porphyrin macrocycles. [56, 57]

In addition to the development of new synthetic methods, these types of molecules have provided insights into the complexities of photo-induced electron/energy transfer processes[58, 59] in terms of chromophores geometry, role of the linker, and dynamics of the molecule. However, the overall yield of discrete molecular systems containing more than a few porphyrins is too low to be commercially viable for all but the most specialized applications.

Similarly, numerous polymers of/with porphyrins have also yielded interesting materials that have a distribution of polymeric and photonic properties because of polydispersity and the subtly different environments of the chromophores. For many of the aforementioned applications, control of both the relative positions of the macrocycles and the nanoscaled size of the system is necessary for the function.[1] Since the first publications on self-organizing[60, 61] and self-assembling porphyrins via H-bonds[62] and coordination chemistry,[63] there has been an exponential annual increase in the number or reports of multiporphyrinic systems made by these methods.[11, 17, 35, 42-44, 60-63] The primary focus of this chapter will be on the developments of the last few years because there are several reviews and papers that cover a large body of work on the chemistry, properties, and applications of porphyrins up to early 2000.[35, 39] There are also a variety of reviews on both self-assembly and multiporphyrin systems.[10]

2. 4. 3. Self-Organization on Surfaces

Because self-organized systems are generally less ordered and more tolerant of defects both in solution and on surfaces than self-assembled systems, these types of systems are generally easier to make. Thus the majority of work on porphyrinic materials on surfaces use self-organizing systems, which can be divided into two categories: (1) thin films[47, 48] deposited as polymers or by layer-by-layer methods,[64-66] and (2) monolayers chemically attached via covalent [45, 67-69] or coordination bonds to the surface,[70] or as (mono)layers adsorbed onto the surface. To date, most of the demonstrated applications for nanoscaled porphyrinic materials on surfaces have been in the area of electrodes, wherein these types of layered films are used to modify electrodes to make them selective for various analytes, and/or to modify surface/electrode chemistry. Other applications in molecular electronics are in the early stages of development.

The self-organization of porphyrins on a variety of surfaces can be accomplished via covalent attachment, coordination chemistry, and electrostatic interaction. The choice of substrate and mode of attachment is dictated by the desired function of the surface-bound photonic material. In general, the relative orientation of the macrocycle to the plane of the substrate can be reasonably designed, but the horizontal two-dimensional structure of the porphyrins is usually much less ordered or organized. The two-dimensional order that is observed results from weak porphyrin–porphyrin interactions, and is generally found only in small domains, rather than globally.

This does not imply that these systems are not well suited for some purposes, but rather that long-range surface organization is not easily achieved by these approaches. The applications of these systems can be as diverse as the mode of assembly, the nature of the porphyrin, the choice of substrate, and the properties of the linkage. All of these parameters can be systematically changed to modulate the material/device properties and to optimize catalytic, sensor, and photonic functions.

2. 5. Self-assembled porphyrinic materials on surfaces

As discussed before in the beginning of this chapter there are several challenges to using self-assembled and self-organized structures in commercial devices, which can be generally ascribed as issues of structural and chemical stability. To construct self-assembled arrays that then self-organize into reasonably uniform films on surfaces, two porphyrinic squares bearing dodecyloxyphenyl group on the periphery were constructed, as shown schematically in Figure 2. 2. The intent was that there would be much less conformational flexibility, compared to the dimer; therefore the intersupramolecular forces would be more defined, and a more ordered film would result. These squares are constructed using the same design strategy as the first discrete porphyrin assemblies reported—pyridyl porphyrins with Pd(II) and Pt(II). [63]

Because the Pt-Py bond is stronger than the Pd-Py bond, assemblies using Pt as a linker are more robust. Consistent with previous findings, these supramolecular squares with dodecyloxy groups are all well characterized in solution by NMR, UV–visible, and mass spectral analyses.

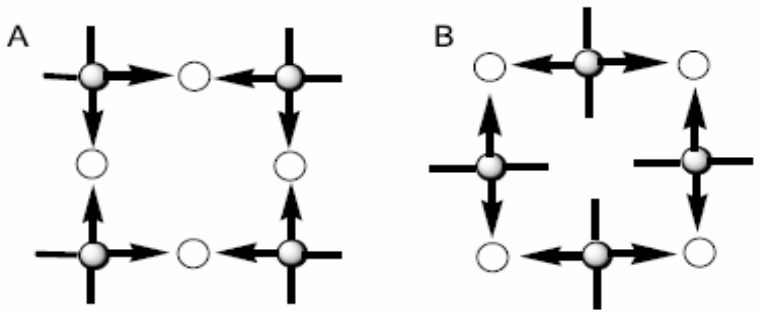

Figure 2. 2. (A) square results from the 90° topology of the pyridyl groups on these porphyrins and the architecturally complementary 180° coordination geometry of Pd(II)Cl_2; and (B) cube results from the 180°topology of the pyridyl groups on the isomeric porphyrins and the architecturally complementary 90°coordination geometry of Pt(II)Cl_2

The conformation of Figure 2. 2. A is largely planar as illustrated because the 90° topology of the rigid corner macrocycles prevents much twisting about the pyridyl Pd(II) bond, but the conformation of Figure 2. 2. B is box like or parallelogram-like because there can be substantial rotation about the pyridyl Pt(II) bonds.

The calculated structure showing the bond rotations is shown in Figure 2. 3. This means that the dodecyloxyphenyl groups of Figure 2. 2. A are essentially coplanar with the plane of the supramolecular square, but in Figure 2. 2. B, these groups are directed along two faces of the box. The orientation of these liquid crystal-forming groups has a significant influence on the resultant structure of the films on glass surfaces, such that films from Figure 2. 2. B-type squares are reasonably uniform, whereas those from Figure 2. 2. A-type squares are much less so. The relative number/strength of the van der Waals forces per supermolecule may be largely responsible for these observations.

Although both Figure 2. 2. A and 2. 2. B have eight alkanes groups, only two per side of Figure 2. 2. A can interact with a coplanar neighbor, but four alkanes interact with the neighbors of Figure 2. 2. B.

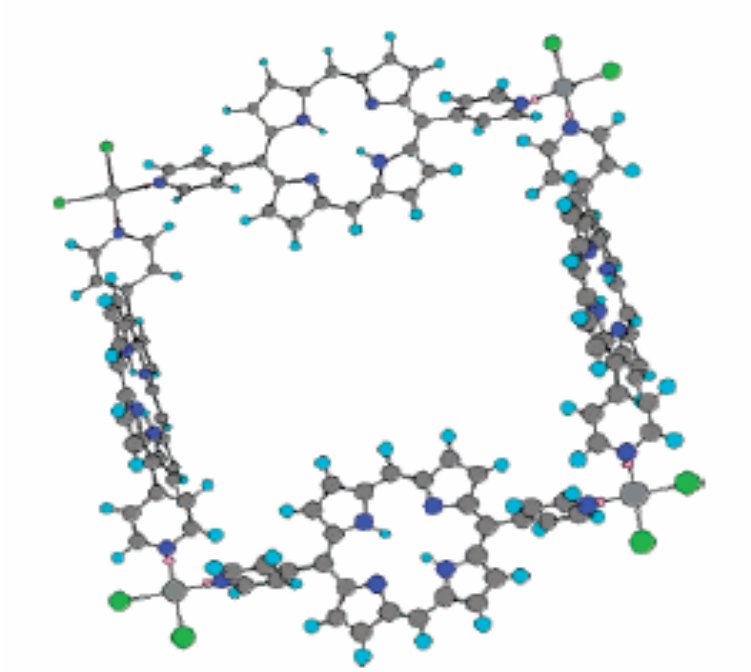

Figure 2. 3. Molecular model of the *cis*-Pt(II) porphyrin assembly based on MM-2 energy minimization using Chem 3D. The figure corresponds to the tetramer array coordinated to four Pt(II) chloride molecules.

This hypothesis is born out by AFM studies of these two supramolecular squares deposited on glass. Figure 2. 2. B tends to form thin films that are 2–5 nm thick, whereas Figure 2. 2. A forms small islands of variable thickness. A Figure 2. 2. B-type square with tert-butylphenyl groups was made for comparison with the supermolecule with dodecyloxyphenyl groups. As expected, the tert-butylphenyl substituted square does not form films but rather small aggregates.

This is a clear indication that the number, position, and nature of the R-groups are of paramount importance to the self-organization of self-assembled arrays of porphyrins. Further studies on the interactions of all of these systems on different surfaces will reveal the role of surface chemistry/energetics in the organization of supramolecular porphyrinic systems. Adsorption of the dodecyloxyphenyl-functionalized porphyrin square on glass shows that a thin (~2 nm) film is formed. The thickness of this film is in general agreement with the dimensions of a single central square unit, as shown schematically in Figure 2. 4. The film is composed of both nanoparticles of these subunits and larger domains/islands (Figure 2. 5.), which are found to be much more uniform in height than those of the porphyrin rings using a Pd-linked dimer.[71, 72]

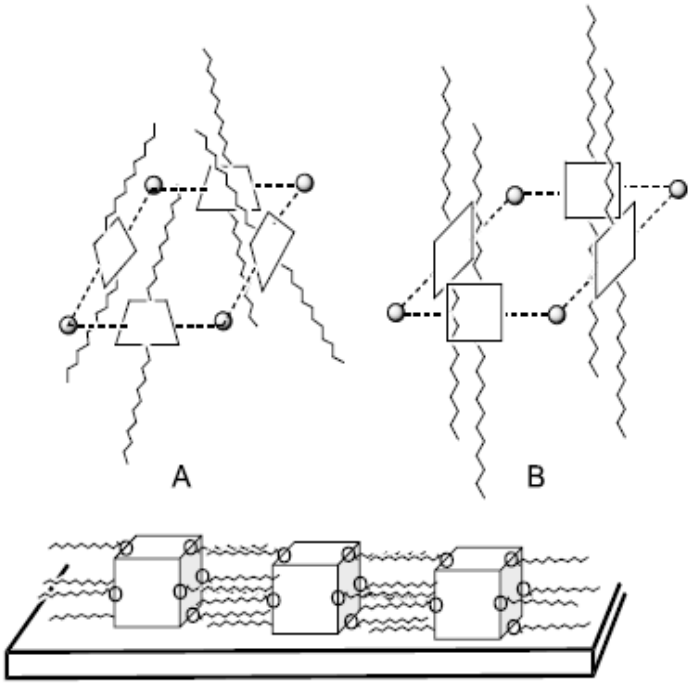

Figure 2. 4. Two possible conformations of the square and possible interactions between the supramolecular squares

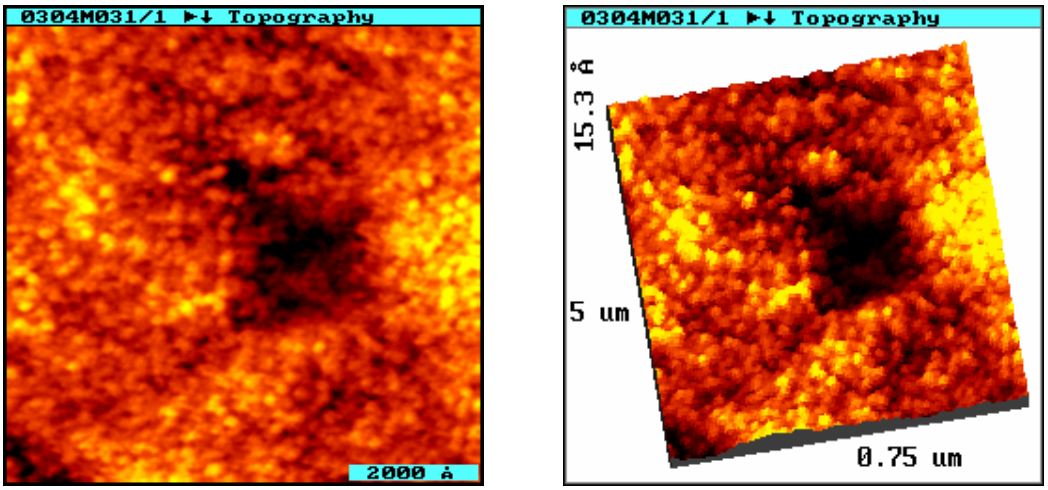

Figure 2. 5. AFM image of the dodecyloxyphenyl film on glass 50 uL drop-dried on glass (2.63 x 10^{-4} M); dried overnight Park E (0.1 N/m) tip; not rinsed with toluene. Imaged in ethanol -- Data worked in collaboration with Dr. Jayne Garno at NIST

The ability to deposit specifically designed self-assembled (discrete) supramolecular structures onto surfaces without change in structure or function remains a significant challenge for the exploitation of this methodology in real-world applications and devices. However, self-organized monolayer systems are more accessible because of the tolerance for local defects, but the horizontal dimensions of these are generally quite large. The layer-by-layer method has both advantages (ease of preparation) and disadvantages (greater defect density than SAMs), but may find numerous applications as sensors, and other systems requiring surface modification.

The overall structure of these systems is likely a grid, but because the cross-linking step results in kinetic rather than thermodynamic products, the degree or order is likely not comparable to self-assembled/organized systems. This research is notable because it is an attempt to organize porphyrin sandwich compounds on surfaces with greater structural stability and a degree of order different from monolayers of similar compounds.

2. 6. Liquid Crystalline porphyrinic arrays

In the liquid crystalline phase, molecules move freely yet retain certain spontaneous orientational order. Liquid crystals respond to weak electric and magnetic fields much more than solids, liquids, or gases, and these changes often induce significant structural reorganization.[73] Because of these morphological changes in response to applied fields, the preparation and characterization of liquid crystalline and mesogenic films have received much attention in recent years, for important applications such as display technologies and light emitting devices. Liquid crystal-forming derivatives of porphyrins and metalloporphyrins are interesting because of their rich photophysical properties, ease of functionalization, and lower melting points in comparison to phthalocyanines,[10] yet they have not been extensively investigated. Certain phthalocyanines with long, flexible hydrocarbon chains are thermotropic mesogenic materials[74-78] and form discotic mesophases at an elevated temperature, while other phthalocyanines derivatives self-assemble into columnar phases in Langmuir-Blodgett (L-B) films and in solution.[79]

Mesotetrasubstituted porphyrins have shown properties of liquid crystalline columnar phases,[80] and phthalocyanines crown ether conjugates form columnar aggregates in the presence of metal ions of appropriate size for the crown ether.[16] One of the early successes in the self-organization of a porphyrin-based device utilized liquid crystal-type interactions to form thin films of a photoconducting zinc porphyrin with eight dodecyloxy groups on the pyrroles.[4, 81] Electron–hole pairs are generated on irradiation of a section of a device that has this porphyrin derivative placed between two optically transparent electrodes with an applied electric field. The device then performs as a high-density nanosecond charge trap that can be used as an optical memory device. Similar porphyrins were used to make liquid crystal thin films between indium tin oxide coated glass slides, which displayed electric-field modulated near-field photo luminescence.[82]

These studies show that there is a correlation between the device's physical properties and the morphology of the self-organized, photoactive, organic layer. Other liquid crystal-forming porphyrins with properties dependent on the nature and position of the hydrocarbon have also been reported.[78, 83, 84]

The placement of long-chain hydrocarbons can dictate the two-dimensional organization of porphyrins[85] (Figure 2. 6.) and phthalocyanines[86-88] on surfaces and can be characterized by scanning probe microscopy. (Figure 2. 7.) Another functional device, in this case a field effect transistor, uses the self-organizing properties of lipid bilayers to organize porphyrins[60, 61, 89, 90] or supramolecular porphyrin arrays.[42] There are several examples of discrete multiporphyrin arrays with long-chain hydrocarbons appended on the periphery that induce the formation of monolayers by the Langmuir–

Blodgett method. Then, these can be transferred to surfaces such as glass with reasonable structural integrity. These films are early examples of using a secondary procedure to self-organize self-assembled supermolecules. The supermolecules with liquid crystal-forming moieties also form three-dimensional crystalline structures at higher deposition concentrations. These observations clearly demonstrate that the number, position, and nature of the peripheral groups and the supramolecular structure and dynamics, as well as the energetics of interactions with the surface, are of key importance to the two-dimensional and three-dimensional self-organization of assemblies such as porphyrins on surfaces.

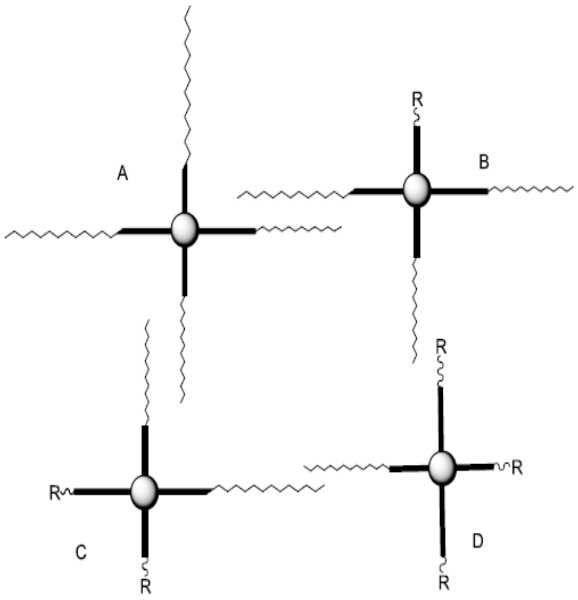

Figure 2. 6. Adsorption of porphyrins bearing long-chain hydrocarbons that serves as liquid crystal-forming motifs. The R-group can be a variety of polar and nonpolar functional groups. The number and topology of the hydrocarbon chains and the nature of R-groups govern the molecule–surface and molecule–molecule interactions, thus the resulting organization on the surface.

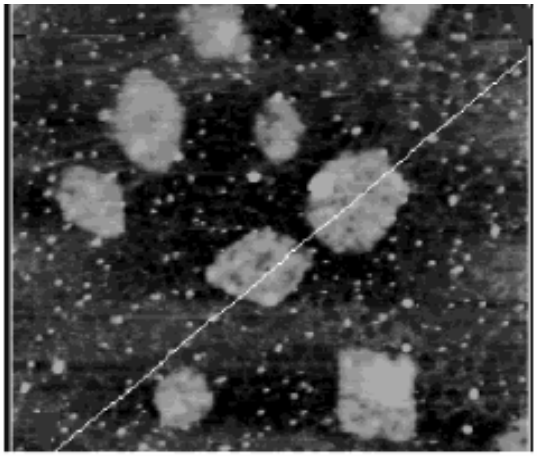

Figure 2. 7. AFM image (7.0x7.0 μm^2) of several nanocrystalline domains of supramolecular porphyrin array formed on glass by depositing solution of ~10-fold-higher concentration.—Tatjana Milic data

2. 7. Conclusions

The use of porphyrins and porphyrinoids for self-assembly and self-organization of molecules and ions to create functional, photonic materials has been the cornerstone of much research because of their structural rigidity, chemical stability, and rich photochemical and electrochemical properties. The facile modulation of the photonic properties of porphyrins[20, 24, 91] is accomplished both by the choice of metal ion and by the choice of substituents on the macrocycle. The placement of self-assembled/organized porphyrinoids on surfaces[45, 46, 49, 85, 92, 93] remains a key issue toward the use of these systems in materials and devices[43, 44] and scanning probe methods for both discerning functional properties and organization have been used.[94]

Although the focus of much of the research discussed herein is on nanoscaled materials[3, 5, 17, 43, 44, 47, 51, 71, 93] in which at least one dimension is less than a few manometers, some applications of porphyrinoids require larger, less defined structures such as nanoscaled colloids between about 100 and 600 nm for catalysis, or less well-defined or controllable surface structures. To date, the methods to self-assemble discrete multiporphyrinic systems of this size are limited, but aggregates of this size have been made and deposited on surfaces.[51] These particles exhibit enhanced catalytic activity and have novel photonic properties. The rapid advances in supramolecular chemistry, surface chemistry, and physical chemistry indicate that molecule-based materials have a bright future.

References:

1. Alivisatos, A. P.; Barbara, P. F.; Castleman, A. W.; Chang, J.; Dixon, D. A.; Klein, M. L.; McLendon, G. L.; Miller, J. S.; Ratner, M. A.; Rossky, P. J.; Stupp, S. I.; Thompson, M. E., *Adv. Mater.* **1998,** 10, (16), 1297–1336.
2. Tour, J. M., *Acc. Chem. Res.* **2000,** 33, (11), 791–804.
3. Lent, C. S., *Science* **2000,** 88, 1597-1599.
4. Fox, M. A., *Acc. Chem. Res.* **1999,** 32, (3), 201-207.
5. Ellenbogen, J. C.; Love, J. C., *Proc. IEEE* **2000,** 88, (3), 386-426.
6. Mauzerall, D. C., *Clin. Dermatol.* **1998,** 16, 195-201.
7. Adler, A. D.; Longo, F. R.; Shergalis, W., *J. Am. Chem. Soc.* **1964,** 86, (15), 3145-3149.
8. Lindsey, J. S., *Eds. Academic Press: New York* **2000,** 1, 45-118.
9. Drain, C. M.; Gong, X., *Chem. Commun* **1997**, 2117-2118.
10. Chou, J.-H.; Kosal, M. E.; Nalwa, H. S.; Rakow, N. A.; Suslick, K. S., *Eds. Academic Press: New York* **2000,** 6, 43-131.
11. Drain, C. M.; Hupp, J. T.; Suslick, K. S.; Wasielewski, M. R.; Chen, X., *J. Porphy. Phthalocyanines* **2002,** 6, (4), 241-256.
12. Chambron, J.-C.; Heitz, V.; Sauvage, J.-P., *Eds. Academic Press: New York* **2000,** 6, 1-42.
13. Valkova, L.; Borovkov, N.; Kopranenkov, V.; Pisani, M.; Bossi, M.; Rustichelli, F., *Mater. Sci. Eng.* **2002,** 22, (2), 167–170.
14. Valkova, L.; Borovkov, N.; Maccioni, E.; Pisani, M.; Rustichelli, F.; Erokhin, V.; Patternolli, C.; Nicolini, C., *Colloids Surf. A Physicochem. Eng. Asp*

2002, 198-200, 891- 896.

15. Lange, S. J.; Nie, H.; Stern, C. L.; Barrett, A. G. M.; Hoffman, B. M., *Inorg. Chem.* **1998,** 37, (25), 6435–6443.

16. Engelkamp, H.; Middelbeek, S.; Nolte, R. J. M., *Science* **1999,** 284, (5415), 785–788.

17. Burrell, A. K.; Wasielewski, M. R., *J. Porphy. Phthalocyanines* **2000,** 4, (5), 401- 406.

18. Fabbrizzi, L.; Licchelli, M.; Pallavicini, P., *Acc. Chem. Res.* **1999,** 32, (10), 846– 853.

19. Wagner, R. W.; Lindsey, J. S.; Seth, J.; Palaniappan, V.; Bocian, D. F., *J. Am. Chem. Soc.* **1996,** 118, (16), 3996–3997.

20. Mines, G. A.; Tzeng, B. C.; Stevenson, K. J.; Li, J.; Hupp, J. T., *Angew. Chem, Int. Ed. Engl.* **2002,** 41, (1), 154-157.

21. Rakow, N. A.; Suslick, K. S., *Nature* **2000,** 406, 710-713.

22. Andrew, R.; Seiji, S., *Coord. Chem. Rev.* **2000,** 205, (1), 157-199.

23. Sun, S.-S.; Lees, A. J., *Coord. Chem. Rev.* **2002,** 230, (1-2), 170–191.

24. Wosnick, J. H.; Swager, T. M., *Chem. Biol.* **2000,** 4, (6), 715-720.

25. Diskin-Posner, Y.; Dahal, S.; Goldberg, I., *Angew. Chem., Int. Ed. Engl.* **2000,** 39, (7), 1288–1292.

26. Diskin-Posner, Y.; Patra, G. K.; Goldberg, I., *Eur. J. Inorg. Chem.* **2001,** 10, (2515-2523).

27. Goldberg, I., *Cryst. Eng. Commun.* **2002,** 4, 109-116.

28. Kumar, R. K.; Diskin-Posner, Y.; Goldberg, I., *J. Incl. Phenom. Macrocycl.*

Chem. **2000,** 37, 219-230.

29. Lu, X.; Jin, J.; Kang, J.; Lv, B.; Liu, H.; Geng, Z., *Mater. Chem. Phys.* **2003,** 77, (3), 952–957.

30. Ikeda, A.; Ayabe, M.; Shinkai, S.; Sakamoto, S.; Yamaguchi, K., *Org. Lett.* **2000,** 2, (23), 3707–3710.

31. Johnston, M. R.; Latter, M. J.; Warrener, R. N., *Org. Lett.* **2002,** 4, (13), 2165-2168.

32. Lehn, J.-M., *Proc. Natl. Acad. Sci.U. S. A* **2002,** 99, (8), 4763–4768.

33. Lehn, J.-M., *Angew. Chem., Int. Ed. Engl.* **1990,** 29, 1304-1319.

34. Lehn, J.-M., *Pure Appl. Chem.* **1994,** 66, (10/11), 1961–1966.

35. Lawrence, D. S.; Jiang, T.; Levett, M., *Chem. Rev* **1995,** 95, (6), 2229–2260.

36. Moulton, B.; Zaworotko, M. J., *Chem. Rev.* **2001,** 101, (6), 1629–1658.

37. Nguyen, S. T.; Gin, D. L.; Hupp, J. T.; Zhang, X., *Proc. Natl. Acad. Sci. U.S.A* **2001,** 98, (21), 11849–11850.

38. Tabellion, F. M.; Seidel, S. R.; Arif, A. M.; Stang, P. J., *J. Am. Chem. Soc.* **2001,**123, (31), 7740–7741.

39. Whitesides, G. M.; Simanek, E. E.; Mathias, J. P.; Seto, C. T.; Chin, D. N.; Mammen, M.; Gordon, D. M., *Acc. Chem. Res.* **1995,** 28, (1), 37–44.

40. Aakeroy, C. B.; Seddon, K. R., *Chem. Soc. Rev.* **1993**, 397–407.

41. Desiraju, G. R., *Acc. Chem. Res.* **2002,** 35, (7), 565–573.

42. Drain, C. M., *Proc. Natl. Acad. Sci. U. S. A.* **2002,** 99, 5178-5182.

43. Drain, C. M.; Batteas, J. D.; Flynn, G. W.; Milic, T.; Chi, N.; Yablon, D. G.; Sommers, H., *Proc. Natl. Acad. Sci.U.S.A.* **2002,** 99, 6498–6502.

44. Milic, T. N.; Chi, N.; Yablon, D. G.; Flynn, G. W.; Batteas, J. D.; Drain, C.M *Angew.Chem., Int. Ed. Engl.* **2002,** 41, 2117–2119.

45. Ishida, A.; Majima, T., *Chem. Commun.* **1999**, 1299-1300.

46. Kong, D.-S.; Wan, L.-J.; Han, M.-J.; Pan, G.-B.; Lei, S.-B.; Bai, C.-L.; Chen, S.- H., *Electrochim. Acta* **2002,** 48, (4), 303–309.

47. Imae, T.; Niwa, T.; Zhang, Z., *J. Nanosci. Nanotechnol.* **2002,** 2, (1), 37–40.

48. Oberg, K.; Eliasson, B., *Mater. Lett* **2001,** 49, (3-4), 147–153.

49. Sarno, D. M.; Grosfeld, D.; Jiang, B.; Afriyie, J. O.; Matienzo, L. J.; Jones, W. E., Jr, *Langmuir* **2000,** 16, (15), 6191–6199.

50. Drain, C. M.; Shi, X.; Milic, T.; Nifiatis, F., *Chem. Commun.* **2001**, 287–288.

51. Gong, X.; Milic, T.; Xu, C.; Batteas, J. D.; Drain, C. M., *J. Am. Chem. Soc.* **2002,** 124, (48), 14290–14291.

52. Kwok, K. S.; Ellenbogen, J. C., *Moletronics: Mater.Today* **2002,** 5, (2), 28–37.

53. Merlau, M. L.; Mejia, M. D. P.; Nguyen, S. T.; Hupp, J. T., *Angew. Chem. Int. Ed. Engl* **2001,** 40, (22), 4239–4242.

54. Borovkov, V. V.; Lintuluoto, J. M.; Sugeta, H.; Fujiki, M.; Arakawa, R.; Inoue, Y., *J. Am. Chem. Soc.* **2002,** 124, (12), 2993–3006.

55. Ogawa, K.; Zhang, T.; Yoshihara, K.; Kobuke, Y., *J. Am. Chem. Soc.* **2002,** 124, (1), 22–23.

56. Aratani, N.; Osuka, A.; Kim, Y. H.; Jeong, D. H.; Kim, D., *Angew. Chem., Int. Ed. Engl.* **2000,** 39, (8), 1458–1462.

57. Aratani, N.; Osuka, A., *Org. Lett.* **2001,** 3, (26), 4214–4216.

58. Ambroise, A.; Wagner, R. W.; Rao, P. D.; Riggs, J. A.; Hascoat, P.; Diers, J.

R.; Seth, J.; Lammi, R. K.; Bocian, D. F.; Holten, D.; Lindsey, J. S., *Chem. Mater.* **2001,** 13, (3), 1023–1034.

59. Benites, M. D. R.; Johnson, T. E.; Weghorn, S.; Yu, L.; Rao, P. D.; Diers, J. R.; Yang, S. I.; Kirmaier, C.; Bocian, D. F.; Holten, D.; Lindsey, J. S., *J. Mater.Chem.* **2002,** 12, (1), 65–80.

60. Drain, C. M.; Christensen, B.; Mauzerall, D., *Proc. Natl. Acad. Sci. U. S. A.* **1989,** 86, 6959–6962.

61. Drain, C. M.; Mauzerall, D., *Bioelectrochem.Bioenerg.* **1990,** 24, 263–266.

62. Drain, C. M.; Fischer, R.; Nolen, E.; Lehn, J. M., *Chem. Commun.* **1993**, 243–245.

63. Drain, C. M.; Lehn, J. M., *Chem. Commun.* **1994**, 2313–2315.

64. Araki, K.; Wagner, M. J.; Wrighton, M. S., *Langmuir* **1996,** 12, (22), 5393–5398.

65. Guldi, D. M.; Pellarini, F.; Prato, M.; Granito, C.; Troisi, L., *Nano Lett* **2002,** 2, (9), 965–968.

66. Qian, D.-J.; Nakamura, C.; Miyake, J., *Chem.Commun.* **2001**, 2312–2313.

67. Imahori, H.; Arimura, M.; Hanada, T.; Nishimura, Y.; Yamazaki, I.; Sakata, Y.; Fukuzumi, S., *J. Am. Chem. Soc.* **2001,** 123, (2), 335–336.

68. Nishimura, N.; Ooi, M.; Shimazu, K.; Fujii, H.; Uosaki, K., *J. Electroanal.Chem.* **1999,** 473, (1-2), 75–84.

69. Imahori, H.; Hasobe, T.; Yamada, H.; Nishimura, Y.; Yamazaki, I.; Fukuzumi, S., *Langmuir* **2001,** 38, (9), 1257–1261.

70. Ashkenasy, G.; Kalyuzhny, G.; Libman, J.; Rubinstein, I.; Shanzer, A., *Angew.*

Chem., Int. Ed.Engl. **1999,** 38, (9), 1257–1261.

71. Foubert, P.; Vanoppen, P.; Martin, M.; Gensch, T.; Hofkens, J.; Helser, A.; Seeger, A.; Taylor, R. M.; Rowan, A. E.; Nolte, R. J. M.; Schryver, F. C. D., *Nanotechnology* **2000,** 11, (1), 16–23.

72. Latterini, L.; Blossey, R.; Hofkens, J.; Vanoppen, P.; De Schryver, F. C.; Rowan, A. E.; Nolte, R. J. M., *Langmuir* **1999,** 15, (10), 3582–3588.

73. Collings, P. J., *Liquid Crystals; Princeton University Press: Princeton, NJ,* **1990**.

74. Simon, J.; Bassoul, P.; Leznoff, C. C.; Lever, A. B. P., *Phthalocyanines: Properties and Applications; VCH: New York,* **1989,** 2.

75. Donnio, B.; Bruce, D. W., *In Structure and Bonding; Springer-Verlag: Berlin* **1999,** 95, 193-247.

76. Monobe, H.; Miyagawa, Y.; Mima, S.; Sugino, T.; Uchida, K.; Shimizu, Y., *Thin Solid Films* **2001,** 393, 217-224.

77. Shimizu, Y.; Matsuno, J.; Miya, M.; Nagata, A., *Chem. Commun.* **1994**, 2411-2412.

78. Patel, B. R.; Suslick, K. S., *J. Am. Chem. Soc.* **1998,** 120, 11802-11803.

79. Van Nostrum, C. F.; Nolte, R. J. M., *Chem. Commun.* **1996**, 2385- 2392.

80. Kugimiya, S.; Takemura, M., *Tetrahedron Lett.* **1990,** 31, 3157-3160.

81. Liu, C.-Y.; Pan, H.-L.; Fox, M. A.; Bard, A. J., *Science* **1993,** 261, 897-899.

82. Adams, D. M.; Kerimo, J.; Liu, C.-Y.; Bard, A. J.; Barbara, P. F., *J. Phys. Chem. B* **2000,** 104, 6728-6736.

83. Kimura, M.; Saito, Y.; Ohta, K.; Hanabusa, K.; Shirai, H.; Kobayashi, N., *J.*

Am. Chem. Soc. **2002,** 124, 5274-5275.

84. Burrows, H. D.; Gonsalves, A. M. R.; Leitao, M. L. P.; Miguel, M. d. G.; Pereira, M. M., *Supramol. Sci.* **1997,** 4, 241-246.

85. Zhang, Z.; Yoshida, N.; Imae, T.; Xue, Q.; Bai, M.; Jiang, J.; Liu, Z., *J. Colloid Interface Sci.* **2001,** 243, 382-387.

86. Lei, S. B.; Wang, C.; Yin, S. X.; Wang, H. N.; Xi, F.; Liu, H. W.; Xu, B.; Wan, L. J.; Bai, C. L., *J. Phys. Chem. B* **2001,** 105, 10838-10841.

87. Ohshiro, T.; Ito, T.; Buhlmann, P.; Umezawa, Y., *Anal. Chem.* **2001,** 73, 878-883.

88. Qui, X.; Wang, C.; Zeng, Q.; Xu, B.; Yin, S.; Wang, H.; Xu, S.; Bai, C., *J. Am. Chem. Soc.* **2000,** 122, 5550-5556.

89. Drain, C. M.; Mauzerall, D. C., *Biophys. J.* **1992,** 63, 1556-1563.

90. Drain, C. M.; Mauzerall, D. C., *Biophys. J.* **1992,** 63, 1544-1555.

91. Holten, D.; Bocian, D. F.; Lindsey, J. S., *Acc. Chem. Res.* **2002,** 35, (1), 57–69.

92. Sharma, C. V. K.; Broker, G. A.; Szulczewski, G. J.; Rogers, R. D., *Chem. Commun.* **2000**, 1023–1024.

93. Zhang, Z.; Imae, T., *Nano Lett.* **2000,** 1, (5), 241–243.

94. Thomas, P. J.; Berovic, N.; Laitenberger, P.; Palmer, R. E.; Bampos, N.; Sanders, J. K. M., *Chem. Phys. Lett.* **1998,** 294, (1-3), 229–232.

3.

COLLOIDAL PORPHYRIN NANOPARTICLES AS SUPRAMOLECULAR SYSTEMS

3. 1. Introduction

Porphyrins and their related macrocycles (phthalocyanines, corroles, and porphyrazines) are versatile organic compounds for supramolecular chemistry because of their topological diversity, minimal conformational flexibility, and well-established synthetic methods which enable the creation of a large number of derivatives with diverse functionalities.[1-3] Porphyrinoids are also ideal organic molecules for materials – especially photonics, sensors, and molecular sieves – because they are remarkably robust under a variety of conditions yet have optical and redox properties that can be readily fine-tuned *via* the choice of metal ion coordinated to the center of the macrocycle and by exocyclic moieties. Nature exploits these properties by using porphyrins to harvest solar energy, transfer electrons, and as redox catalysts.[4] Because of these properties and functions, the supramolecular chemistry of porphyrins in terms

of solid state structures *self-organized* by non-specific interactions such as dispersion forces combined with specific interactions such as coordination chemistry and hydrogen bonding continues to be of intense interest even after decades of research.[1, 5] This vigorousness is largely due to a better understanding of intermolecular forces mediated by specific interactions and to developments in synthetic and separation methodologies for the preparation of target macrocycles. Porphyrins can also be designed to *self-assemble* into discrete, predefined nano-architectures or arrays by using specific intermolecular interactions.[1] Though not *a priori* required, discrete systems usually utilize all available recognition or assembly motifs. Since the initial reports of discrete porphyrin nano-assemblies by electrostatic interactions,[6-9] hydrogen-bonding,[10-13] and coordination chemistry,[14, 15] there have been numerous reports on the properties of self-assembled porphyrin arrays.[1, 5]

There is a distinction between self-assembly and self-organization.[16] Self-assembly is intolerant of errors and results in discrete (mono-dispersed) supramolecular arrays, albeit with varying yields. For example, the absence of a porphyrin unit in a self-assembled square array is a fatal flaw because the product is not square and has significantly different dynamic, thermodynamic, and photonic properties. Self-organization, on the other hand, is more tolerant of defects and results in non-discrete systems with varying dispersity. For example the absence of a monomer unit from a large coordination polymer slightly alters the dimensions but not the overall structure and usually not the properties. An exception to the latter is represented by the imidazolyl polymers of Kobuke et. al.[17-19] The supramolecular structure of any material can be delineated, as in structural biology, by four levels of hierarchical

organization.[16] The primary structure describes the monomeric units and the algorithms of molecular recognition – in the present case the porphyrin serves as the core platform. The supramolecular architectures formed by self-assembly/organization are the secondary structures. Tertiary structures result from the self-organization of the supramolecular entities into solid-state materials, thin films, and colloids. The quaternary structure includes the interactions between the supramolecular materials and their environment, e.g. surfaces/matrices of the supports, thus include the interconnections with the macroscopic world.

Of course there is overlap between the various levels of organization and structure, but these concepts aid in the design of functional supramolecular materials. Self-organized systems can be used to construct colloids and to achieve maximal surface area or deployment of chromophores, such as for use as catalysts and functional coatings on surfaces. Discrete supramolecular systems are almost always less than about 10 nm. Crystals and most solid-state structures of both discrete and polymeric supramolecular systems have dimensions from microns to many millimeters. Thus there is a void between the 3-10 nm arrays and the micron to millimeter crystals and polymers that may be filled by melding the concepts and methods of supramolecular chemistry, colloid chemistry, and surface chemistry.[5] Part of our hypothesis is that supramolecular systems of porphyrins and related macrocycles with 5-500 nm dimensions will yield materials that will exhibit catalytic, photonic, and sensor properties that are unobtainable by either the molecular compounds or the macroscopic solids. At present the general goal is to understand and define the principles and conditions that may lead to the construction of supramolecular

nanostructures of high structural integrity and provide effective algorithms for the design – by self-organization – of supramolecular materials of this intermediate, 5–500 nm scale. For the formation of 5-500 nm materials from supramolecular polymers and other aggregates of porphyrins, the key issue is how to stabilize and isolate systems of the desired dimensions with acceptable polydispersity and in high yields.[5]

There are three basic strategies for the stabilization of nanoscaled supramolecular materials. (1) The use of stabilizing agents that are either grafted onto the porphyrin monomers or added into the solution can prevent agglomeration of the nanoparticles and result in stable colloidal dispersions.[20] (2) Kinetically trapping self-organizing materials can remove them from the conditions that allow equilibrium – usually by removing the solvent. Practically this often means isolating the nanoparticles on a surface and/while removing them from solution.[15, 16, 20-28] (3) Adjusting the environmental conditions to favor or force the formation of nano aggregates by, for example, encapsulation into a solid[29] or a gel matrix.[30-33] Each of these strategies has advantages and disadvantages, depending on the intended function and application of the material.

3. 2. Applications of Porphyrin Nanoparticles

The advantages of self-organizing particles over self-assembled entities arise from the use of commercially available dyes and pigments, ease of preparation, and material stability.[20] There are a variety of possible applications of nanoparticles of organic

chromophores that derive from the photonic properties of both the component molecule and the nanoscaled dimensions of the particle.[2, 3, 5, 28, 34]

Many of these nanoparticles, when the porphyrin contains a redox-active transition metal (e.g. Fe, Co, Mn), are more efficient catalysts on a per porphyrin basis than the individual porphyrins in solution or individual porphyrins adsorbed onto supports.[20] An understanding of nanoparticles surface interactions can be exploited to dictate the size of the deposited nanoparticles.[21, 22, 34] For example, 50 nm diameter nanoparticles of hydrophilic porphyrins can be deposited onto glass surfaces passivated with a monolayer of organic 'grease' without further aggregation or falling apart; conversely, these nanoparticles de-aggregate into 5-20 nm particles and 5 nm high disks on hydrophilic glass surfaces. The fluorescence properties of nanoparticles containing the free base or closed-shell metalloporphyrins, or the phosphorescence of these or other metallo derivatives such as the Pd(II) and Pt(II) can be exploited for sensors and displays.[35-37]

Since our initial report on the formation of nanoparticles of hydrophilic and hydrophobic porphyrins,[20] there has been a large body of work on the formulation of drug nanoparticles. The advantages of <60 nm diameter aggregates of drugs are manifold, including the reduction or elimination of isomorphic solid state structures, increased rate of bio-availability, and possible functionalization of the stabilizer for targeted cell delivery.[38]

3. 3. Preparation of Porphyrin Nanoparticles

The formation of nanoscaled colloidal particles of hydrophobic porphyrins such as 5,10,15,20-tetraphenylporphyrin (TPP), 5,10,15,20-tetratolylphenylporphyrin (TTP), 5,10,15,20-tetratbutylphenylporphyrin (TtbutylPP), 5,10,15,20-tetramethoxyphenylporphyrin (TMPP), 5,10,15,20-tetracarboxyphenylporphyrinmethylether (TCPP-ME), 5,10,15,20-tetraoctyloxyphenylporphyrin (TOOPP), 2,3,7,8,12,13,17,18-octaethylporphyrin (OEP), 5,10,15,20-Tetrakis(pentafluorophenyl)porphyrin (TPPF20) and many of their metallo derivatives can be accomplished by adding water (guest solvent) to a solution of a hydrophobic porphyrin in THF, DMSO, DMF (host solvent) with a few percent of a low molecular weight PEG (MW=164) such as $HO(C_2H_4O)_3CH_3$ [20, 39] (Scheme 3. 1.).

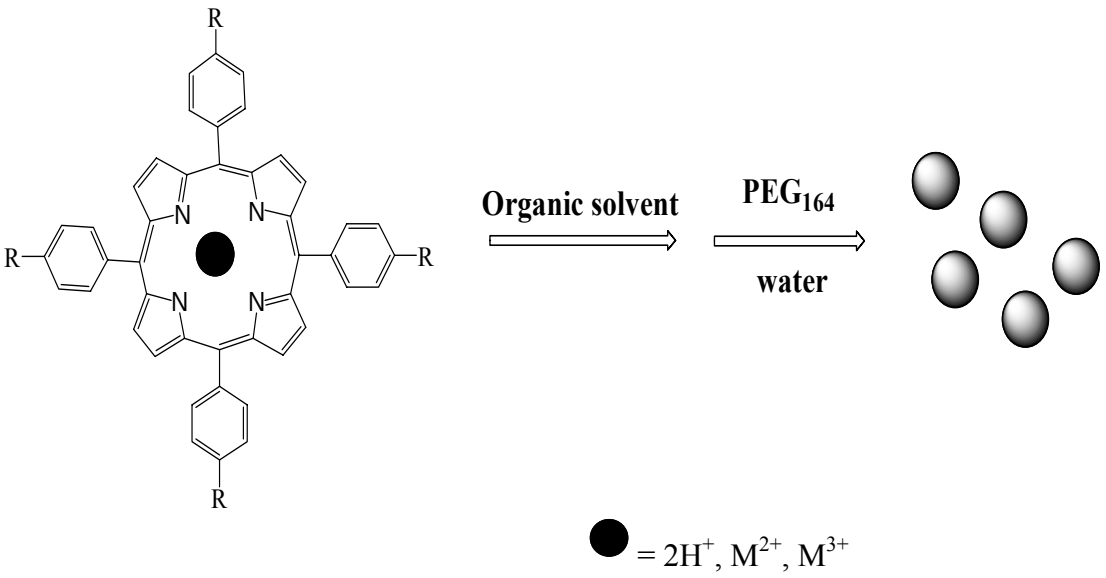

R = H, CH_3, $C(CH_3)_3$), OCH_3, $COOCH_3$, $O(CH_2)_7CH_3$, Ethyl or aryl groups are C_6F_5

Scheme 3. 1. Preparation of porphyrin nanoparticles

See Appendix for the preparation and characterization of 17 different porphyrins and metalloporphyrins nanoparticles.

Stabilizers such as PEG are essential for the formation of stable colloidal systems by host/guest solvent methods; reports on nanoparticles systems of porphyrinoids without this component are misleading or inaccurate since the porphyrins rapidly and quantitatively precipitate.[40] Other inquiries into the formation and activity of nanoparticles of dyes such as phthalocyanines have been reported.[40-43]

The mixed solvent approach is an efficient means to make large quantities of nanoparticles colloids (5 nm – 150 nm) of a variety of porphyrins. In terms of scale-up, the particle size and distribution of batches using 20 g of porphyrin correlate well with the small batches of 20 mg.

Porphyrin concentration, solvent, solvent ratios, amount of stabilizer, mixing speed, and temperature are significant processing variables that dictate the size and stability of the nanoparticles. The complex interplay amongst the various intermolecular interactions between solute, solvent, and stabilizer are difficult to predict de novo. Free base porphyrins generally need less stabilizer and less vigorous mixing compared to their metalloporphyrin analogues to form stable colloidal suspensions. For example, Zn(II)TPP requires about twice the PEG stabilizer as the free base TPP and sonication rather than vortex mixing. This observation can be heuristically explained by the increased intermolecular forces between the metalloporphyrins compared to the free bases. In this case, Zn(II) porphyrins generally have an increased proclivity to pi-stack compared to the free base analogues.

Conversely, the free base pyrroles N and N-H may participate in hydrogen bonding to the solvent, and in the case of nanoparticles, to the stabilizer.

Macrocycle symmetries, dipoles, and exocyclic moieties are important as well. The perfluorophenyl groups of 5,10,15,20-tetra-(2,3,4,5,6-pentafluorophenyl)porphyrin, ($TPPF_{20}$) are widely recognized to impart stability to redox catalysts of the metallo derivatives,[44-46] and to enhance the luminesce properties of especially the Pd(II) and Pt(II) species in applications such as organic LEDs and oxygen sensors.[35-37]

Since $TPPF_{20}$ is of wide interest we focus on some of the variables that affect colloid size and stability of this compound. $TPPF_{20}$ forms stable nanoparticles under a wide variety of conditions: stabilizer type and concentration, host solvents, and solvent/water ratios. One reason for the wide range of processing conditions that yield stable colloids of $TPPF_{20}$ may be attributed to the unique solvation properties of the perfluoro-phenyl moieties. The effect of various groups on TPP derivatives on particle size and stability is also discussed for comparison.

Changes in the peripheral substituents on the porphyrin can have dramatic effects on the resultant nanoparticles size even when using identical preparative methods. Nanoparticles of 17 different porphyrins and metalloporphyrins bearing a wide range of functional groups have been prepared by mixing solvents techniques.[20, 39] (See Appendix)

Batch-to-batch consistency for a given porphyrin is demonstrated by dynamic light scattering (DLS) data which shows that each macrocycle results in a specific particle size with a specific dispersity for a given method [39] (See Appendix). Small changes in

the structure of the substituents on the macrocycle can have profound consequences in particle size. *E.g.* for TPP derivatives, when the 4-phenyl position bears an H ~22 nm diameter particles are formed, when it bears a methyl group ~120 nm particles result, but the presence of methoxy group at the same position affords ~70 nm diameter particles. The metal ion within the macrocycle plays a role in determining particle size. [Fe(III)TPP]Cl^-, Co(II)TPP, and [Mn(III)TPP]Cl^-, yield 80 nm, 56 nm and 98 nm diameter particles, respectively.

Thus the metal oxidation state and the presence of counter ions are also important. It is likely that similar preparative methods will result in formation of nanoparticles of many other porphyrins, metalloporphyrins and other dyes, but that the size, stability, and physical chemical properties will vary with each.[41, 42]

In addition to molecular structure, different preparative procedures also dictate particle size and stability.[20] The choice of miscible solvent, the ratio of host to guest solvent, and the rate of mixing of the two solutions, also can dictate particle size. It should be noted that not all variations in the procedures result in stable dispersions for a give porphyrin. An important consideration pertaining to metalloporphyrins is the nature of the counter ion when the oxidation state of the central metal is greater than two.

3. 4. Characterization of Porphyrin Nanoparticles

3. 4. 1. Structure

The detailed structure inside these nanoparticles remains unknown. Densely packed, a 100 nm diameter particle of TPP (1.75nm x 1.75nm x 1nm ~3nm^3) can contain up to ~164,000 porphyrins, but density studies and the catalytic activities of the iron porphyrins indicate that there are far fewer molecules in the aggregate. Our working hypothesis is that the nanoparticles consist of sub-domains of the macrocycles and solvent/stabilizer-filled voids or channels of unknown size and distribution, so that the number of chromophores per nanoparticle is substantially less. The structural organization of the porphyrins within the nanoparticles likely depends on the specific structure of the macrocycle used because this dictates the intermolecular interactions between the porphyrins, the solvent, and the stabilizer. Results from assays designed to probe the functional size of the domains in colloidal nanoparticles of 5,10,15,20-tetratolylporphyrin (TTP), in terms of energy/electron transfer, indicate that domains of 15-25 porphyrins act cooperatively to harvest light energy and effect electron transfer to a Fe(III)TPP acceptor. Two well-established methods were used: (i) varying the mole ratios of an acceptor dopant, and (ii) examining the optical cross section by varying the light intensity.[47]

The caveat is that the antenna domain size may or may not correlate well with the physical domain size. The presence of subdomains is also consistent with AFM studies that reveal that some porphyrin nanoparticles fall apart into smaller 5-10 nm

high particles on surfaces and the observation that 5-10 nm diameter nanoparticles can be prepared by sonicating the solutions as they are mixed (See Appendix). These smaller particles can contain up to 20 and 160 porphyrins, respectively and surface deposition studies indicate they are more robust than the much larger colloidal particles.

3. 4. 2. Optical Properties

The UV-Vis. spectra of porphyrin nanoparticles are significantly different compared to the spectra of the corresponding porphyrin solutions. Soret bands are found to be broadened and/or split. The arrangement of macrocycles in aggregates generally fall into two types, "J" (edge-to-edge) interactions are characterized by red shifts, and "H" (face-to-face) interactions are characterized by blue shifts.[48] The optical spectra suggest both types of interactions in the nanoparticles and are well understood to be indicative of electronic coupling of the chromophores. The extent of J versus H aggregation depends on the specific porphyrin used. These spectra are consistent with other nanoscaled porphyrin aggregates, e.g. those encapsulated in MCM-41.[29]

The aggregation of porphyrins generally results in the quenching of the fluorescence by a variety of factors such as shading the inner chromophores from light irradiation, and energy transfer and concomitant branching pathways for deactivation.[49-51]

Preliminary results from steady-state fluorescence measurements indicate that many of the freebase nanoparticles that are <150 nm in diameter are anomalously luminescent. Comparison of the fluorescence intensity of non-aggregated porphyrins in toluene to the same porphyrin concentration in the form of colloidal nanoparticles in water, show that the latter intensity is reduced by only 20-50%. Notably, the luminescence of 140 nm diameter particles of $TPPF_{20}$ in water is nearly that of the same concentration of the fully solvated $TPPF_{20}$. This luminescence likely arises from the small ~ 10 nm diameter domains within the particles, rather than from the entire particle. The luminescence of the ~10 nm sub-domains is then analogous to the bright luminescence of nanoscaled aggregates of hydrophilic porphyrins[29, 50, 51] and those encapsulated in zeolite-types of materials.[52, 53] Time resolved luminescence studies of the free base and Zn(II) nanoparticles may further reveal the mechanism of luminescence, domain size, and quantum efficiency.

3. 5. Particles Stability and Dynamics

Particle stability was assayed by both DLS and UV-Vis over time on batches of nanoparticles stored as they were made in closed vials in the dark in air. As noted above, the exact procedure used to prepare the nanoparticles depends on the specific porphyrin, but conditions were found that resulted in colloids that were stable for at least a month for a range of substituted macrocycles (See Appendix). Many preparations are stable for more than a year. The nanoparticle solutions can be diluted

and somewhat concentrated, but cannot be dried as this leads to irreversible agglomeration.

An inter-nanoparticle material exchange assay was designed to examine the stability of porphyrinic nanoparticles in the presence of other porphyrinic nanoparticles. In addition to examining the dynamics of particle-particle interactions, these studies were designed to assess the feasibility of using solutions with two different porphyrinic nanoparticles. The manifold applications of solutions containing two different porphyrinic nanoparticles include: (1) two different catalytic processes may be achieved concomitantly, (2) one nanoparticle is used as a sensor for the catalytic product(s) of another nanoparticle, (3) when the different luminescent properties (e.g. lifetime and/or wavelength) of two or more nanoparticles are needed. Nanoparticles of free base TTP with an average particle diameter of 120 nm were mixed with nanoparticles of Fe(III)TPP with an average particle diameter of 80 nm. Two methods to assay material exchange were used.

DLS indicates no changes in the two particle sizes or dispersities over the course of two weeks. A second assay monitors the fluorescence of free base TTP nanoparticles in the presence of non-luminescent Fe(III)TPP nanoparticles. Because the free base luminescence is quenched by electron transfer from the TTP to the Fe(III)TPP, any change in fluorescence intensity of this mixture over time would indicate that porphyrins form the two types of nanoparticles had exchanged. (Nanoparticles composed of both chromophores exhibit significantly reduced luminescence, vide supra.) The fluorescence is observed to be constant for at least six days, indicating no dynamic exchange of porphyrins between particles. (Figure 3. 1.)

This is expected because of the PEG stabilizer and the water of hydration inhibit interactions between the particles and prevent agglomeration and precipitation.

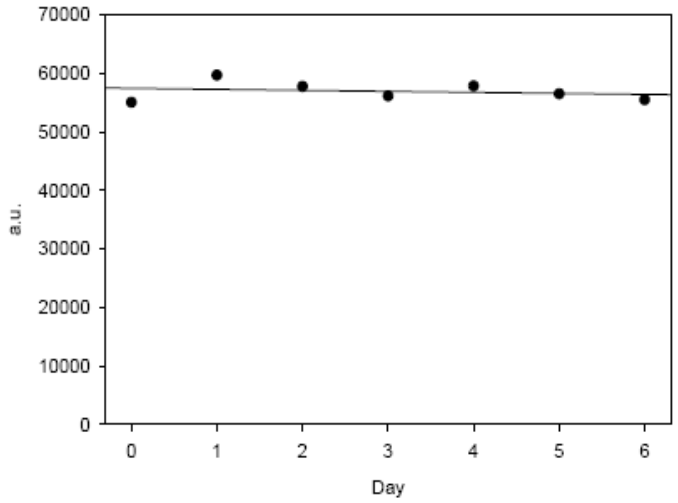

Figure 3. 1. The fluorescence intensity of a 1:1 mixture of Fe(III)tetratolylporphyrin nanoparticles and free base TPP nanoparticles remains constant for six days, indicating no exchange of porphyrins between the two types of nanoparticles. This also shows that the nanoparticles of TPP fluoresce (~50% of the same concentration in THF and same instrumental conditions) -- S. Patel Data

3. 6. Characterization and Preparation of $TPPF_{20}$ colloids

As mentioned above, colloidal nanoparticles of $TPPF_{20}$ are of interest because of the diverse photonic and catalytic applications. Various factors that dictate the particle size, dispersity, and stability of a variety of porphyrin nanoparticles were examined, and the results for $TPPF_{20}$ are illustrative of general trends. Note that the particle size and stability depends on the structure of the porphyrin/metalloporphyrin, the exact

preparative procedures, and conditions in which they are examined (e.g. in solution, concentration, on a surface).

3. 6. 1. Stabilizer

Different stabilizers were chosen to study the effects the molecular weight and molecular properties of this component on the particle size and stability. In general, porphyrins bearing only hydro- or fluoro- carbon groups (e.g. $TPPF_{20,}$ TPP, TTP) tend to from nanoparticles with sizes and distributions that are modestly dependent on the exact chemical structure and concentration of the stabilizer (Table 3. 1., Figure 3. 2.). Conversely, porphyrins with polar functional groups (e.g. *meso* pyridyl groups, and hydroxy, carboxy, amino, or sulfonatto groups on the phenyl) exhibit a greater range of particle size with different kinds and amounts of the stabilizer.

Table 3. 1. Stabilizer effects on nanoparticle size -- X.Gong and S.Patel data

Stabilizer	TPP[1] (average diameter, nm)	$TPPF_{20}$[1] (average diameter, nm)
Without stabilizer[2]	200-300	140-185
$HO(CH_2CH_2O)_3CH_3$	25	162
$HO(CH_2CH_2O)_4CH_3$	30	181
$HO(CH_2CH_2O)_6H$	--	182
$HO(CH_2CH_2CH_2O)_3CH_3$	--	168
PEG400	colloids not formed	152
$(CH_2OCH_2CH_2NH_2)_2$	232	234
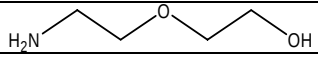	214	112
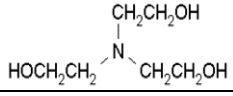	260	98

[1] Preparation method: 50 μL stabilizer was added to 0.4 mL of stock solution in DMSO (1.22 mM for TPP and 0.039 mM for $TPPF_{20}$), followed by adding 5 mL water with vigorous mixing. [2]There is large batch-to-batch variability and these solutions are unstable since the porphyrins precipitate after a couple of days. The preparations with TPP precipitate in less than 24 hrs. $HO(CH_2CH_2O)_3CH_3$ = triethyleneglycolmonomethylether (TriEGMe); $HO(CH_2CH_2O)_4CH_3$ = tetrethyleneglycolmonomethylether (TetraEGMe); $HO(CH_2CH_2O)_6H$= hexaethyleneglycol (HEG); $HO(CH_2CH_2CH_2O)_3CH_3$ = tripropyleneglycolmonomethylether (TriPGMe)

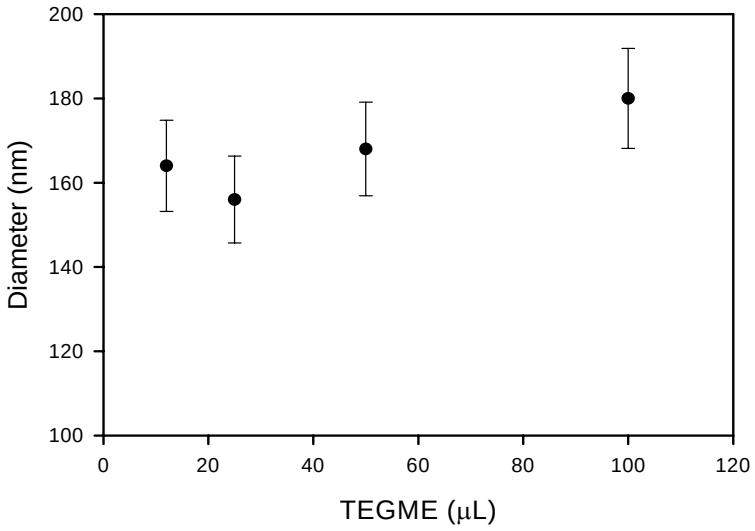

Figure 3. 2. DLS reveals the slight dependence of the size of $TPPF_{20}$ nanoparticles on TetraEGME stabilizer concentration. The graph shows the average of three trials with error bars representing the distribution of particle sizes. --X.Gong and S.Patel data

This latter observation is likely due to the stronger interactions between the solute and the solution components (host and guest solvents, and stabilizer). Thus for polar porphyrins it is possible to tune the sizes and morphology of particles over a greater range by changing the chemical nature and the quantity of the stabilizer. The complex intermolecular interactions between amphipathic molecules such as the polyethylene glycols with water, the polar host solvent, and the porphyrin solute are essential for the formation of stable colloids.

3. 6. 2. Temperature

As expected for a process dependent on intermolecular interactions, the temperature used during the preparation affects the particle size (Figure 3. 3.) in that the particles become ~25% smaller as the temperature used to the prepare the TPPF sample increases from 20° C to 100° C. Since the particle sizes of these preparations do not change for many weeks, the stabilizer must be preventing material exchange between nanoparticles and thus preventing re-equilibration towards the larger sized nanoparticles found at room temperature. Since increasing temperatures decreases the strength of the intermolecular interactions as well as the interactions between sub-domains, smaller particle sizes are expected. This kinetic trapping of nanoparticles is akin to what is observed for stacks of porphyrin nonamers.[15, 21, 22, 54]

3. 6. 3. Concentration

The widest range of particle sizes, about a factor of three for $TPPF_{20}$, can be achieved by varying the concentration of the macrocycle in the host solvent (Figure 3. 4.). The formation of the porphyrin nanoparticles likely represents a process governed by kinetics as well as the equilibrium of intermolecular interactions between all the components. The importance of kinetics is supported by the strong dependence of particle size on concentration in the host solvent. The nonlinearity in the plot of the data suggests that the formation of these nanoparticles is a complex process; note that the largest particles form at the lowest concentrations.

At the highest porphyrin concentration in the host solvent, there are some differences in the intermolecular interactions of the chromophores since a ~15% broadening of the Soret band is observed compared to the lowest concentration. The observed larger nanoparticles at lower concentrations may indicate that there is a minimum, critical aggregate size that nucleates the growth, and smaller particles eventually aggregate into larger ones.

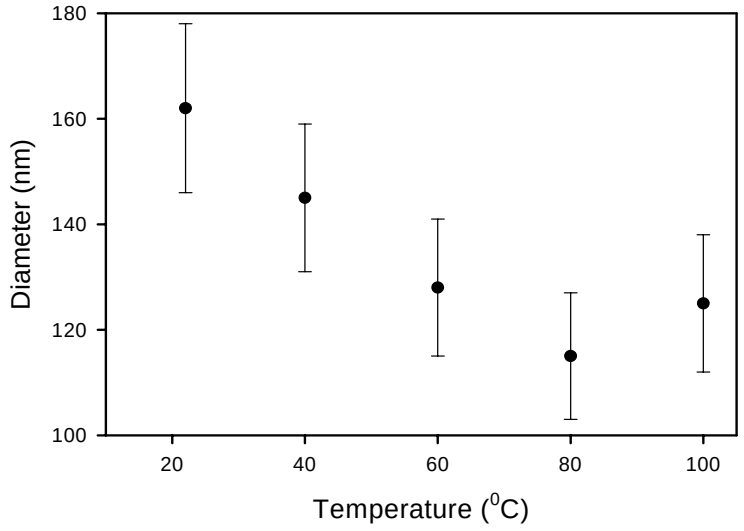

Figure 3. 3. The temperature during nanoparticle preparation affects the particle size. The DLS measurements were taken at 25 °C upon cooling and 24 hours after preparation. The graph shows the average diameters of three trials with error bars representing the distribution of particle sizes. -- X.Gong and S.Patel data

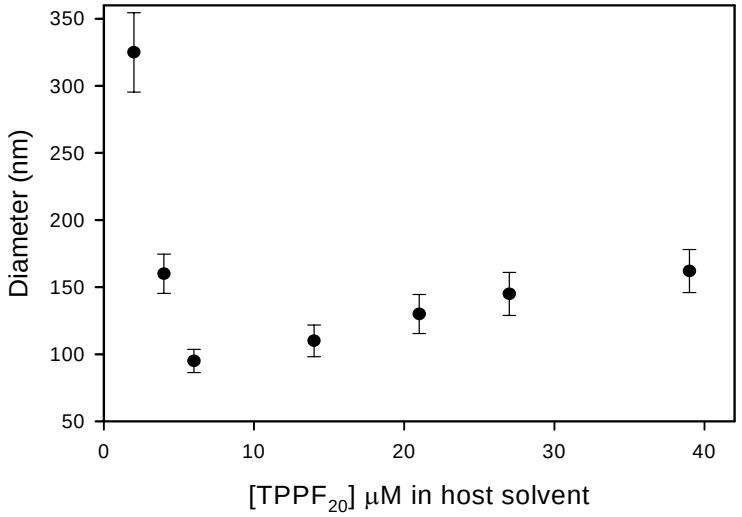

Figure 3. 4. The concentration of $TPPF_{20}$ in the DMSO host solvent strongly affects nanoparticle size as measured by DLS. The graph shows the average diameters of three trials with error bars representing the distribution of particle sizes. -- X.Gong and S.Patel data

3. 6. 4. Host/guest solvent ratio and intermolecular forces.

For the same considerations outlined above regarding the intermolecular forces between the components in the milieu (host solvent, guest solvent, stabilizer, and solute) the chemical properties of the host solvent can have profound effects on the size and stability of the porphyrin nanoparticles (Table 3. 2.). The favorable entropy of mixing the host solvent with the guest solvent and stabilizer, as well as any enthalpic contributions such as those arising from the formation of hydrogen bonds between host and guest solvents and between the guest solvent and solute, is countered by the strength of the interactions between the dye and the host solvent. Both dipolar interactions and hydrogen bonding between the various solvents (including the

stabilizer) and $TPPF_{20}$ are present. In addition to dipolar and H-bonding interactions, aromatic host solvents such as pyridine also afford π-π interactions with the macrocycle and the peripheral phenyl moieties.

The solubility of the dye in the host solvent, the guest solvent, and the stabilizer affect the particle size and dispersity. The observed trend, that the greater relative quantity of the host solvent to the guest solvent the smaller the particle size (Figure 3. 5.), is consistent with other nanoparticle preparations[20] and the diminished intermolecular interactions between solute molecules. Kinetics must also play a role here, since the diffusion/mixing the components in the mixture must be part of the agglomeration process. The greater the quantity of the host solvent results in less guest solvent to induce precipitation. Since the colloids are likely composed of sub-domains, the increased quantity of host solvent may reduce the magnitude of the inter-sub-domain interactions as well.

Table 3. 2. Effects of host solvent on the size of $TPPF_{20}$ nanoparticles

Host solvent	Nanoparticle size (average diameter, nm)
DMSO	162
DMF	166
Dimethylacetimide	400
THF	150
Pyridine	288

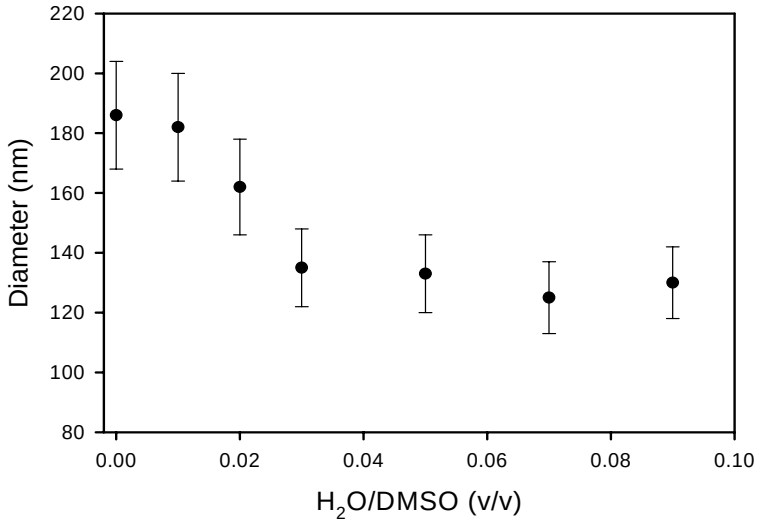

Figure 3. 5. The volume ratio of host solvent to guest solvent, DMSO to water in this case, affects $TPPF_{20}$ nanoparticle size as measured by DLS. The graph shows the average of three trials with error bars representing the distribution of particle sizes. -- X.Gong and S.Patel data

3. 6. 5. Mixing

The rate and efficiency of mixing the host and guest solvents have a profound effect on the size and stability of the porphyrinic nanoparticles – especially when metalloporphyrins are used. In general for a given derivative and using the same rate of addition, the greater the mixing the smaller the nanoparticles; however, we have not quantified mixing rates and efficiencies. The size of the colloidal particles of free base TPP decreases in the order: no stirring, a magnetic stir-bar with a vortex, a vortex mixer, and sonication. Conversely for $TPPF_{20}$ the rate of mixing has a smaller effect on particle size: stirring, vortex mixer, and sonication 140 nm, 100 nm, and 60 nm

diameters. To date we have found that for most metalloporphyrins stable particles are generally formed only when sonication is used.

3. 6. 6. Surfaces

The aforementioned data indicate that the interactions of the porphyrins within the subdomains are stronger than the interactions between the subdomains. Therefore, it should be possible to break up the ~100 nm diameter colloids into the subdomains by introducing an energetic perturbation that is greater than that holding the colloid together but less than that holding the molecules in the subdomains together.

Refluxing a solution of $TPPF_{20}$ nanoparticles formed at room temperature (see row 3 in Table 3. 1.) for 20 minutes and allowing the solution to cool produces nanoparticles that are 20-50 nm in diameter, and reassembly into the larger structures is not observed over the course of three days. The colloidal nanoparticles also can be induced to disassemble on surfaces that have a strong affinity for the constituent porphyrin and/or the solvents. AFM studies of nanoparticles of hydrophobic $TPPF_{20}$ deposited on hydrophobic glass surfaces reveal a distribution of 5-20 nm particles that are much smaller than the sizes observed in the colloidal dispersion. Conversely, AFM studies show that most of the colloidal nanoparticles of a hydrophilic porphyrin, tetra(N-alkylpyridinium)porphyrin^{4+} (water host solvent and THF guest solvent), remain in tact on hydrophobic surfaces (Table 3. 3.).

These observations also support the notion that the porphyrins in the sub-domains are held together by intermolecular interactions that are substantially greater than the forces holding the sub-domains together in the colloid. For surfaces with similar

hydrophobicities as the macrocycle and host solvent, as the solvent evaporates the colloids can disassemble to produce smaller, 5–20nm nanoparticles. These results indicate that tuning of surface energetics in terms of hydrophobicity can be used to dictate particles size. This observation also suggests that solvent flow and evaporation dynamics may enable the patterning of these small nanoparticles.

Samples were prepared by drop-deposition on freshly cleaved mica (0001) and cleaned glass slides. (See Appendix)

Table 3. 3. Average AFM heights of $TPPF_{20}$ colloids deposited onto hydrophilic glass surfaces

Stabilizer	Average diameter of colloids in solution by DLS	Average diameter of nanoparticles on glass by AFM (nm)
None	185	5 ± 40
$HO(CH_2CH_2O)_4H$	170	9 ± 4
$HO(CH_2CH_2O)_4CH_3$	180	30 ± 15
$HO(CH_2CH_2CH_2O)_3CH_3$	167	6 ± 4

3. 7. Conclusions

Recent reports on nanoparticles of other porphyrinoids, and nanoarchitectures with different morphologies such as nanotubes, have shown that the formation of nanostructured materials by self-organization is general. The hierarchical organization is dictated by both the molecules and by the preparative methods. The nanoscale size imparts functionalities unobtainable by the molecule or macroscopic material.[41, 42, 54-59]

The evaluation of the physical, chemical, and functional properties of nanoparticles of other dye systems will also provide a portal to materials that exhibit enhanced or new functionalities (e.g. catalytic, sensing, and luminescent) compared to the known properties of the component molecules, for example the free base and closed shell metalloporphyrin nanoparticles discussed above.

The variety of other complex porphyrinic materials with nanostructured features[5] indicates the richness of the possible structures that can be obtained using these ~1 nm rigid macrocycles appended with appropriate motifs for specific or non-specific supramolecular interactions. The richness of the supramolecular chemistry and the ability to kinetically trap the self-organized porphyrinic systems affords nanoscaled colloids of various sizes. Surfactants that form nanoscaled, metastable structures such as those used to form zeolites, trimethylcetylammonium bromide and Triton x-100, may well serve to template the formation of other nanoscaled tubular or rod-like architectures of porphyrins.[5] Since porphyrinic compounds are the basis of Photo Dynamic Therapy – which has a multi-billion dollar yearly market world wide – formulations of porphyrinic nanoparticles may significantly improve the delivery of these types of therapeutics.

3. 8. Appendix

Preparation and characterization of porphyrin nanoparticles [39]

All free bases and metallated nanoparticles were made by adding a large volume of an insoluble guest solvent (H_2O), while vigorously stirring it into a small volume of the porphyrin dissolved in a host solvent (e.g. THF, DMF, DMSO), mixed with some poly(ethylene glycol) derivative. Preparations were made in 10mL vials while sonicated. The formation and characterization of these nanoparticles are discussed using different techniques like UV-Vis, DLS and AFM (contact and tapping mode).

Our goal in all these preparations are 1) to find the right conditions to obtain porphyrin nanoparticles (guest solvent, stabilizer, concentrations, ratio guest/host solvent, order of adding the solutions) 2) the best method for preparation of stable porphyrin and metallated porphyrin nanoparticles 3) see how different metals or different external groups on porphyrins will affect particles sizes 4) find a good method to get smaller size nanoparticles for use in drug delivery 5) see how distribution/nanoparticles size will be affected by the surface (e.g. clean or unclean glass, mica)

All data for 17 porphyrin nanoparticles solutions : TPP(R = H), TtolylPP (R = CH_3), TbutylPP (R= $C(CH_3)_3$), TMPP (R = OCH_3), TCPP-ME (R = $COOCH_3$), TOOPP (R = $O(CH_2)_7CH_3$), OEPP (Octaethyl porphyrin), $TPPF_{20}$ (tetra C_6F_5 porphyrin) and their metallated correspondents are illustrated below.[39] The size of particles are in nm, diameter for DLS and H=horizontal (length) and V=vertical (height) for AFM.

Table 3. 4. TPP nanoparticles characterization

Structure	Absorption Spectrum
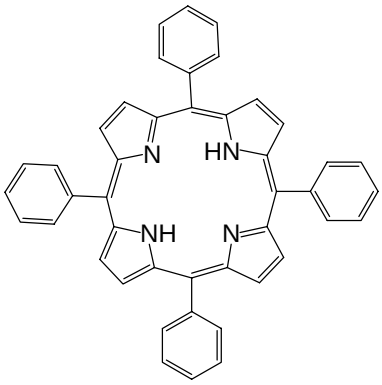	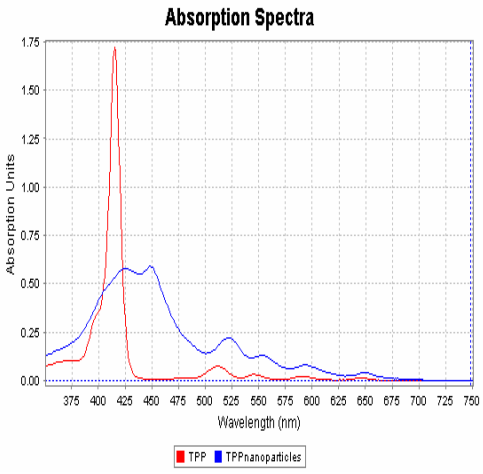
DLS histogram (diameter)	**AFM histogram**
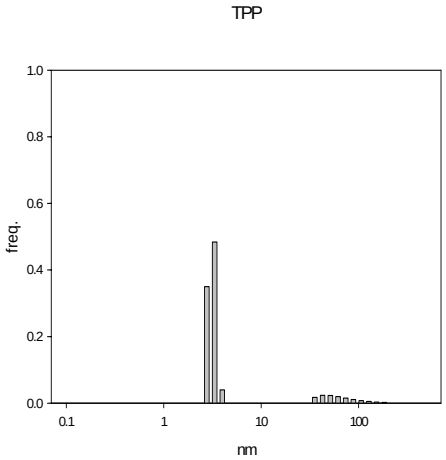	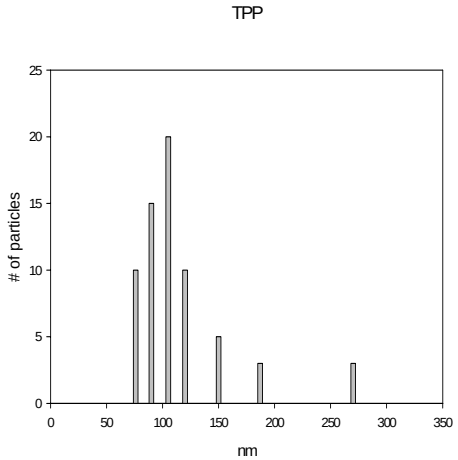
AFM image contact mode (glass)	**AFM image tapping mode (glass)**
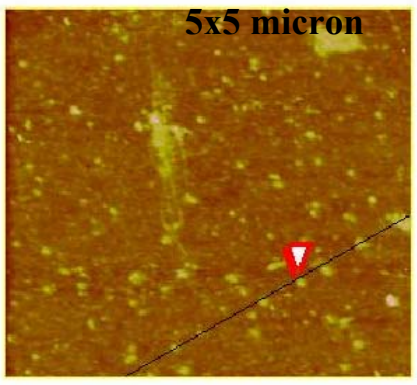	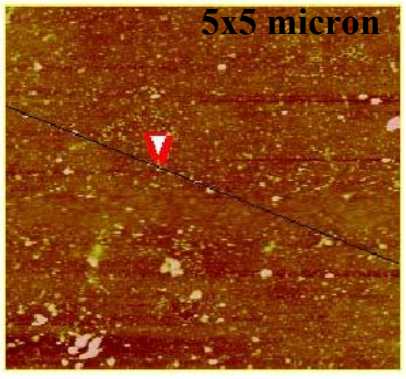
H: 90-170 nm V: 5-20 nm	**H: 70-100 nm V: 3-10 nm**

Table 3. 5. TtolylPP nanoparticles characterization

Structure

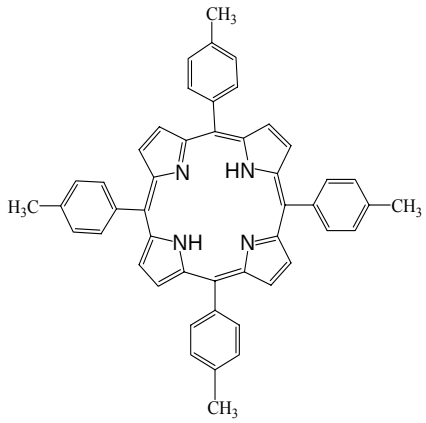

Absorption Spectrum

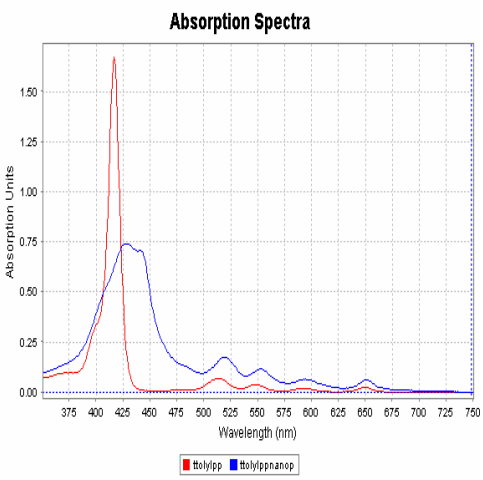

DLS histogram (diameter)

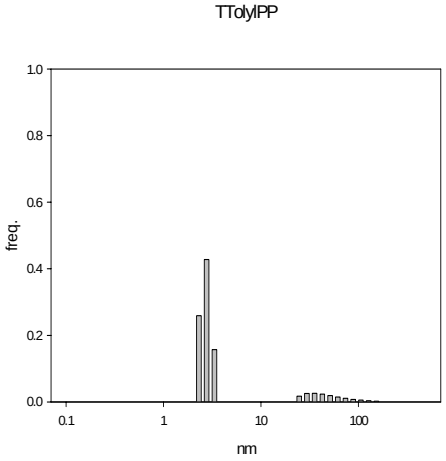

AFM histogram

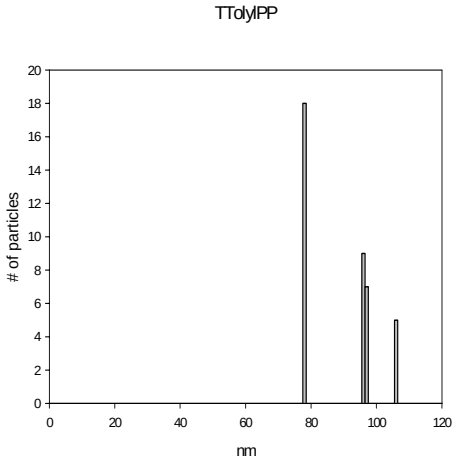

AFM image contact mode (glass)

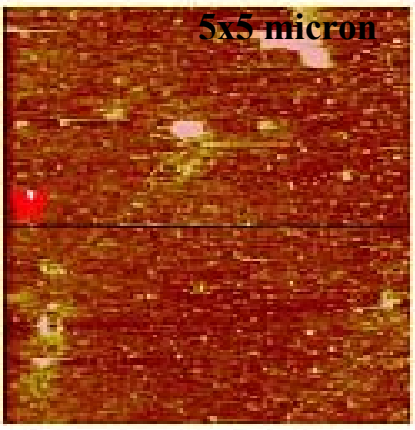

H:70 -200 nm V: 7-20 nm

AFM image tapping mode (glass)

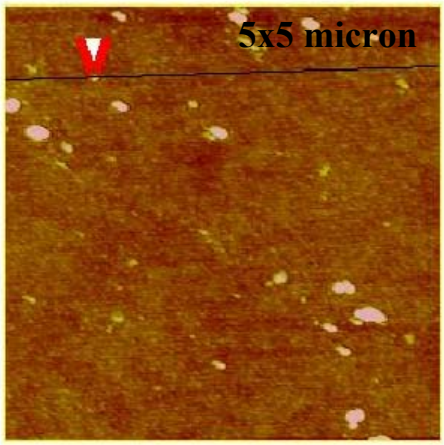

H: 70-150 nm V: 3-10 nm

Table 3. 6. TtbutylPP nanoparticles characterization

Structure

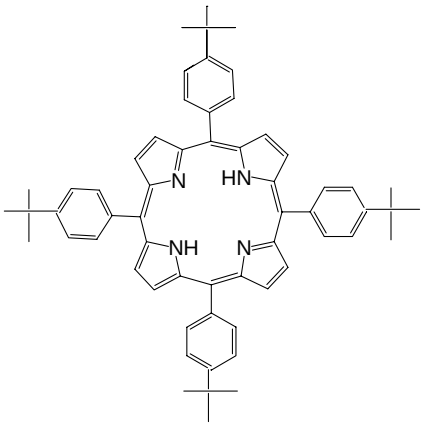

Absorption Spectrum

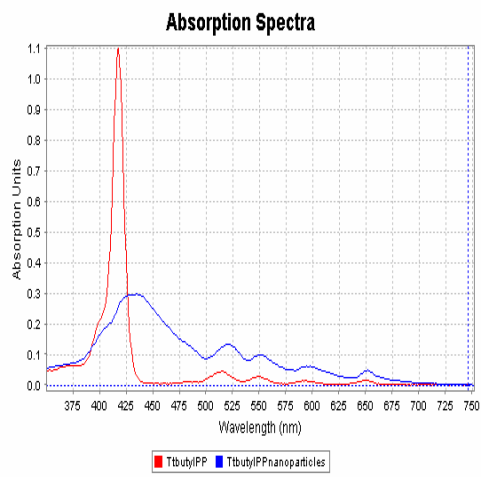

DLS histogram (diameter)

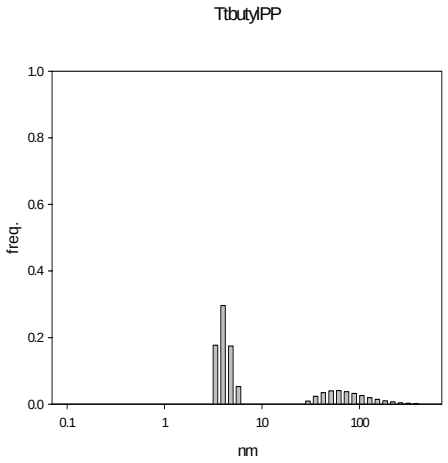

AFM histogram

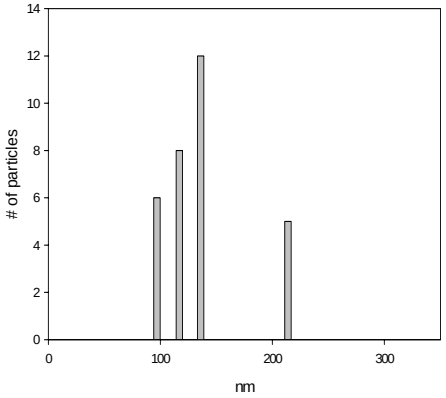

AFM image contact mode (glass)

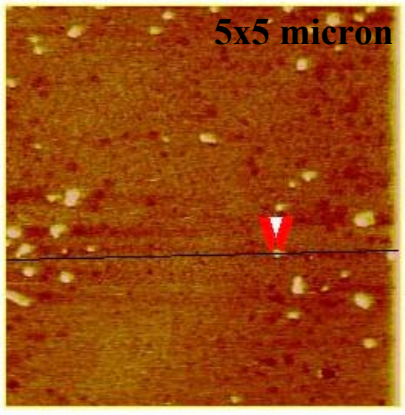

H: 120-200 nm V: 12-25 nm

AFM image tapping mode (glass)

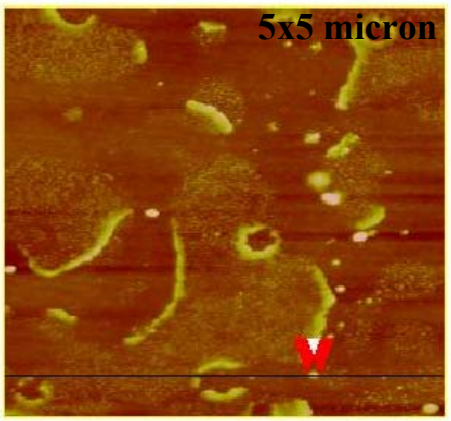

H: 90-140 nm V: 5-12 nm

Table 3. 7. $TPPF_{20}$ nanoparticles characterization

Structure

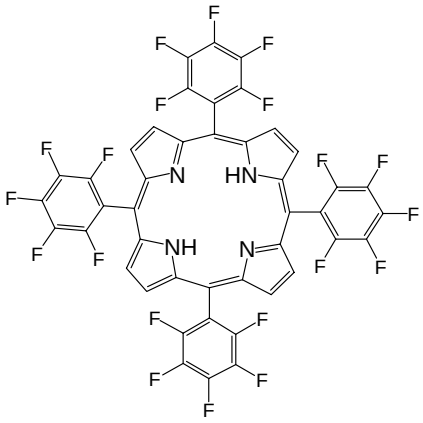

Absorption Spectrum

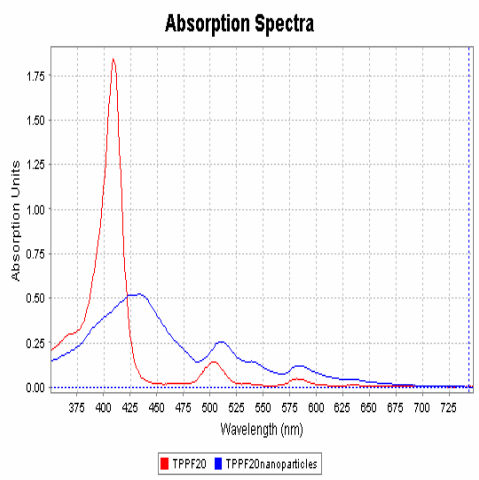

DLS histogram (diameter)

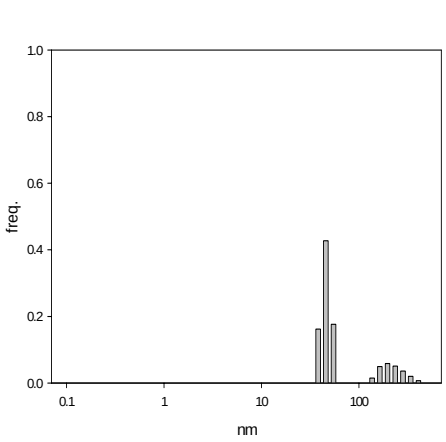

AFM histogram

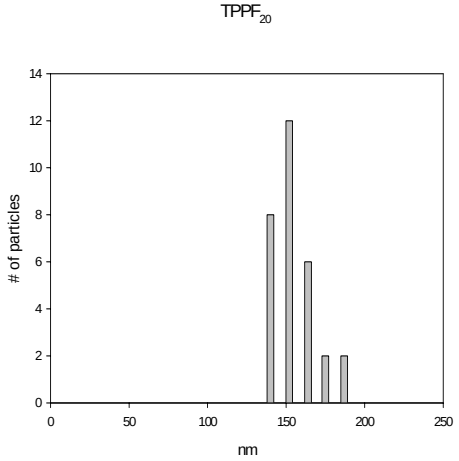

AFM image contact mode (glass)

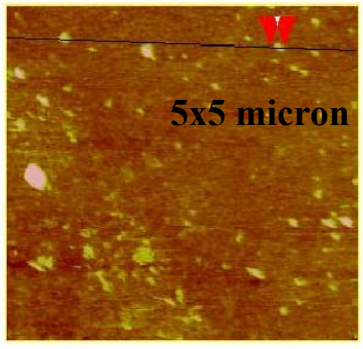

H: 120-200 nm V: 15-30 nm

AFM image tapping mode (glass)

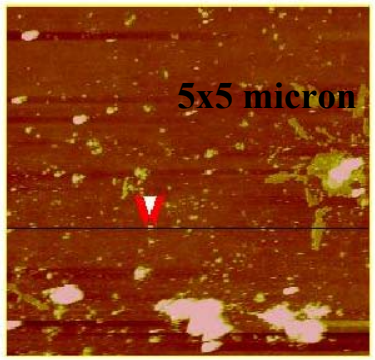

H: 70-120 nm V: 5-15 nm

Table 3. 8. TCPP Me nanoparticles characterization

Structure

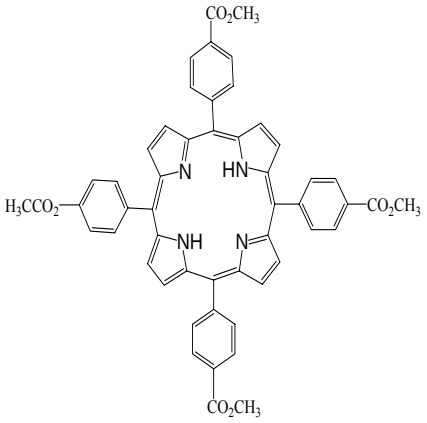

Absorption Spectrum

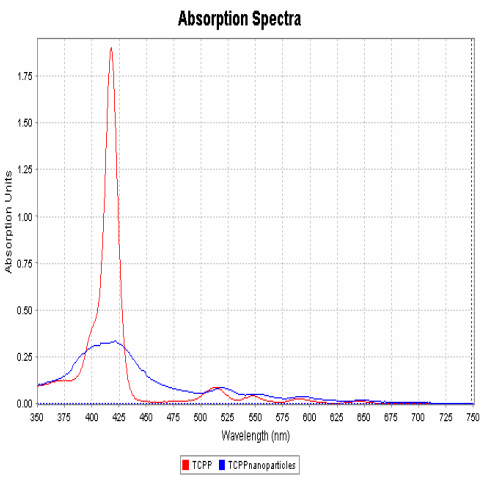

DLS histogram (diameter)

TCPP Me

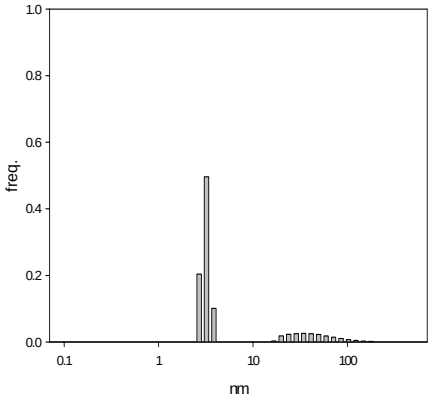

AFM histogram

TCPP Me

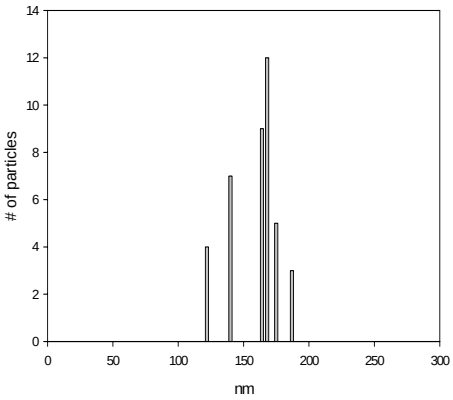

AFM image contact mode (glass)

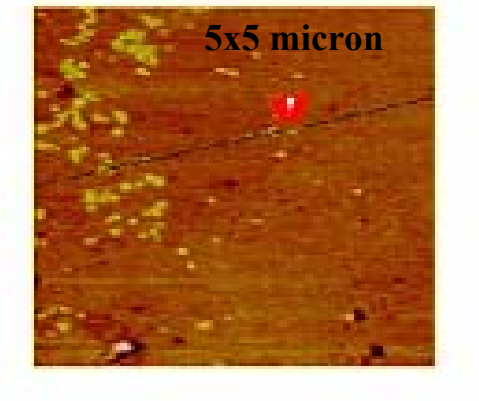

H: 93-140 nm V: 5-15 nm

AFM image tapping mode (glass)

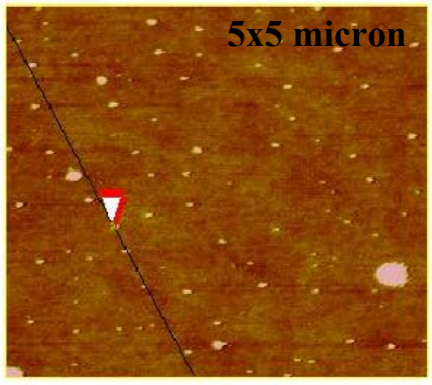

H: 50-100 nm V: 5-10 nm

Table 3. 9. TmethoxyPP nanoparticles characterization

Structure

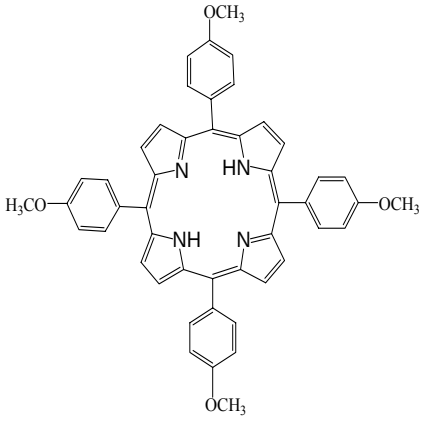

Absorption Spectrum

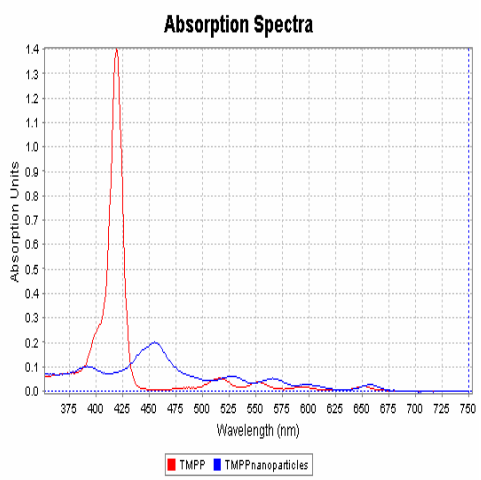

DLS histogram (diameter)

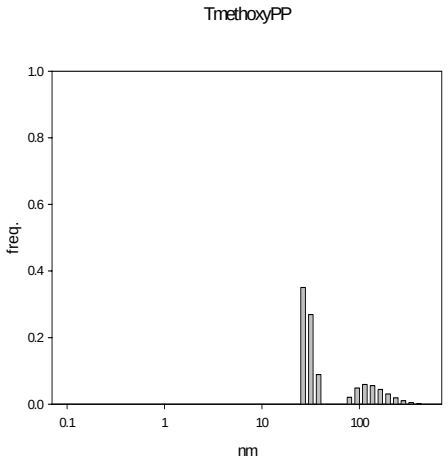

AFM histogram

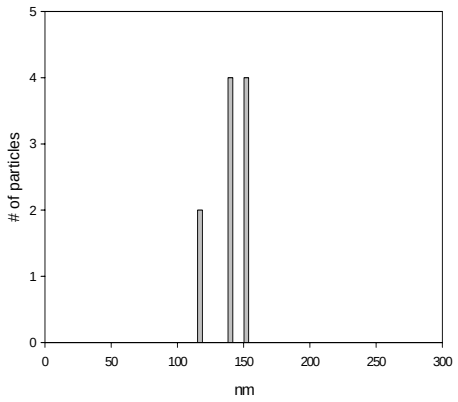

AFM image contact mode (glass)

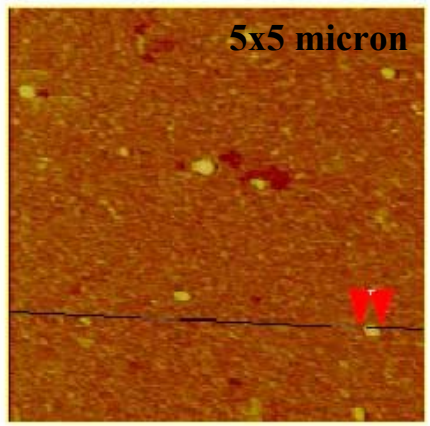

H: 105-200 nm V: 20-30 nm

AFM image tapping mode (glass)

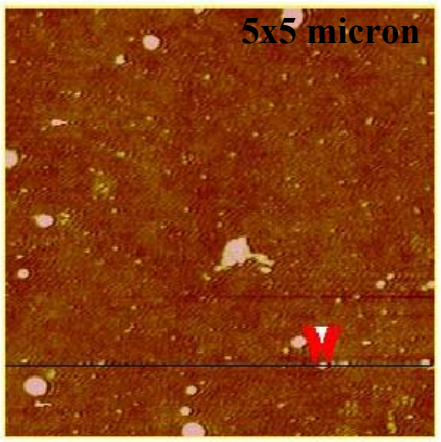

H: 70-120 nm V: 5-10 nm

Table 3. 10. ToctyloxyPP nanoparticles characterization

Structure

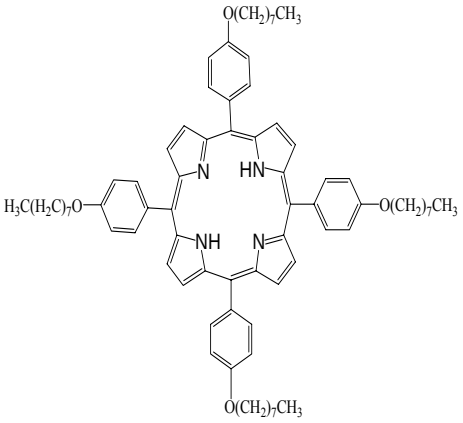

Absorption Spectrum

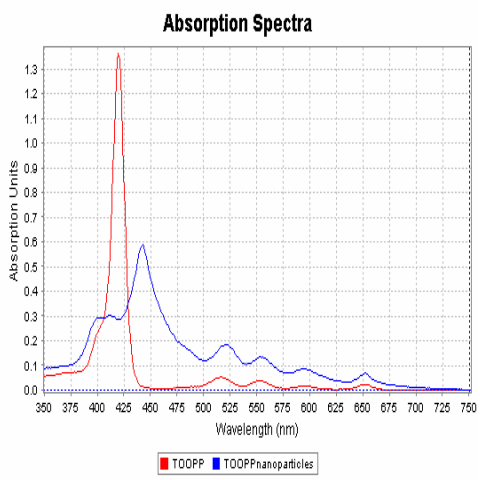

DLS histogram (diameter)

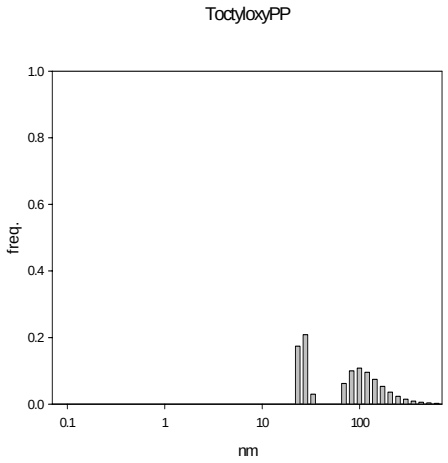

AFM histogram

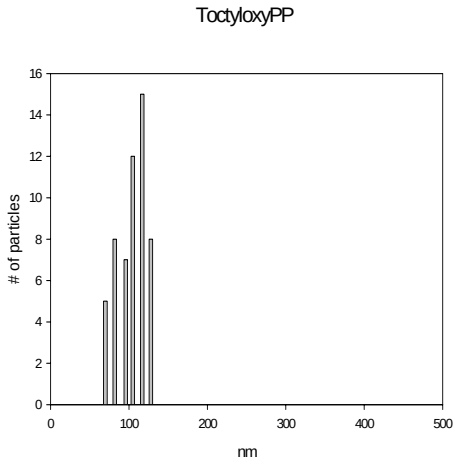

AFM image contact mode (glass)

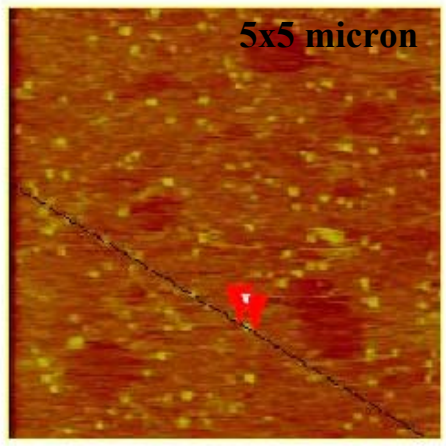

H: 70-130 nm V: 20-35 nm

AFM image tapping mode (glass)

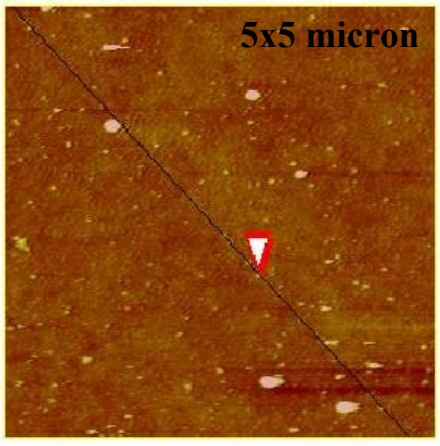

H: 50-100 nm V: 5-15 nm

Table 3. 11. OEP nanoparticles characterization

Structure

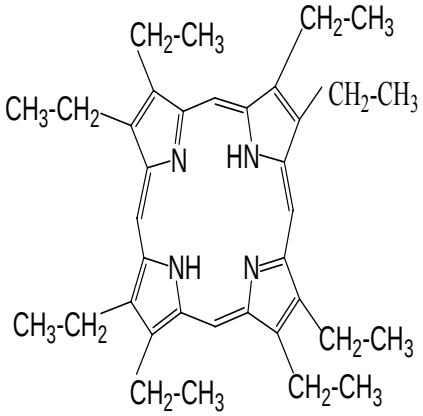

Absorption Spectrum

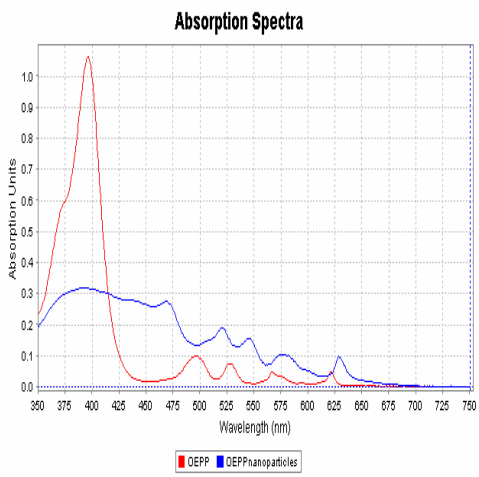

DLS histogram (diameter)

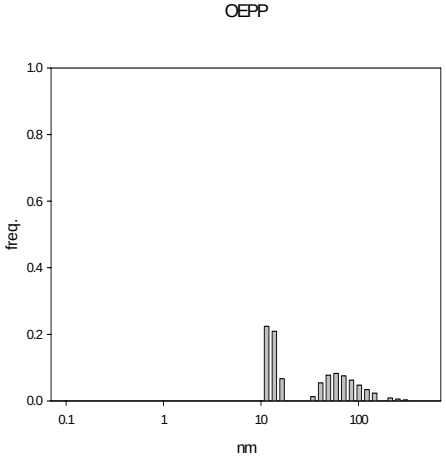

AFM histogram

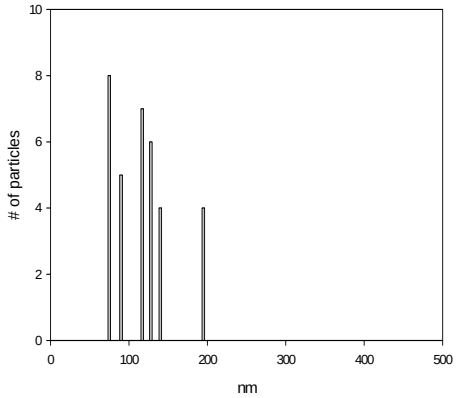

AFM image contact mode (glass)

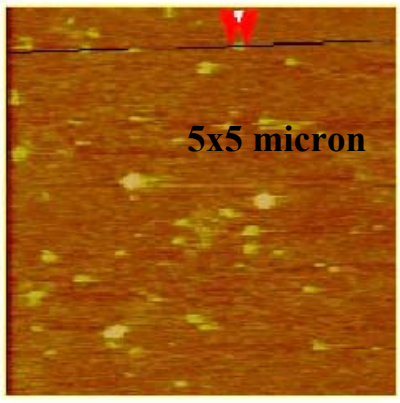

H: 93-140 nm V: 10-20 nm

AFM image tapping mode (glass)

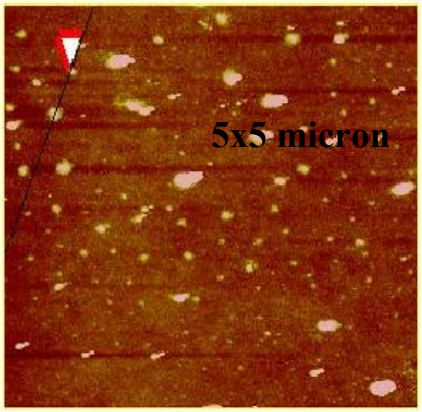

H: 90-120 nm V: 4-10 nm

Table 3. 12. Summary of free bases porphyrin nanoparticles characterization data

Compound	AFM contact	AFM tapping	DLS (diameter)
TPP	H: 90-170 nm V: 5-20 nm	H: 70-100 nm V: 3-10 nm	5-7 nm in THF 60-200 nm(solvent)
TtolylPP	H: 70 -200 nm V: 7-20 nm	H: 70-150 nm V: 3-10 nm	4-6 nm in THF 50-200 nm(solvent)
TtbutylPP	H: 120-200 nm V: 12-25 nm	H: 90-140 nm V: 5-12 nm	5-8 nm in THF 60-400 nm(solvent)
TPPF20	H: 120-200 nm V: 15-30 nm	H: 70-120 nm V: 5-15 nm	60-80 nm in THF 200-300 nm(solvent)
TmethoxyPP	H: 105-200 nm V: 20-30 nm	H: 70-120 nm V: 5-10 nm	40-60 nm in THF 90-300 nm(solvent)
TCPP Me	H: 93-140 nm V: 5-15 nm	H: 50-100 nm V: 5-10 nm	5-7 nm in THF 40-200 nm(solvent)
OEP	H: 93-140 nm V: 10-20 nm	H: 90-120 nm V: 4-10 nm	10-30 nm in THF 60-200 nm(solvent)
ToctyloxyPP	H: 70-130 nm V: 20-35 nm	H: 50-100 nm V: 5-15 nm	50-60 nm in THF 90-500 nm(solvent)

Table 3. 13. CoTPP nanoparticles characterization

Structure

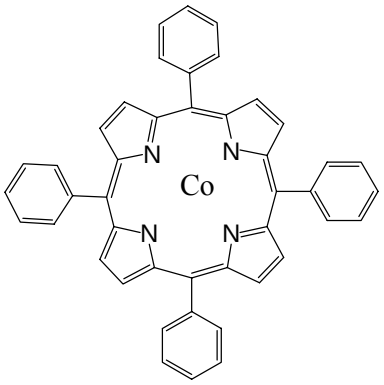

Absorption Spectrum

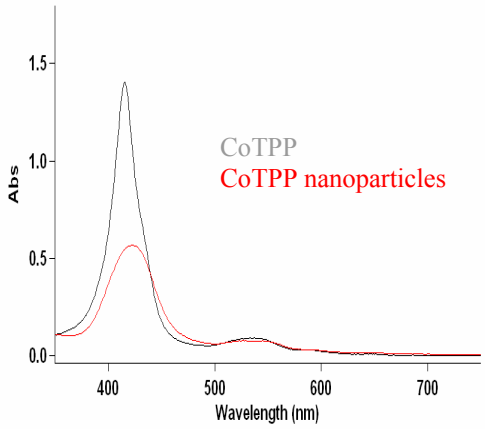

DLS histogram (diameter)

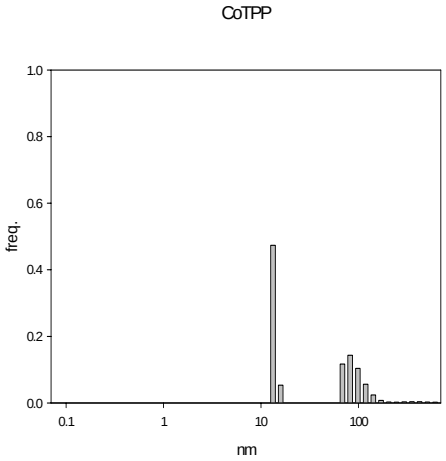

AFM histogram

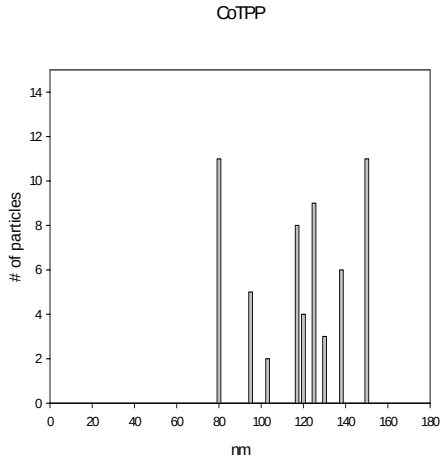

AFM image contact mode (glass)

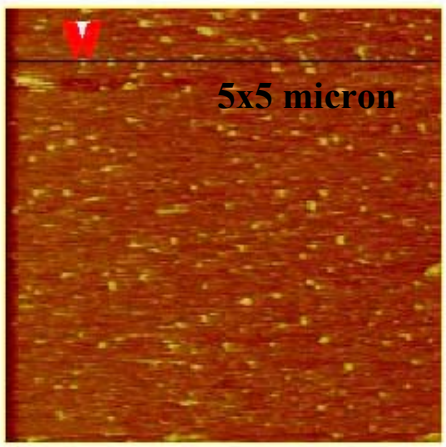

H: 80-117 nm V: 18-26 nm

AFM image tapping mode (glass)

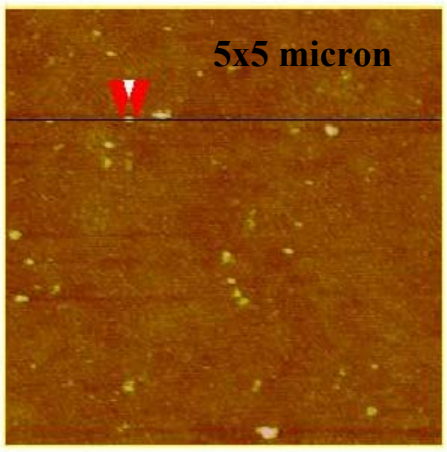

H: 80-150 nm V: 7-15 nm

Table 3. 14. ZnTPP nanoparticles characterization

Structure

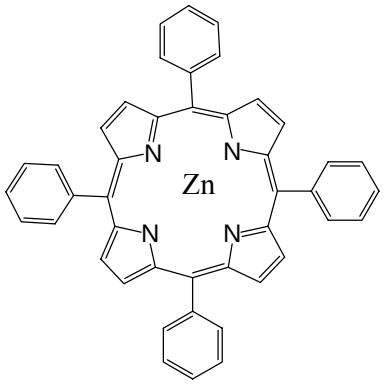

Absorption Spectrum

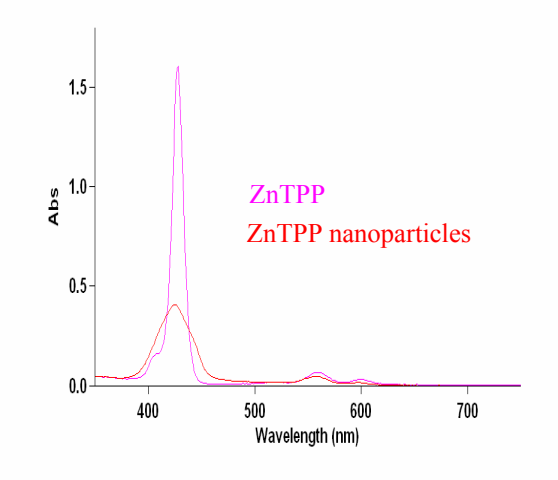

DLS histogram (diameter)

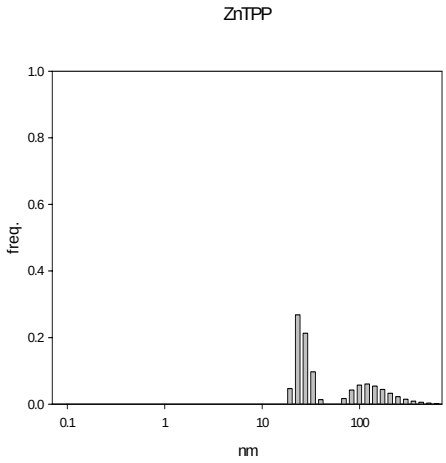

AFM histogram

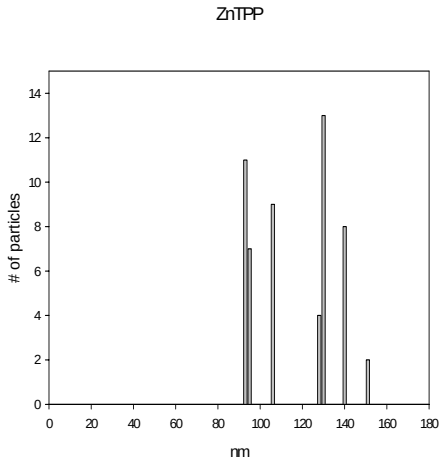

AFM image contact mode (glass)

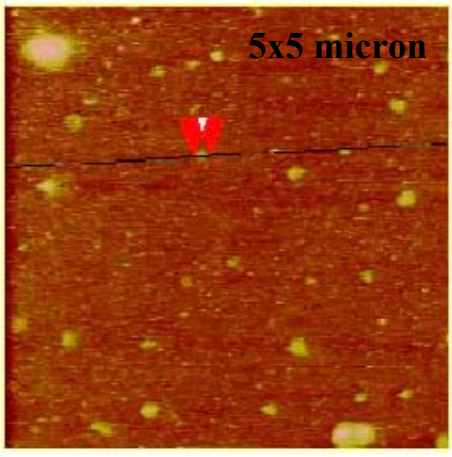

H: 95-130 nm V: 14-30 nm

AFM image tapping mode (glass)

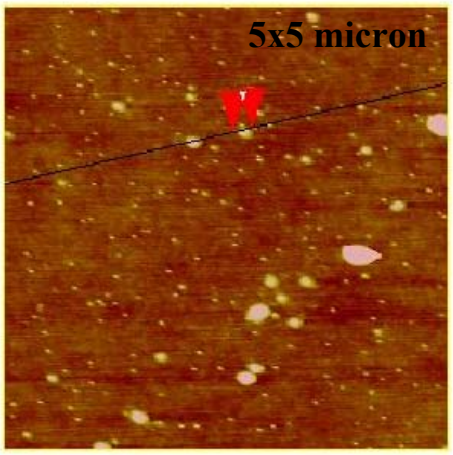

H: 93-140 nm V: 5-15 nm

Table 3. 15. FeTPP nanoparticles characterization

Structure

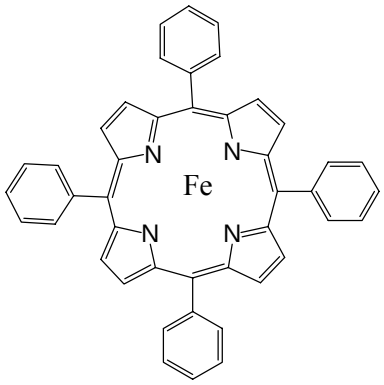

Absorption Spectrum

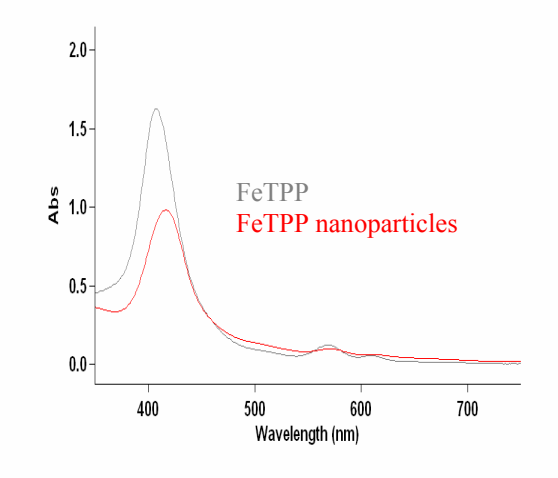

DLS histogram (diameter)

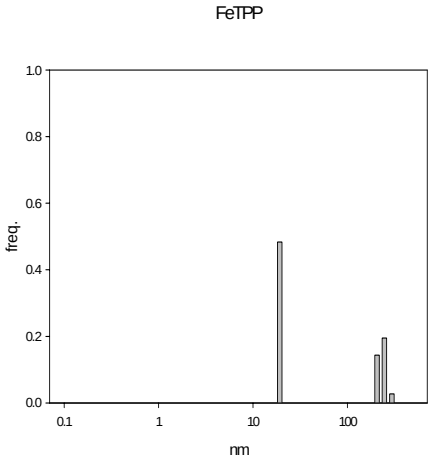

AFM histogram

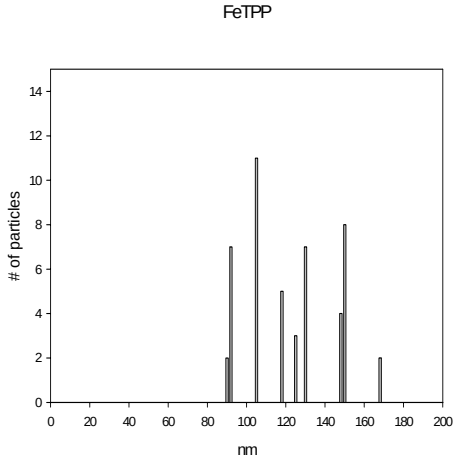

AFM image contact mode (glass)

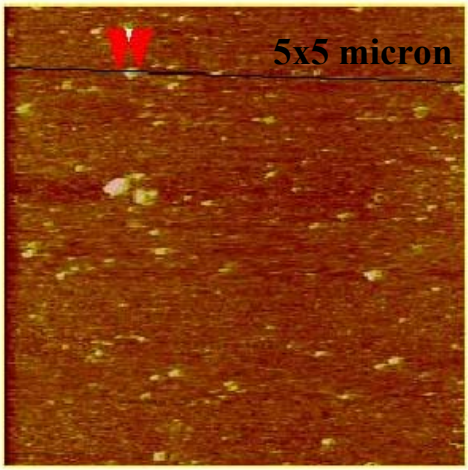

AFM image tapping mode (glass)

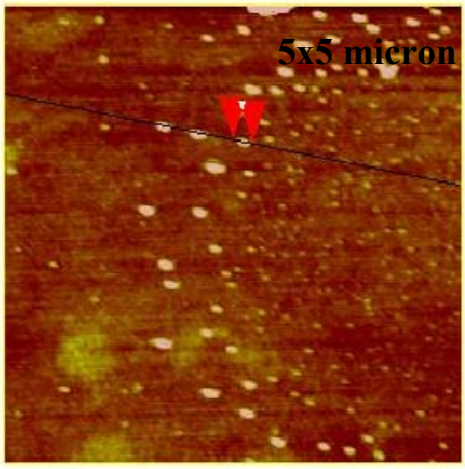

H: 105-130 nm V: 25-35 nm

H: 92-150 nm V: 4-10 nm

Table 3. 16. CoTTbutylPP nanoparticles characterization

Structure

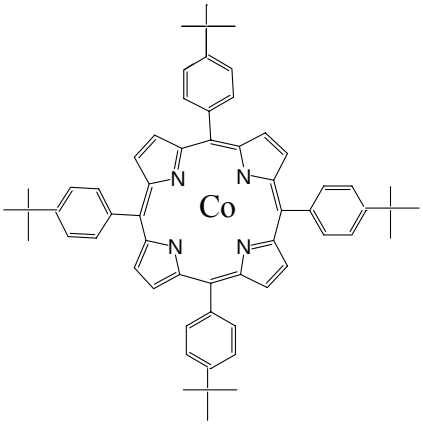

Absorption Spectrum

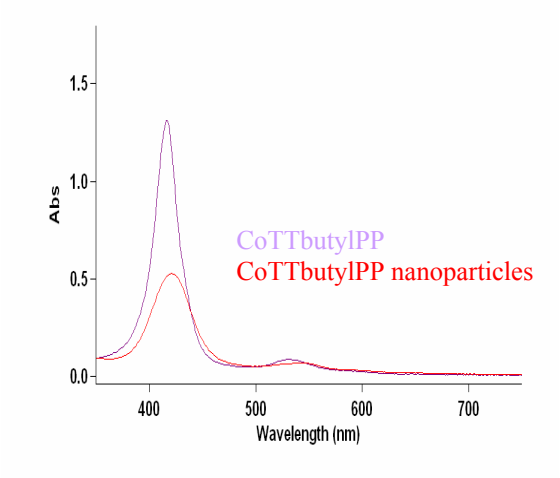

DLS histogram (diameter)

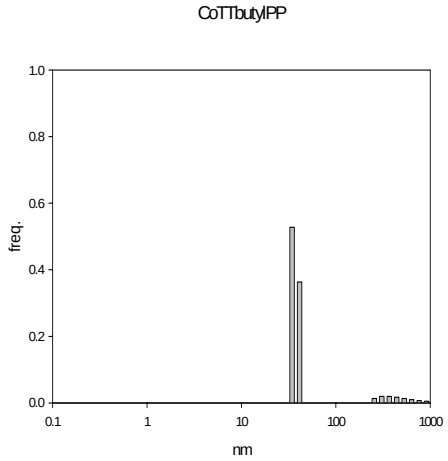

AFM histogram

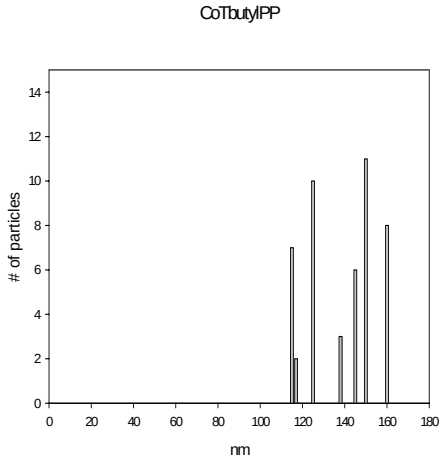

AFM image contact mode (glass)

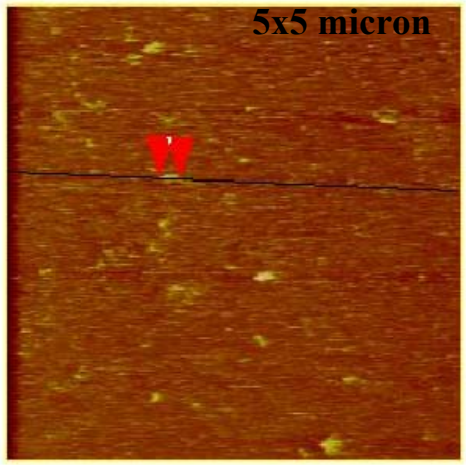

H: 125-160 nm V: 30-40 nm

AFM image tapping mode (glass)

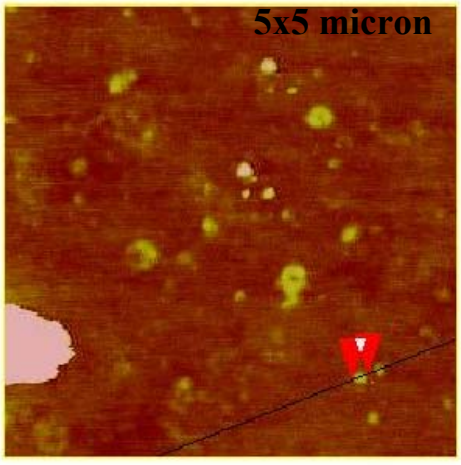

H: 117-150 nm V: 6-20 nm

Table 3. 17. ZnTTbutylPP nanoparticles characterization

Structure

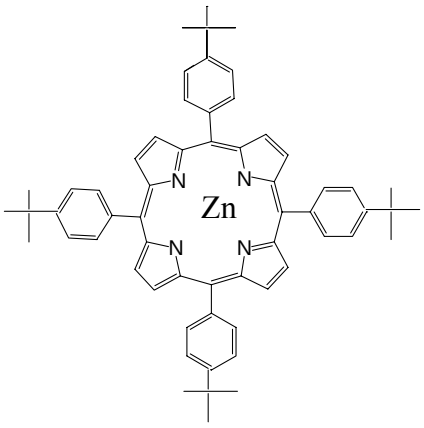

Absorption Spectrum

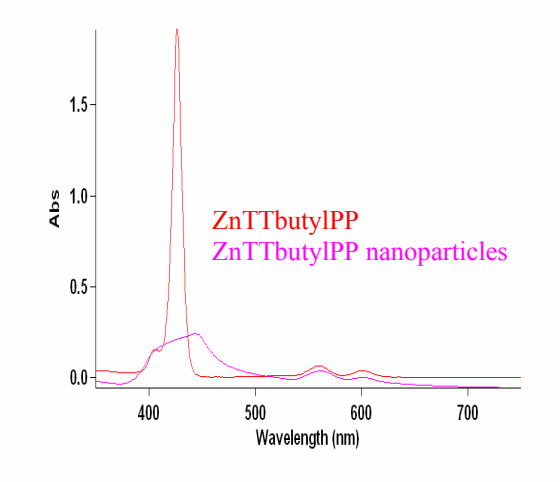

DLS histogram (diameter)

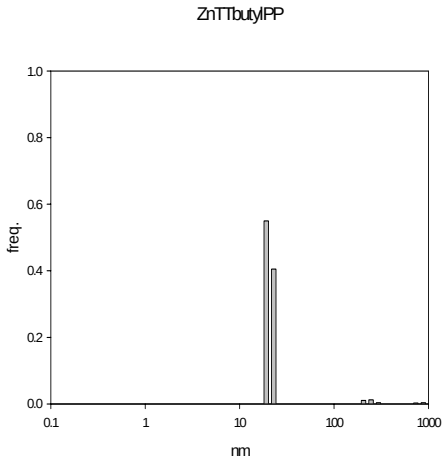

AFM histogram

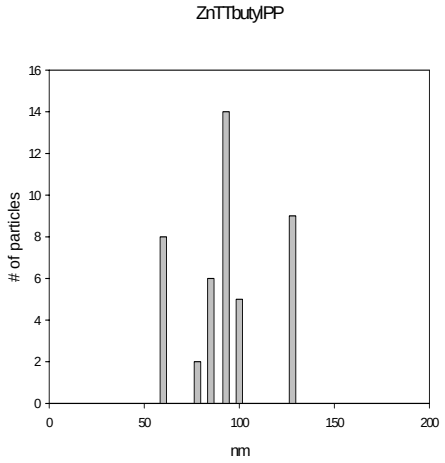

AFM image contact mode (glass)

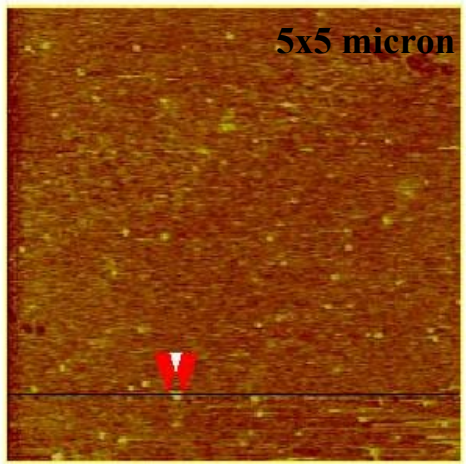

H: 93-128 nm V: 25-45 nm

AFM image tapping mode (glass)

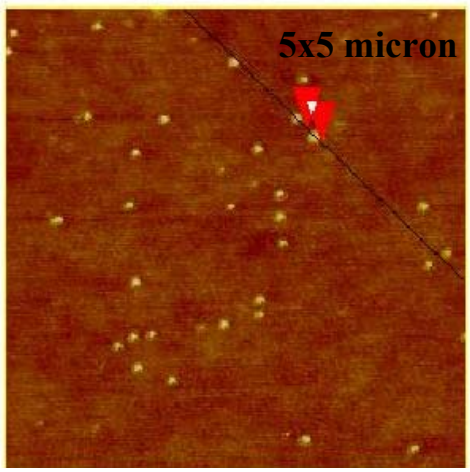

H: 60-100 nm V: 4-10 nm

Table 3. 18. ZnTCPP Me nanoparticles characterization

Structure

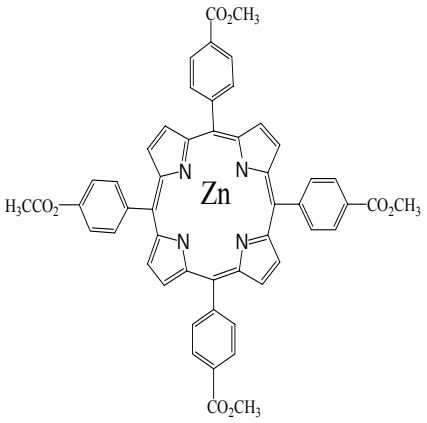

Absorption Spectrum

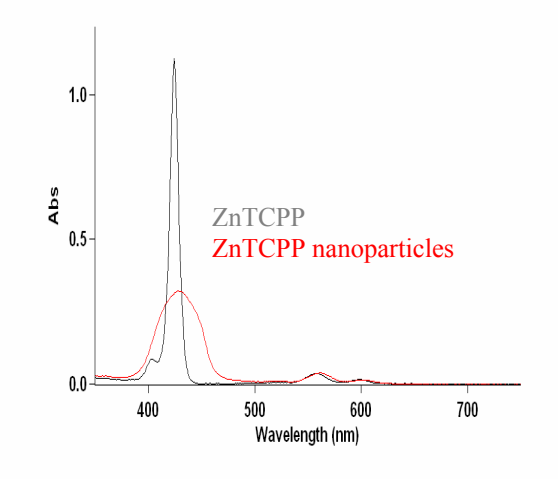

DLS histogram (diameter)

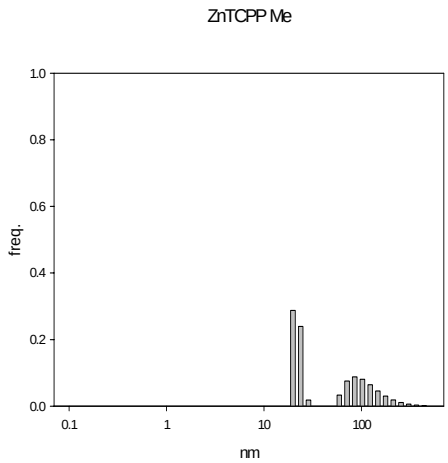

AFM histogram

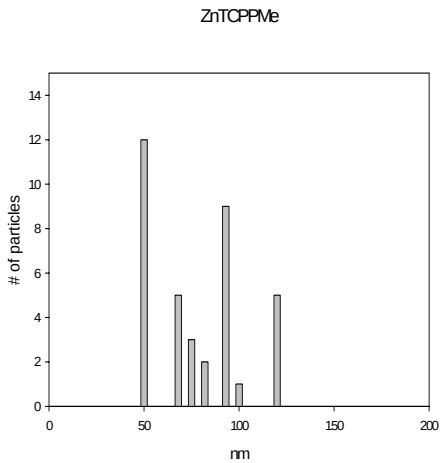

AFM image contact mode(glass)

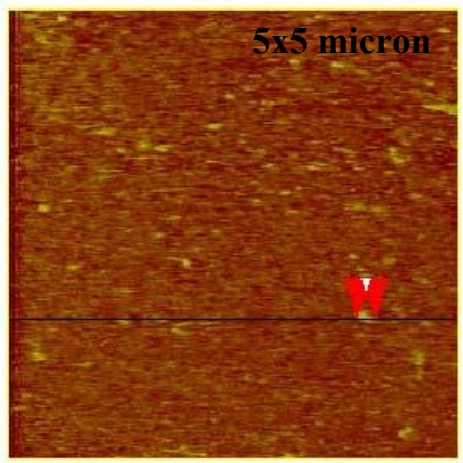

H: 50-100 nm V: 20-30 nm

AFM image tapping mode (glass)

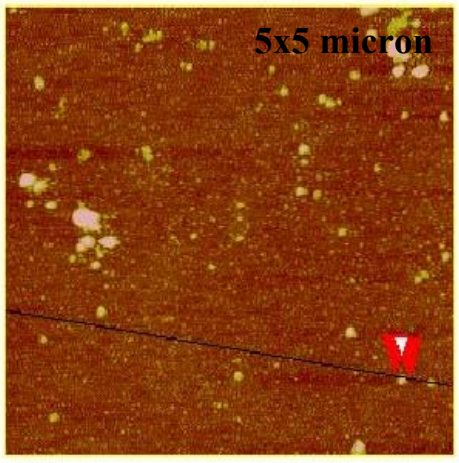

H: 93-120 nm V: 8-20 nm

Table 3. 19. ZnOEP nanoparticles characterization

Structure

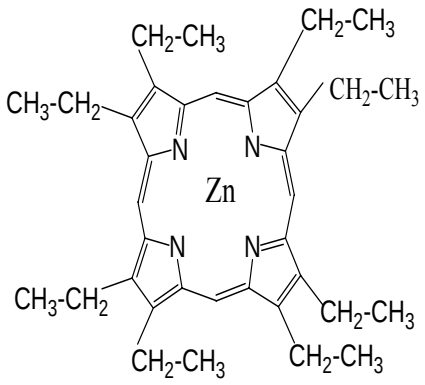

Absorption Spectrum

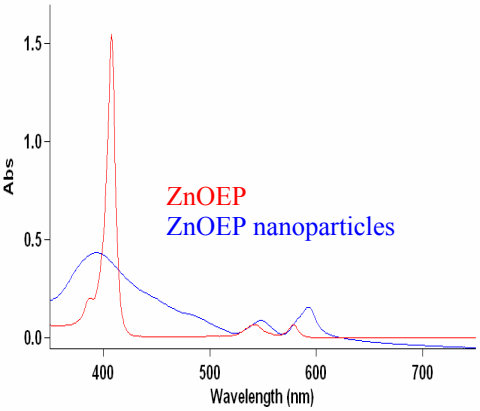

DLS histogram (diameter)

ZnOEPP

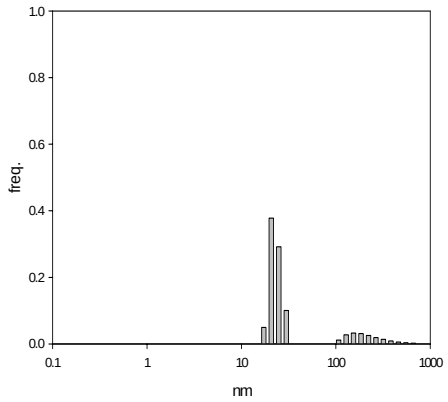

AFM histogram

ZnOEPP

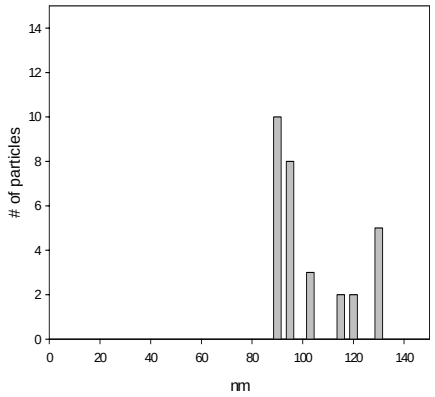

AFM image contact mode (glass)

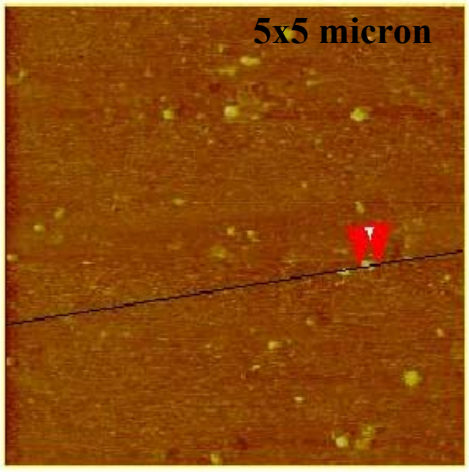

H: 95-130 nm V: 19-30 nm

AFM image tapping mode (glass)

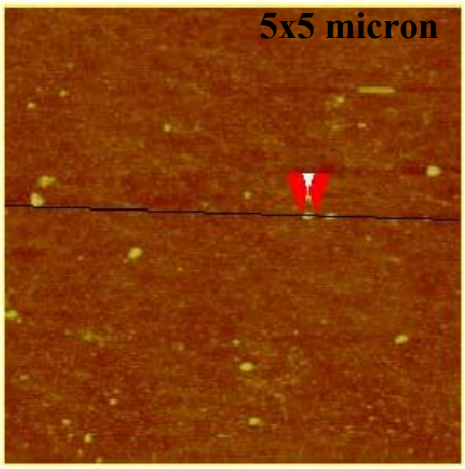

H: 90-120 nm V: 7-15 nm

Table 3. 20. MgOEP nanoparticles characterization

Structure

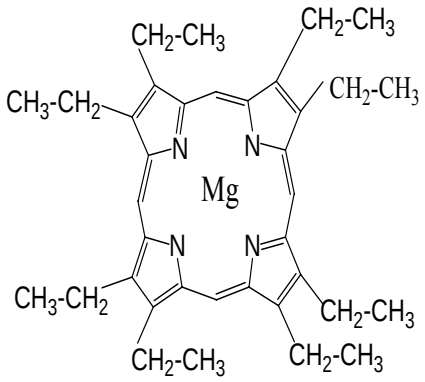

Absorption Spectrum

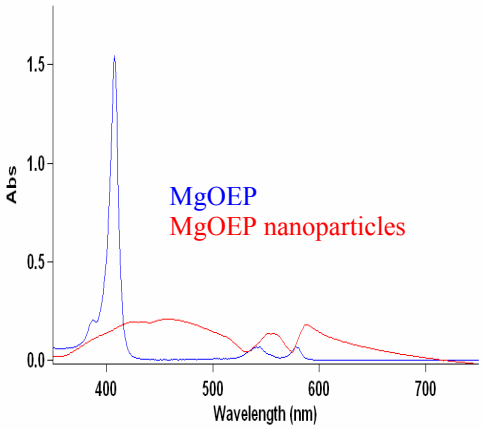

DLS histogram (diameter)

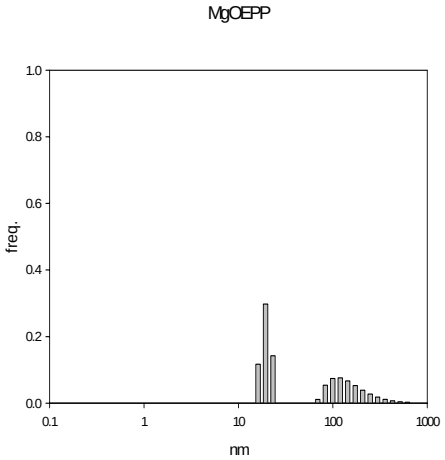

AFM histogram

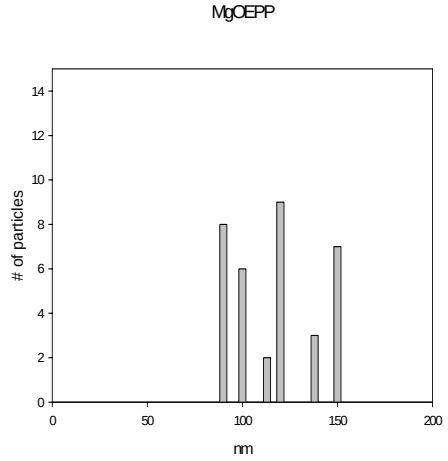

AFM image contact mode (glass)

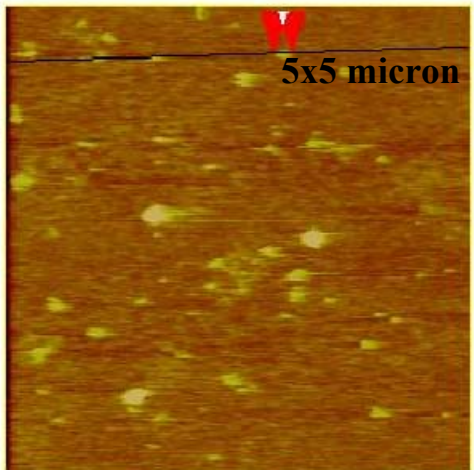

H: 100-150 nm V: 15-25 nm

AFM image tapping mode (glass)

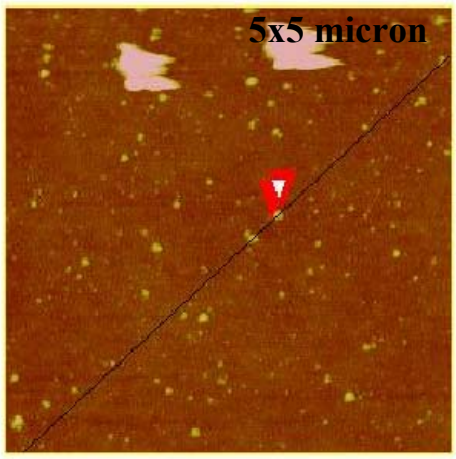

H: 90-120 nm V: 6-20 nm

Table 3. 21. $FeTPPF_{20}$ nanoparticles characterization

Structure

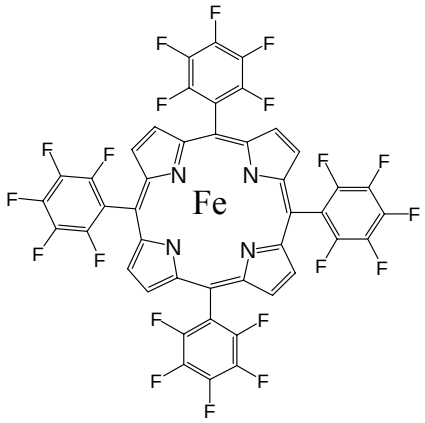

Absorption Spectrum

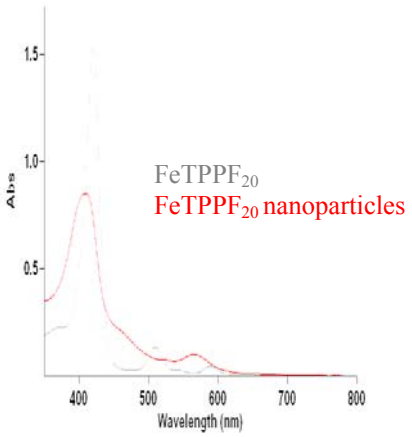

DLS histogram (diameter)

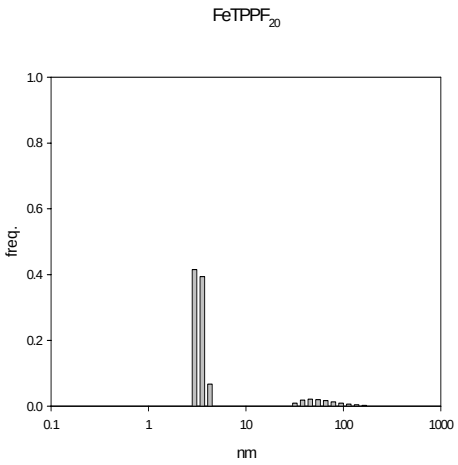

AFM histogram

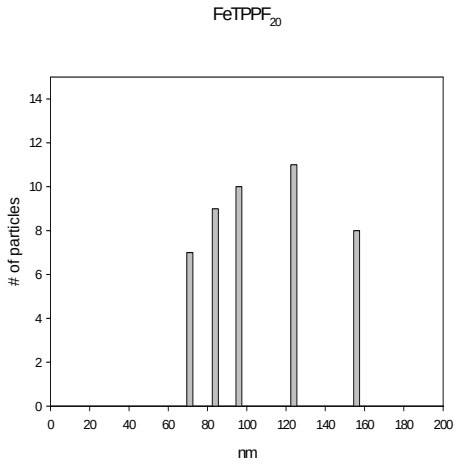

AFM image contact mode (glass)

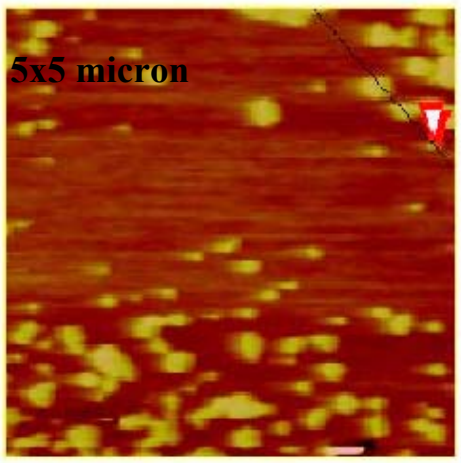

H: 70-150 nm V: 3-10 nm

AFM image tapping mode (glass)

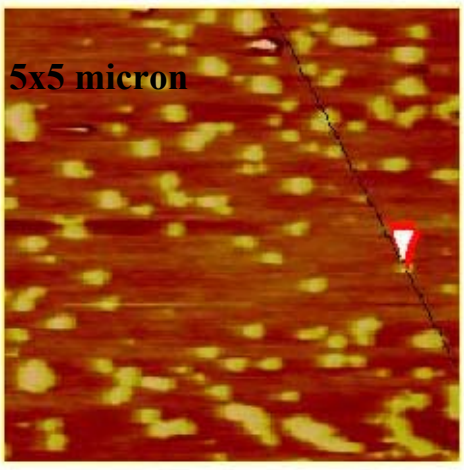

H: 60-140nm V: 6-10 nm

Table 3. 22. Summary of metal porphyrin nanoparticles characterization data

Compound	AFM contact	AFM tapping	DLS (diameter)
CoTPP	H: 80-117 nm V: 18-26 nm	H: 80-150 nm V: 7-15 nm	20-30 nm in DMF 80-500 nm (solvent)
ZnTPP	H: 95-130 nm V: 14-30 nm	H: 93-140 nm V: 5-15 nm	40-70 nm in DMF 90-1000 nm (solvent)
FeTPP	H: 105-130 nm V: 25-35 nm	H: 92-150 nm V: 4-10 nm	30 nm in DMF 300-800 nm (solvent)
CoTtbutylPP	H: 125-160 nm V: 30-40 nm	H: 117-150nm V: 6-20nm	50-60 nm in DMF 500-1000 nm (solvent)
ZnTtbutylPP	H: 93-128 nm V: 25-45 nm	H: 60-100nm V: 4-10nm	30-40 nm in DMF 300-500 nm (solvent)
ZnTCPP	H: 50-100 nm V: 20-30 nm	H: 93-120nm V: 8-20nm	30-50 nm in DMF 90-800 nm (solvent)
ZnOEP	H: 95-130nm V: 19-30 nm	H: 90-120nm V: 7-15nm	30-50 nm in DMF 200-600 nm (solvent)
MgOEP	H: 100-150 nm V: 15-25 nm	H: 90-120nm V: 6-20 nm	20-50 nm in DMF 90-600 nm (solvent)
$FeTPPF_{20}$	H: 70-150 nm V: 3-10 nm	H: 60-140nm V: 6-10 nm	5-8 nm in THF/DMF 60-300 nm (solvent)

Concluding from these data 1) UV-Vis spectrum we can see formation of both J (red shift) and H (blue shift) aggregates 2) Contact mode AFM shows bigger size particles then Tapping mode AFM due to the movement around with the tip 3) The size of particles obtained by DLS measurements doesn't necessary correlate with what we find by AFM because the nanoparticles are soft and they easy disassemble and reorganize upon deposition on surface 4) If stirring is used as mixing method we have seen some changes in nanoparticles sizes when we have different external group (size particles increase in this order H → methyl → t-butyl) or different metals and also the particles sizes increase when we have big external groups attached to the porphyrin (e.g. ToctyloxyPP, $TPPF_{20}$) 5) If sonication is used there is no change in particles sizes when we go from H→ CH_3→ t-butyl 6) Some changes in nanoparticles sizes are as well when we have different metals (Fe, Co, Zn, Mg), M^{2+} metals giving bigger sizes nanoparticles then M^{3+} 7) Porphyrin concentration, solvents, type and amount of stabilizer, mixing speed or order of adding the solutions can also dictate particles sizes.

References:

1. Drain, C. M.; Goldberg, I.; Sylvain, I.; Falber, A., *Topics in Current Chemistry* **2005,** 245, 55–88.
2. Drain, C. M.; Smeureanu, G.; Batteas, J.; Patel, S., *Dekker Encyclopedia of Nanoscience and Nanotechnology,* **2004,** 5, 3481-3502.
3. Drain, C. M.; Chen, X., *Encyclopedia of Nanoscience & Nanotechnology* **2004,** 9, 593-616.
4. Mauzerall, D. C., *Clin. Dermat.* **1998,** 16, 195-201.
5. Drain, C. M.; Bazzan, G.; Milic, T.; Vinodu, M.; Goeltz, J. C., *Israel J. Chem.* **2005,** 45, 255-269.
6. Drain, C. M.; Christensen, B.; Mauzerall, D. C., *Proc. Natl. Acad. Sci., USA* **1989,** 86, 6959-6962.
7. Drain, C. M.; Mauzerall, D., *Bioelectrochem. Bioenerg.* **1990,** 24, 263-266.
8. Drain, C. M.; Mauzerall, D. C., *Biophys. J.* **1992**, 1544-1555 .
9. Drain, C. M.; Mauzerall, D. C., *Biophys. J.* **1992,** 63, 1556-1563.
10. Drain, C. M.; Fischer, R.; Nolen, E.; Lehn, J. M., *Chem. Commun.* **1993**, 243-245.
11. Drain, C. M.; Gong, X., *Chem. Commun.* **1997**, 2117-2118.
12. Shi, X.; Barkigia, K. M.; Fajer, J.; Drain, C. M., *J. Org. Chem* **2001,** 66, 6513-6522.
13. Drain, C. M.; Shi, X.; Milic, T.; Nifiatis, F., *Chem. Commun.* **2001**, 287-288.
14. Drain, C. M.; Lehn, J.-M., *Chem. Commun.* **1994**, 2313-2315.

15. Drain, C. M.; Nifiatis, F.; Vasenko, A.; Batteas, J. D., *Angew. Chem. Int. Ed.* **1998,** 37, 2344-2347.

16. Drain, C. M., *Proc. Natl. Acad. Sci., USA* **2002,** 99, 5178-5182.

17. Kuramochi, Y.; Satake, A.; Kobuke, Y., *J. Am. Chem. Soc* **2004,** 126, 8668-8669.

18. Kobuke, Y., *J. Porph. Phthal.* **2004,** 8, 156-174.

19. Kobuke, Y.; Nagata, N., *Mol. Cryst. Liq. Cryst.* **2000,** 342, 51-56.

20. Gong, X.; Milic, T.; Xu, C.; Batteas, J. D.; Drain, C. M., *J. Am. Chem. Soc* **2002,** 124, 14290-14291.

21. Milic, T. N.; Chi, N.; Yablon, D. G.; Flynn, G. W.; Batteas, J. D.; Drain,C. M., *Angew. Chem., Int. Ed.* **2002,** 41, 2117-2119.

22. Drain, C. M.; Batteas, J. D.; Flynn, G. W.; Milic, T.; Chi, N.; Yablon, D. G.; Sommers, H., *Proc. Natl. Acad. Sci., USA* **2002,** 9, 6498-6502.

23. Lensen, M. C.; Takazawa, K.; Elemans, J.; Jeukens, C.; Christianen, P. C. M.; Maan, J. C.; Rowan, A. E.; Nolte, R. J. M., *Chem . Eur. J.* **2004,** 10, 831-839.

24. Elemans, J.; Rowan, A. E.; Nolte, R. J. M., *J. Mater. Chem.* **2003,** 13, 2661-2670.

25. Elemans, J.; Nolte, R. J. M.; Rowan, A. E., *J. Porph. Phthal.* **2003,** 7, 249-254.

26. Latterini, L.; Blossey, R.; Hofkens, J.; Vanoppen, P.; De Schryver, F. C.; Rowan, A. E.; Nolte, R. J. M., *Langmuir* **1999,** 15, 3582-3588.

27. Foekema, J.; Schenning, A. P. H. J.; Vriezema, D. M.; G., B. B.; Norgaard, K.; Kroon, J. K. M.; Bjornholm, T.; Feiters, M.; A. Rowan, E.; Nolte, R. J. M., *J. Phys. Org. Chem.* **2001,** 14, 501-512.

28. Chen, X.; Hui, L.; Foster, D. A.; Drain, C. M., *Biochem* **2004,** 43, 10918-10929.

29. Xu, W.; Guo, H.; Akins, D. L., *J. Phys. Chem. B* **2001,** 105, 1543-1546.

30. Komatsu, T.; Tsuchida, E.; Böttcher, C.; Donner, D.; Messerschmidt, C.; Siggel, U.; StockerW. ; Rabe, J. P.; Fuhrhop, J.-H., *J. Am. Chem. Soc.* **1997,** 119, 11660-11665.

31. Shirakawa, M.; Kawano, S.-i.; Fujita, N.; Sada, K.; Shinkai, S., *J. Org. Chem.* **2003,** 68, 5037-5044.

32. Togashi, D. M.; Costa, S. M. B.; Sobral, A.; Gonsalves, A., *J. Phys. Chem. B* **2004,** 108, 11344-11356.

33. Terech, P.; Scherer, C.; Deme, B.; Ramasseul, P., *Langmuir* **2003,** 19, 10641-10647.

34. Milic, T.; Garno, J. C.; Smeureanu, G.; Batteas, J. D.; Drain, C. M., *Langmuir* **2004,** 20, 3974-3983.

35. Khalil, G.; Gouterman, M.; Ching, S.; Costin, C.; Coyle, L.; Gouin, S.; Green, E.; Sadilek, M.; Wan, R.; Yearyean, J.; Zelelow, B., *J. Porph. Phthal.* **2002,** 6, 135-145.

36. Zelelow B; Khalil G. E; Phelan G; Carlson B; Gouterman M; Callis J. B; Dalton L. R, *Sensors and Actuators, B: Chemical* **2003,** 96, 304-314.

37. Khalil, G. E.; Chang A. ; Gouterman, M.; Callis, J. B.; Dalton, L. R.; Turro, N. J.; Jockusch, S., *Review of Scientific Instruments* **2005,** 76, 1-8.

38. Chen, X.; Drain, C. M., *Drug Design Review - Online* **2004**, (1), 215-234.

39. Drain, C. M.; Smeureanu, G.; Patel, S.; Gong, X.; Garno, J.; Arijeloye, J.,

New J. Chem. **2006,** 30, (12), 1834-1843.

40. Takahashi, Y.; Kasai, H.; Nakanishi, H.; Suzuki, T. M., *Angew. Chem. Int. Ed* **2006,** 45, 913-916.

41. Nitschke, C.; O'Flaherty, S. M.; Kroll, M.; Blau, W. J., *J. Phys. Chem. B* **2004,** 108, 1287-1295.

42. Nitschke, C.; O'Flaherty, S. M.; Kroll, M.; Doyle, J. J.; Blau, W. J., *Chem. Phys. Lett.* **2004,** 383, 555-560.

43. Denisyuk, I. Y.; Kamanina, N. V., *Optics and Spectroscopy* **2004,** 96, 235-239.

44. Grinstaff, M. W.; Hill, M. G.; Labinger, J. A.; Gray, H. B., *Science* **1994,** 264, 1311-1313.

45. Selke, M.; Sisemore, M. F.; Valentine, J. S., *J. Am. Chem. Soc* **1996,** 118, 2008- 2012.

46. Ikeue, T.; Ohgo, Y.; Saitoh, T.; Yamaguchi, T.; Nakamura, M., *Inorg. Chem.* **2001,** 40, 3423-3434.

47. Mauzerall, D.; Greenbaum, N. L., *Biochim. Biophys. Acta* **1989,** 974, 119-140.

48. Kasha, M.; Rawls, H. R.; El-Bayoum, M. A., *Pure Appl. Chem.* **1965,** 11, 371-381.

49. Sun, S.-S.; Lees, A. J., *Coord. Chem. Rev.* **2002,** 230, 170-191.

50. Udal'tsov A. V. ; Kazarin L. A. ; A., S. A., *J. Mol. Struct* **2001,** 562, 227-239.

51. Okada, S.; Segawa, H., *J. Am. Chem. Soc.* **2003,** 125, 2792-2796.

52. Akins, D. L.; Ozcelik, S.; Zhu, H. R.; Guo, C., *J. Phys. Chem. B* **1996,** 100, 14390-14396.

53. Akins, D. L.; Zhu, H. R.; Guo, C., *J. Phys. Chem. B* **1996,** 100, 5420-5425.

54. Drain, C. M.; Hupp, J. T.; Suslick, K. S.; WasielewskiM. R. ; Chen, X., *J. Porph. Phthal.* **2002,** 6, 241-256.

55. Hasobe, T.; Imahori, H.; Fukuzumi, S.; Kamat, P. V., *J. Mater. Chem.* **2003,** 13, 2515-2520.

56. Konan, N.; Cerny, R.; Favet, J.; Berton, M.; Gurny, R.; Allemann, E., *Eur. J. Pharmaceutics and Biopharmaceutics* **2003,** 55, 115-124.

57. van der Boom, T.; Hayes, R. T.; Zhao, Y.; Bushard, P. J.; Weiss, E. A.; Wasielewski, M. R., *J. Am. Chem. Soc.* **2002,** 124, 9582-9590.

58. Nazeeruddin, K.; Hunphry-Baker, R.; Officer, D. L.; Campbell, W. M.; Burrell, A. K.; Graetzel, M., *Langmuir* **2004,** 20, 6514-6517.

59. Ahrens, J.; Sinks, L. E.; Rybtchinski, B.; Liu, W. H.; Jones, B. A.; Giaimo, J. M.;Gusev, A. V.; Goshe, A. J.; Tiede, D. M.; Wasielewski, M. R., *J. Am. Chem. Soc.* **2004,** 126, 8284-8294.

4.

NEW CATALYTIC OXIDATION OF CYCLOHEXENE BY NANOPARTICLES OF 5, 10, 15, 20-TETRAKIS-(2,3,4, 5,6-PENTAFLUOROPHENYL) PORPHYRIN IRON (III)

4. 1. Introduction

Under ambient conditions the catalytic oxidation of alkenes by most iron porphyrins using a variety of oxygen sources, but generally not dioxygen, yield the epoxide with only minor quantities of other possible products. The turnover numbers for these catalysts are modest, ranging from a few hundred to about a few thousands depending on the degree of halogenation of the porphyrin, the substrate catalysts ratio, axial ligands, and other conditions. Halogenation of the macrocycle makes the metalloporphyrin catalyst more robust to oxidative degradation and/or increases the rates. The oxidation of cyclohexene by Fe(III)perfluorophenyl porphyrin is typical of the latter: the epoxide accounts for more than 99% of the product with turnover numbers of ca. 350.[1]

The discovery by Groves and coworkers[2-7] that iron porphyrins in organic solvents with oxygen sources such as iodosylbenzene can mimic the oxidative catalysis observed for cytochrome P-450[8-14] led to a huge amount of research on the reactivity and mechanism of this reaction. It was quickly realized that different metals exhibited different chemical reactivities, which included different products or product ratios.[15-20] Other major findings included (a) appropriate modification of the porphyrin macrocycle alters reactivity in terms of site selectivity,[21-23] (b) halogenation generally makes the metalloporphyrins more efficient catalysts, [1, 24-35] (c) the axial ligand can alter reactivity,[36-39] (d) the solvent can also affect the reactivity, and (e) other oxygen sources[33] such as H_2O_2, and O_2, can be used with some systems.[25, 39-41] Various metalloporphyrins are now used in laboratory scale reactions. Heterogeneous porphyrin systems include those in lipid bilayers, micelles, zeolites[21, 42, 43] or on supports such as silica[29, 44] or montmorillonite clay.[18, 44] Several reaction types have been catalyzed by metalloporphyrins, but perhaps the most well studied are oxidation reactions. Self-assembled metalloporphyrin catalysts relevant to the present work are pioneered by Hupp et al.[20, 45, 46] which can be remarkably robust, but require macrocycles that are difficult to obtain in high yields. Conversely, the metalloporphyrin nanoparticles are self-organized because they are neither discrete arrays nor mono-dispersed assemblies.[47-50]

The catalytic oxidation of cyclohexene by iron tetra aryl porphyrins is a standard reaction that has been thoroughly investigated over the last few decades, and the epoxide is the major product under a range of experimental conditions using a variety of porphyrin derivatives.

In general the turnover number is a few hundred because of the degradation of the iron porphyrin catalyst, but this increases to about ca. 350 when 5,10,15,20-tetrakis(2,3,4,5,6,-pentafluorophenyl) porphyrin iron(III) (Fe(III)$TPPF_{20}$) is used because this is a more active catalyst and may be more resistant to oxidative degradation. There are numerous studies on the catalytic activity of this porphyrin,[1, 24, 25, 27, 28, 34, 35, 41] including the catalytic oxidation of cyclohexene by Fe(III)$TPPF_{20}$ in acetonitrile which requires methanol as a co solvent to yield over 98% of the epoxide and traces of the 2-cyclohexene-1-one and the 2-cyclohexene-1-ol (Scheme 4.1.).[1,34,35]

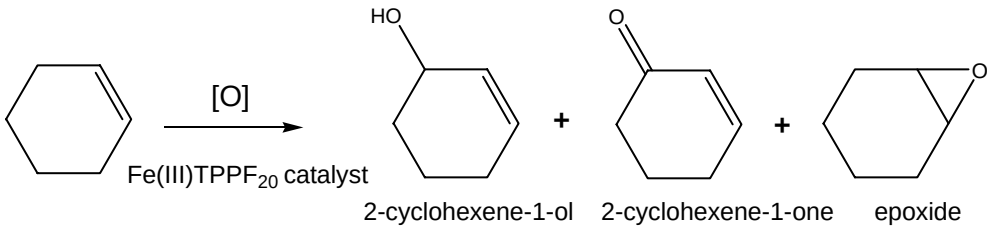

Scheme 4. 1. Catalytic oxidation reaction of cyclohexene by $FeTPPF_{20}$

Given the enhanced catalytic activity Fe(III)$TPPF_{20}$, there are also a considerable number of reports on other halogenated metalloporphyrins, such as perhalogenated porphyrins. Gray and coworkers reported significantly different oxidation chemistry for a derivative of Fe(III)$TPPF_{20}$ wherein the eight pyrroles β positions are also halogenated.[27, 28]

When the β positions are chlorinated the activity of ethylbenzene oxidation using oxygen at 100 ^{o}C is increased but not the stability to oxidative degradation in reactions wherein the substrate was also the solvent.[41] The differences in the catalytic oxidation of perhalogenated porphyrins arise from both distortions in the otherwise planar macrocycle and electronic effects.[27, 28] Another example is $FeTPPF_{20}$ linked to polystyrene, which catalyzes the oxidation of ethylbenzene with dioxygen at elevated temperatures.[41]

We have found that 10 ± 5 nm nanoparticles of $Fe(III)TPPF_{20}$ formed by host/guest solvent methods[51, 52] (Scheme 4. 2.), catalytically oxidize cyclohexene to exclusively yield 2-cyclohexene-1-one and 2-cyclohexene-1-ol, rather than the epoxide with ca. 10-fold greater turnover number (TON) than the completely solvated species in acetonitrile/methanol[1, 34, 35] when oxygen is used rather then H_2O_2.

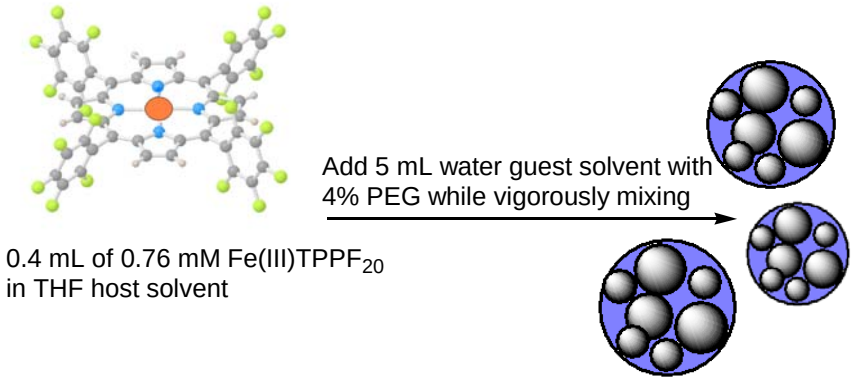

Scheme 4. 2. Preparation of 10 nm $FeTPPF_{20}$ nanoparticles in water

Moreover, dioxygen is efficiently used as oxidant in place of H_2O_2 or other synthetic oxygen sources that are required by most other metal-porphyrin catalysts of this reaction. This reactivity is quite non-intuitive because the metalloporphyrins are in close proximity in the nanoparticles, and so their oxidative degradation should be enhanced, thus causing a significant *decrease* in catalytic turnovers. Furthermore, the allylic products suggest a different oxidative mechanism compared to that of the corresponding solvated metalloporphyrin.[1, 34, 35]

4. 2. Experimental

Materials and instrumentation

Fe(III)TPPF_{20}Cl, cyclohexene oxide, 2-cyclohexene-1-ol, 2-cyclohexene 1-one, polyethylene glycol monomethyl ether (PEG $_{164}$) were purchased from Aldrich Chemical Co. The solvents (Tetrahydrofuran, 99.9% acetonitrile, 99.9%, methanol, toluene and HPLC grade dichloromethane), cyclohexene and 30% H_2O_2 were purchased from Fisher Scientific Co. Nanopure water was obtained using Barnstead Nanopure water system. D_2O 99.6% was obtained from Cambridge Isotope laboratories, Inc., and 10% $H_2{}^{18}O$, and 98 %$^{18}O_2$ were obtained from Sigma-Aldrich.

Product analyses were performed using GC-MS Agilent 5975 series system with HP-5 column. A Carey Bio-3 UV-Visible spectrophotometer, a Precision Detectors PD2000DLS Cool-Batch 90T dynamic light scattering instrument was used in batch mode at 20°C. A Fisher scientific SF15 sonicator was used in nanoparticle preparations.

Reactions

Reactions were performed at ambient temperature. All reactions were run a minimum of ten times except the isotope experiments, which were repeated three times, and the reported data represent the average of these reactions.

For the homogeneous protic solvent reactions[34] the iron porphyrin complex was dissolve in methanol : acetonitrile = 1 : 3. Then reaction was initiated in a 9.5 mL screw capped vial by mixing 250 μL of the iron porphyrin solution in 2.5 mL solvent (MeOH: ACN=1:3) ($2.5x10^{-7}$moles, $9.5x10^{-5}$M) and 50 μL cyclohexene, whereupon 80 μL of 30% H_2O_2 was slowly added to the reaction via a Teflon cannula tube securely fitted to a hole in the cap using a syringe pump through a over the course of 80 min. and the reaction was stirred for 4 hours. The ratio of porphyrin: substrate: H_2O_2 = 1:2000:3000 equivalents. An aliquot of the reaction was analyzed by GC-MS and product yields were determined in relation with the internal standard added (toluene). (Figure 4. 4.) Of the three possible products, cyclohexene oxide was obtained in greater than 99% . The results are shown in Table 4. 1.

For porphyrin nanoparticles reactions the Fe(III)$TPPF_{20}$ nanoparticles were prepared in 10mL vial or test tube in which 5.6 mL batches were obtained by adding 5 mL of nanopure water to a mixture of 0.2 mL PEG and 0.4 mL of a $0.7x10^{-3}$ M solution of Fe(III)$TPPF_{20}$ in THF while sonicating ($2.8x10^{-7}$ moles, $5x10^{-5}$ M). The solution was further sonicated for 1min. The nanoparticle preparations are stable for more than 4 weeks and stored in a refrigerator at ~ 4 ^{0}C. Each batch of nanoparticles was checked by DLS (Figure 4. 1.) and UV-visible (Figure 4. 2.) and AFM (contact and tapping mode) (Figure 4. 3.). The solutions appear slightly cloudy.

2.5 mL of the porphyrin nanoparticles stock solution ($1.25x10^{-7}$ moles, $5x10^{-5}$ M) were mixed in a 9.5 mL screw capped vial with 25 μL of cyclohexene, and 40 μL 30% H_2O_2 which was slowly added to the reaction via a Teflon cannula tube securely fitted to a hole in the cap over the course of 40 minutes. The ratio of porphyrin: substrate: H_2O_2 = 1:2000:3000 equivalents. The reaction mixture was stirred for ca. 20 hours.
Or 2.5 ml of the porphyrin nanoparticles stock solution ($1.25x10^{-7}$ moles,$5x10^{-5}$ M) were mixed with 200 μL of cyclohexene and 125 mL O_2 was added by opening the reaction to a separatory funnel at 1 atm and reacted for 24 hours (porphyrin: substrate: O_2 = 1:16000:40000).

The 2.6 mL reaction mixture volume was extracted once with 2.8 mL dichloromethane and the layers were allowed to separate. The water fraction and some of the organic fraction was removed to leave a total volume of 2 mL (this assures the same volume for every reaction assay). To this volume reaction is added 20 μL toluene (1.88×10^{-4} moles). 4μL of the extract was diluted into 1 mL dichloromethane and then 2 μL of this solution was injected into GC-MS.

For oxygen reaction the 2.6 mL reaction mixture volume was extracted once with 8 mL dichloromethane and the layers were allowed to separate. The water fraction and some of the organic fraction was removed to leave a total volume of 6 mL (this assures the same volume for every reaction assay). To this volume reaction is added 20 μL toluene (6.2×10^{-5} moles). 4μL of the extract was diluted into 1 mL dichloromethane and then 2 μL of this solution is injected into GC-MS.

In both cases the product yields were determined in relation with the internal standard added (toluene) (Figure 4. 6. and Figure 4. 7.).

This reaction exclusively yields 2-cyclohexene-1-one and 2-cyclohexene-1-ol, rather than the epoxide. The data is shown in Table 4. 1.

The TON for each reaction was calculated based on the corrected area for each peak using the internal standard (toluene) and the response factor (obtained in standardization response of GC-MS areas for each compound, Table 4. 4) (See calculation in Appendix).

4. 3. Results and Discussion

The results of the catalytic reactions, controls, and homogeneous reactions used for comparison are presented in Table 4. 1. Control reactions in the absence of an oxygen source or metalloporphyrins result in no product formation, and adding water to the homogeneous reaction has no effect on the product ratios or TON (see Table 4. 2.).

Nanoparticle Structure

The detailed structural arrangement of the Fe(III)TPPF$_{20}$ within the nanoparticles described herein is not known, because the intermolecular forces used to self-organize the molecules into nanoparticles are weak and reversible.[51, 52] The nanoarchitecture of porphyrin molecules within the nanoparticle varies according to the chemical structure of the porphyrinoids, the molecular properties of the host and guest solvents, and of the stabilizer because the chemical properties of the components dictate the intermolecular interactions.[47-50] Densely packed, a 10 nm diameter particle of Fe(III)TPPF$_{20}$ (1.75nm x 1.75nm x 1.0nm ~3 nm^3) can contain up to ~170 porphyrins, but density studies indicate that there are fewer molecules in the aggregate.

Our working hypothesis is that the nanoparticles consist of sub-domains of the macrocycles and solvent/stabilizer-filled voids or channels of unknown size and distribution, so that the number of chromophores per nanoparticle is less. Results from electron transfer experiments in nanoparticles containing free base TPP and ca. 5% Fe(III)TPP indicate sub-domains of 15-25 porphyrins within the nanoparticle. The presence of sub-domains is also consistent with AFM studies that reveal that some porphyrin nanoparticles fall apart into smaller 5-10 nm high and 60-150 nm wide particles on surfaces.[52]

These smaller particles (3 nm diameter) can contain up to 35 porphyrins. Several experiments indicate that in solution under ambient conditions, the porphyrins do not exchange between nanoparticles and that the diameter of the nanoparticles does not change over time.

The data in Table 4. 1. shows that catalytic activity depends on particle size, composition and oxygen source which may indicate differences in the nanoarchitectures of the porphyrins within the nanoparticles and subdomains. A striking example of the dependence of catalytic oxidation on particle size is that the oxidation of cyclohexene by large (ca. 120 nm diameter) nanoparticles of Fe(III)TPPF_{20} requires iodosyl benzene and results in epoxidation similar to the homogeneous system,[51, 52] rather than the ene-ol or ene-one described above for the 10 nm nanoparticles of the same porphyrin.

4. 4. Mechanistic Insights

There is considerable debate over the mechanisms of hydrocarbon oxidation by iron porphyrins and other metalloporphyrins, [1, 6, 7, 11, 13, 27, 34, 35, 53] wherein the two dominant proposed mechanisms are: (1) a radical hydrogen-abstraction–oxygen-rebound mechanism, and (2) an oxygen (or hydroxyl) insertion reaction that proceeds through a cationic ROH_2^+ species. It may be that the spin state of the iron in the macrocycle dictates which of these dominate a particular reaction. In addition to the differences in ligand field and core size effects, axial ligands play an important role.[54] For the nanoparticle systems an additional consideration are the intermolecular interactions, such as pi-stacking, which may have significant effects on electronic structure and substrate accessibility compared to the solvated metalloporphyrin. Considering the close proximity of the Fe(III)$TPPF_{20}$ in the nanoparticles, the formation of μ-oxo and/or dioxo dimers may also play an important role, as the former species is known to have increased catalytic activity in benzylic oxidations at elevated temperatures.[41]

Isotope Experiments

Since the activation of O_2 is of primary interest, we focus on this aspect of the catalysis. Preliminary investigations into possible differences in the mechanism between the nanoparticle and the homogeneous reactions are consistent with previously reported mechanisms for reactions that result in allylic oxidations. These latter reactions can be affected using Mn, Sn, or Ru porphyrins and are akin to the P450 reactions.[8, 12] The source of the oxygen in the product may be from the water and/or the O_2 in the closed reaction vessel. Reactions run with nanoparticle

preparations made with 10% $H_2{}^{18}O$ results in incorporation of ca. 10% ^{18}O into the ketone product (no incorporation in alcohol), which is consistent with a previous study that concluded a high valent iron oxo species is a key intermediate in room temperature oxidations by Fe(III)$TPPF_{20}$[55] (Figure 4. 8, Figure 4. 9). Similarly, when 97% $^{18}O_2$ is used there is ca. 60% incorporation of ^{18}O into the products (>95% incorporation in alcohol and only 10% in ketone) (Figure 4. 10, Figure 4. 11). These results indicate that the oxygen comes primarily from O_2 but suggest that some of the radical intermediates react with water. Note that reactions run in D_2O result in no incorporation of deuterium into the products other than some exchange with the alcohol proton. These reactions are quite pH sensitive and must be run between pH 6.5 and 7.0. No products are found in reactions run outside of this pH range. The presence of an alcohol to form an active axially bound $[(TPPF_{20})Fe(HOCH_3)]^+$ adduct is reported to be essential for cyclohexene epoxidation reactions by this complex in solution,[34] and in the case of the nanoparticles the alcohol moiety on the PEG can serve in this capacity, yet since the products are different an alcohol adduct may not be necessary. Nanoparticles that are stabilized by other PEG's can be made[52], and may be used to address this issue.

Our hypothesis is that the close proximity of the iron porphyrins in the nanoparticles facilitates the formation of μ-oxo-bridged dimers which have known enhanced catalytic activity in terms of alkane hydroxylation[41, 56] and/or μ-dioxo-bridged dimers. Under the reaction conditions, the oxo bridged dimers and monomers may be in equilibrium. Water, hydroxide, and the alcohol moiety of the PEG can serve as axial ligands, which in turn affect the stability of the iron oxo complexes. This is

consistent with the observation that imidazole axial ligands block the incorporation of the oxygen from water in epoxidation by Fe(III)$TPPF_{20}$.[55] The absence of cyclohexene oxide as a significant product in nanoparticle catalysis, argues against the presence of significant amounts of solvated Fe(III)$TPPF_{20}$. Homogeneous reactions in acetonitrile/methanol with a few percent water and PEG yield only the epoxide, so solvent effects can be ruled out, as can differences arising solely from these serving as axial ligands. The absence of the large porphyrin Soret band in the UV-visible spectra of the exhausted reaction mixture reveals that eventually the porphyrin does decompose (Figure 4. 5.). Deformation of the otherwise planar macrocycle by steric crowding of the peripheral substituents has been proposed as a major source of reactivity differences in the perhalogenated porphyrins relative to $TPPF_{20}$ and other arylporphyrins.[27, 28] Nonplanar metalloporphyrins are known to have significantly different photonic properties,[57, 58] including the dynamics of axial ligand binding.[59] The Fe(III)$TPPF_{20}$ molecules likely adopt a similar planar conformation in the nanoparticles as in solution because the intermolecular forces between the nanoparticle components are too weak to force the macrocycle into energetically unfavorable configurations. Also, nonplanar porphyrins are characterized by broad, red-shifted Soret bands. Fe(III)$TPPF_{20}$ in acetonitrile:methanol shows a normal porphyrin optical spectra but the optical spectra of the nanoparticles are broad and contain several underlying peaks both to the red and blue of those of the parent complex, indicating aggregation. The narrow, mildly acidic pH range may indicate an aqua axial ligand allows the reaction to proceed and that hydroxide deactivates the catalyst.

4. 5. Conclusions

These results further illustrate the unique properties of organic nanoparticles relative to the component molecules and that the principles of supramolecular chemistry can be used to create new materials with enhance functions or activities. Since they do not require specifically designed recognition motifs in predefined geometries, self-organized materials are generally easier to make than self-assembled materials,[49, 50, 52, 60] thus obviating the need for macrocycles that are synthetically challenging or the result of low-yield procedures. Symmetric porphyrins, wherein all the meso positions are the same aryl moiety, are easy to prepare in large scales, and can be prepared in a solventless reaction that further reduces production costs.[61] These results and previous reports indicate the mechanism of catalytic oxidation of hydrocarbons by Fe(III)$TPPF_{20}$ is exquisitely dependent on specific environmental conditions and organization or aggregation state of the complex. The Fe(III)$TPPF_{20}$ nanoparticle catalyst system represents an advance in green chemistry since despite numerous efforts in catalyst discovery and design there are still few molecular-based catalysts that can perform oxidation reactions under mild conditions by activation of O_2. The use of water as the primary reaction solvent for the $FeTPPF_{20}$ nanoparticle catalysis is also an additional environmental benefit.

Table 4. 1. Fe(III)TPPF$_{20}$ nanoparticles: a green catalysis of cyclohexene oxidation

Solution[A] / nanoparticle[B]	**Conditions**	**Oxide %**	**ene-1-ol %**	**ene-1-one %**	**TON#**	**comment**
Solution	CH_3OH/CH_3CN H_2O_2	98	<1	<1	350-400	
Solution [1, 34, 35]	CH_3OH/CH_3CN H_2O_2	95 ±5	5±1	<1	Not reported	
10 nm NP	H_2O_2	<1	30	70	150-200	
10 nm NP	6.5 mL air	<1	23	77	80-100	
10 nm NP	6.5 mL O_2	<1	24	76	525-550	
10 nm NP	125 mL O_2	<1	28	72	3000-3500	
10 nm NP	95% D_2O, 125 mL O_2	<1	20	80		No D in products
10 nm NP	10% $H_2{}^{18}O$, 125 mL O_2	<1	34	66		^{18}O in ~ 5% of products (10% in ketone and 0% in alcohol)
10 nm NP	125 mL 97 % $^{18}O_2$	<1	23	76		^{18}O in ~ 60% of products (95% in alcohol and 10% in ketone)
10 nm NP	125 mL O_2 0.5 mL cyclohexene	<1	28	72	3500	
35 nm NP[C]	H_2O/DMF C_6H_5IO	70	11	19	16,500	
120 nm NP[C]	H_2O/DMF C_6H_5IO	85	6	10	12,000	

NP = nanoparticles. [A] Solution reactions: 0.1 mM in 1:3 methanol: acetonitrile, 50 μL cyclohexene, and 80 μL 30% H_2O_2 (added slowly to the reaction with a syringe pump) in 9.5 mL vial (porphyrin: substrate: H_2O_2 = 1:2000:3000) was reacted for 4 h.

[B] 2.5 ml porphyrin nanoparticles (0.05 mM in porphyrin content) were mixed with 25 μL of cyclohexene and 40 μL 30% H_2O_2 (porphyrin: substrate: H_2O_2 = 1:2000:3000, H_2O_2 slowly added to the reaction with a syringe pump) and reacted for 20-24h. Or, 2.5 ml porphyrin nanoparticles (0.05 mM in porphyrin content) were mixed with 200 μL of cyclohexene and 125 mL O_2 was added by opening the reaction to a separatory funnel at 1 atm and reacted for 24 h (porphyrin: substrate: O_2 = 1:16000:40000).

[C] Nanoparticles made from THF host solvent in ratios used to obtain this size nanoparticle. All reactions run exhaustively for 20-24h, error in products and TON = ± 3%, pH = 6.5 - 7.0. In the case of nanoparticles reactions, the products were extracted into CH_2Cl_2 and analyzed using an Agilent 5975 series GC-MS with a HP-5 column. Results of control reactions: (a) H_2O_2 and O_2 do not react directly with cyclohexene under these conditions, and both an oxygen source (O_2 or H_2O_2) and FeTPPF$_{20}$ as either the nanoparticle or the solvated molecule are needed for product formation.

Table 4. 2. Fe(III)$TPPF_{20}$ nanoparticles : Control reactions

Solution[A] / nanoparticle[B]	**Conditions**	**Oxide %**	**ene-1-ol %**	**ene-1-one %**	**TON#**	**comment**
Solution	CH_3OH/CH_3CN without H_2O_2	-	-	-	-	No reaction
Solution	CH_3OH/CH_3CN H_2O_2 with 5% H_2O and PEG	95 ±5	5±1	<1		
Solution	CH_3CN no CH_3OH H_2O_2	Trace	-	-	-	References[1, 34, 35]
Cyclohexene	H_2O_2 or O_2	-	-	-	-	No reaction
No porphyrin	$H_2O/PEG164/H_2O_2$	-	-	-	-	No reaction
No porphyrin	$H_2O/PEG164/O_2$	-	-	-	-	No reaction
10±5nm NP	Argon atmosphere	-	-	-	-	No reaction
10±5nm NP	pH 7.5	-	-	-	-	No reaction
10±5nm NP	pH 7.0	-	-	-	-	No reaction

Other control reaction involve temperature experiment (the reaction was run at about 29-30 °C) and also shaker experiment (to confirm that using a magnetic stir bar the reaction occur not because of magnetic spin sate of Fe(III)).

2.5 mL of the porphyrin nanoparticles stock solution ($1.25x10^{-7}$ moles, $5x10^{-5}$ M) were mixed in a 9.5 mL screw capped vial with 25 μL of cyclohexene, and 40 μL 30% H_2O_2 which was slowly added to the reaction via a Teflon cannula tube securely fitted to a hole in the cap over the course of 40 minutes. The ratio of porphyrin: substrate: H_2O_2 = 1:2000:3000 equivalents. The reaction mixture was stirred for ca. 20 hours at 29-30 °C. The yield of products and the TON was the same with the reactions run at room temperature. So this confirms that the temperature has a small any effect on the nanoparticles catalysis reaction. (Table 4. 3).

Also the same reaction but with O_2 addition (2.5 ml of the porphyrin nanoparticles stock solution ($1.25x10^{-7}$ moles,$5x10^{-5}$ M) were mixed with 200 μL of cyclohexene and 125 mL O_2 was added by opening the reaction to a separatory funnel at 1 atm and reacted for 24 hours (porphyrin: substrate: O_2 = 1:16000:40000)) was run using a protein shaker system (instead of a magnetic stirrer) to demonstrate that a magnetic field has no effect on the reaction products. In this case, because the mixing speed is lower then the stirring bar, the TON are lower but we obtained the same products and same distribution products. (Table 4.3)

Table 4. 3. Fe(III)$TPPF_{20}$ nanoparticles catalyst experiments
Control reactions (temperature and mixing method)

Method	Ratio alcohol/ketone	TON
Stirrer (with O_2)	28%: 72% = 1: 2.57	3000-3500
Shaker (with O_2)	28%:72% = 1: 2.57	1000
Room temperature (23° C) (with H_2O_2)	30%: 70% = 1: 2.33	150-200
29-30 ° C (with H_2O_2)	34% : 66% = 1:1.94	134-160

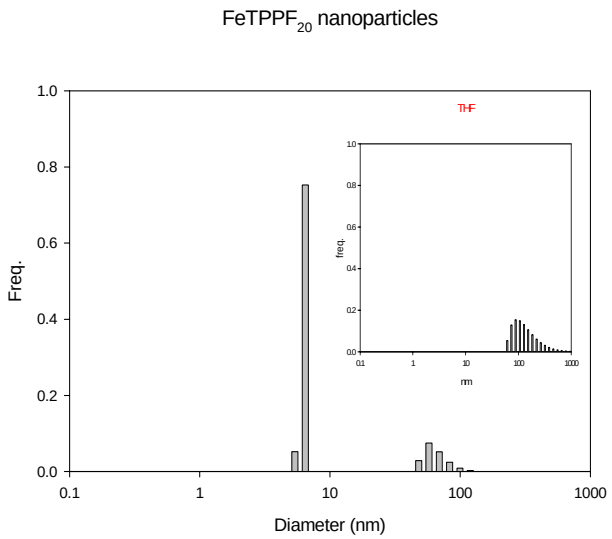

Figure 4. 1. Typical dynamic light scattering data indicating the diameter of the catalytic nanoparticles The peaks at 70-100 nm are due to the mixture of solvents

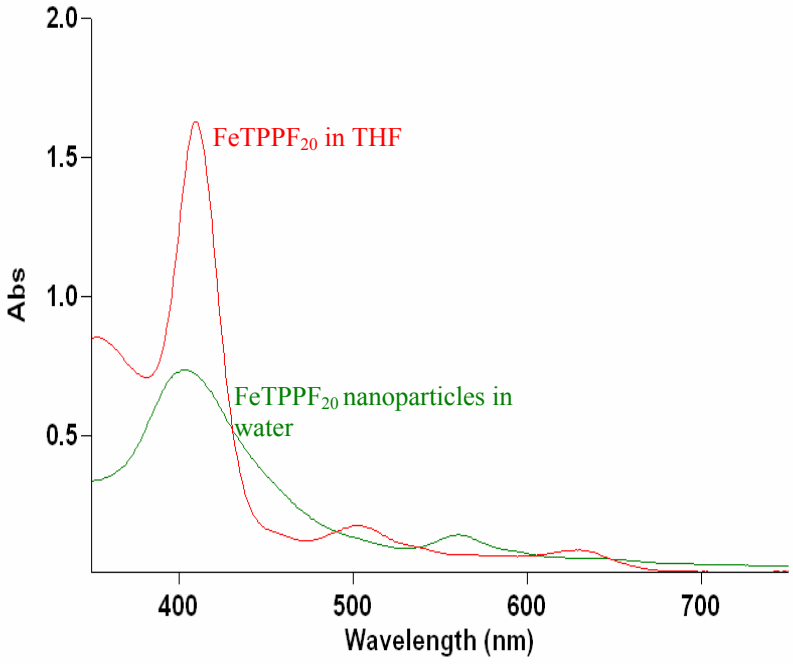

Figure 4. 2. Typical UV-Vis spectrum for $FeTPPF_{20}$ in THF and correspondent nanoparticles in water

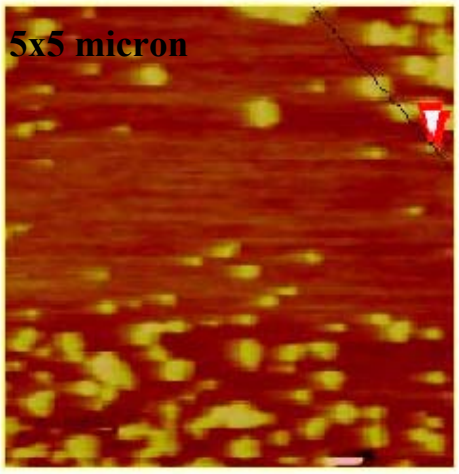

A) Contact mode glass

H: 70-150 nm V: 3-10 nm

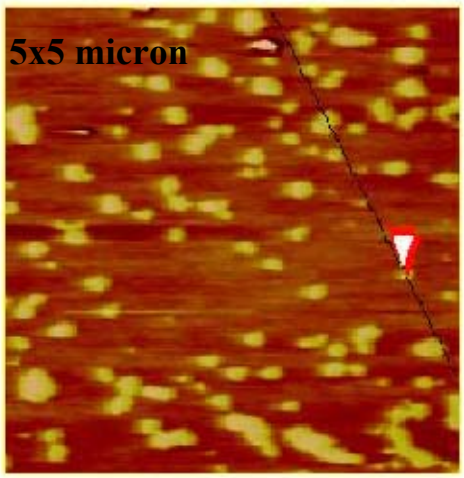

B) Tapping mode glass

H: 60-140nm V: 6-10 nm

Figure 4. 3. Typical AFM of the nanoparticles deposited on ozone-cleaned glass. A) Contact mode B) Tapping mode. Samples were prepared by drop-deposition on cleaned glass slides, dried overnight, imaged in air.
These indicate that the nanoparticles reorganize during the deposition process to form large-flat aggregates and do not reflect the nanoparticles in solution

Figure 4. 4. GC of a standard, solution phase reaction as reported previously. [1, 34, 35] 3.06-cyclohexene, 4.71-toluene, 6.04-cyclohexene oxide

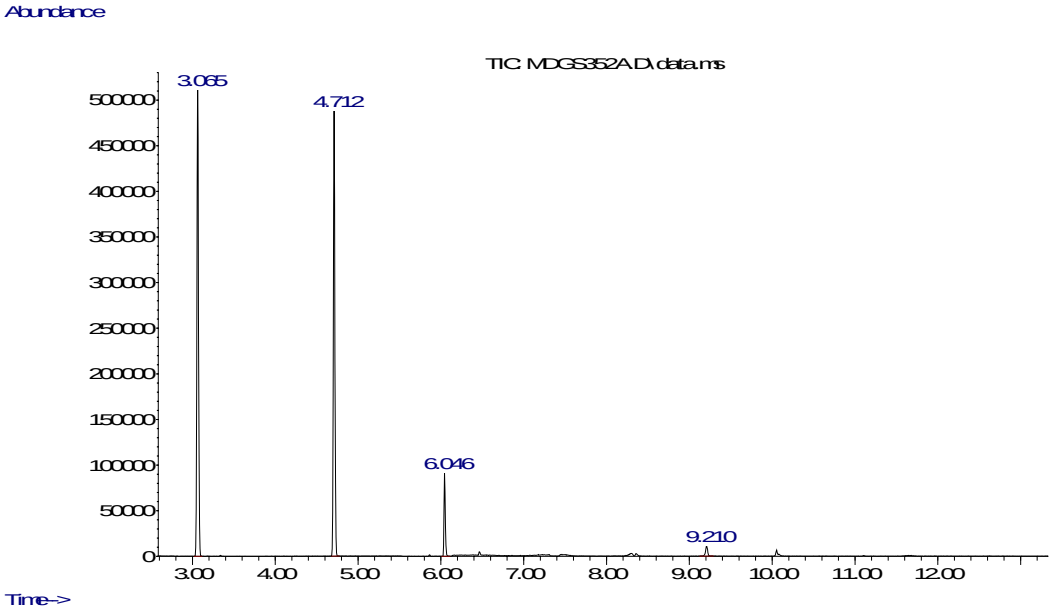

Figure 4. 5. Typical UV-visible spectra of the solvated Fe(III)$TPPF_{20}$ in CH_3CN/CH_3OH after 30 min/4h reaction (top), and 10±5 nm nanoparticles of the complex in water (bottom) after 20 hours reaction

Figure 4 .6. GC of a typical nanoparticle catalyst reaction using H_2O_2
3.06-cyclohexene, 4.71-toluene, 6.38-ene-1-ol, 6.84-ene-1-one

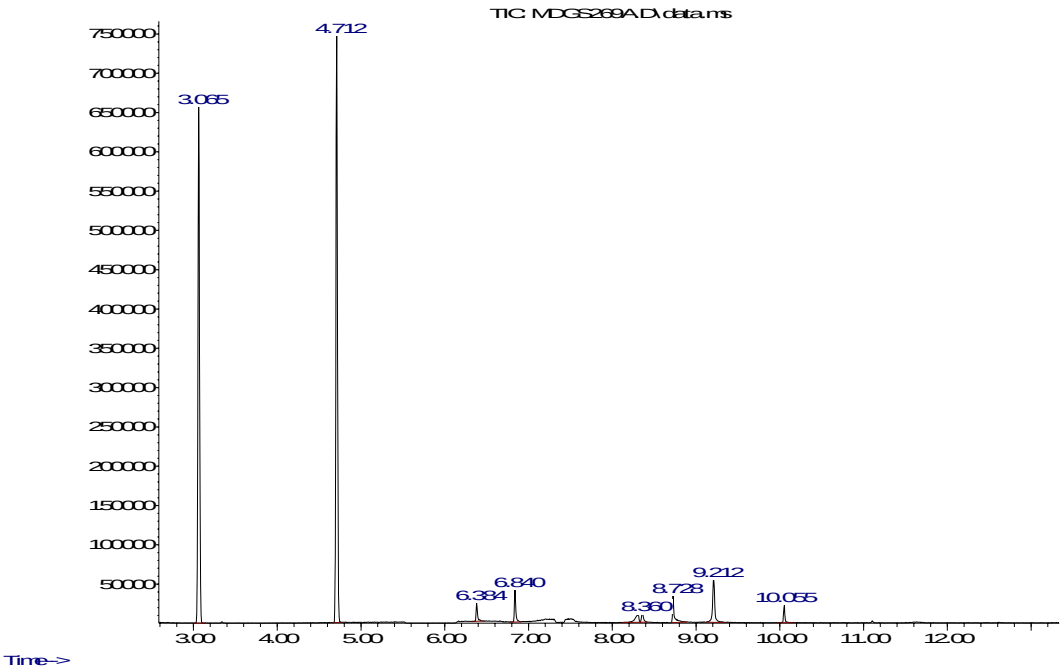

Figure 4. 7. GC of a typical nanoparticle catalyst reaction using 125mL O_2
3.06-cyclohexene, 4.71-toluene, 6.38-ene-1-ol, 6.84-ene-1-one

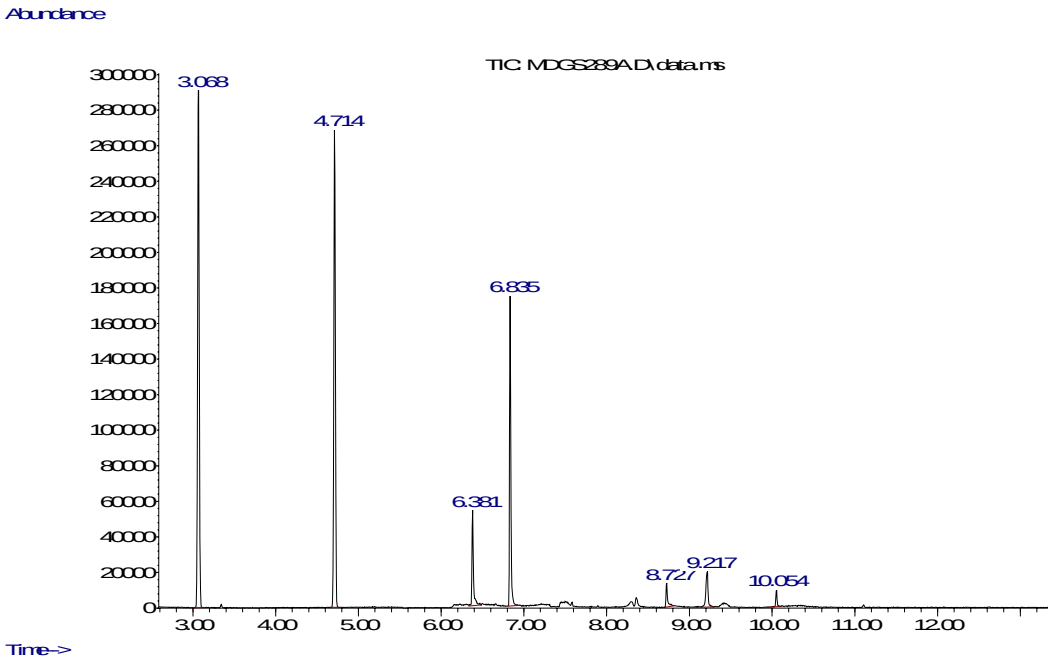

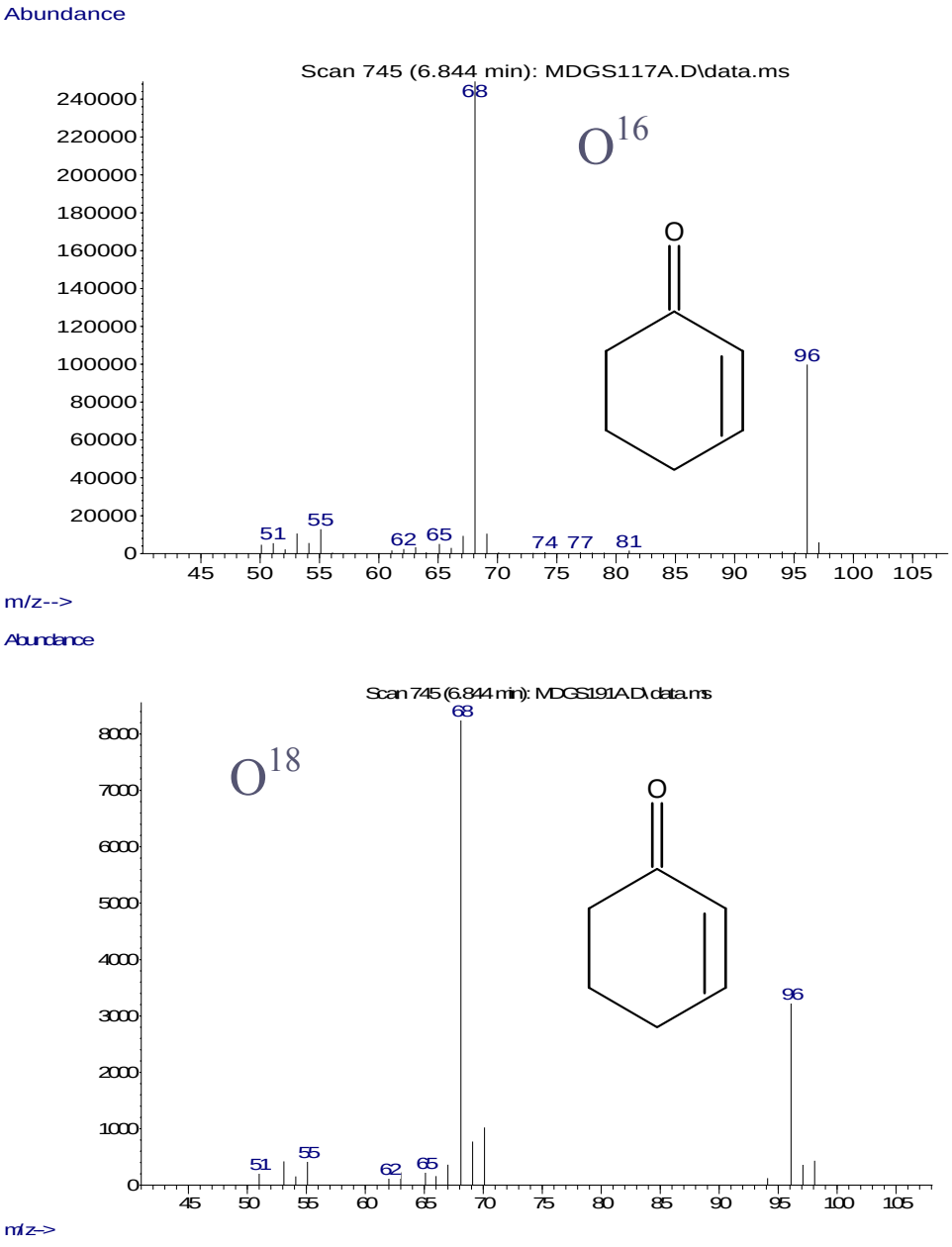

Figure 4. 8. Mass Spectra profile when using nanoparticles in 10% H_2O^{18} showing ~ 10% ^{18}O incorporation into ketone. Top O^{16} profile, bottom O^{18} profile.

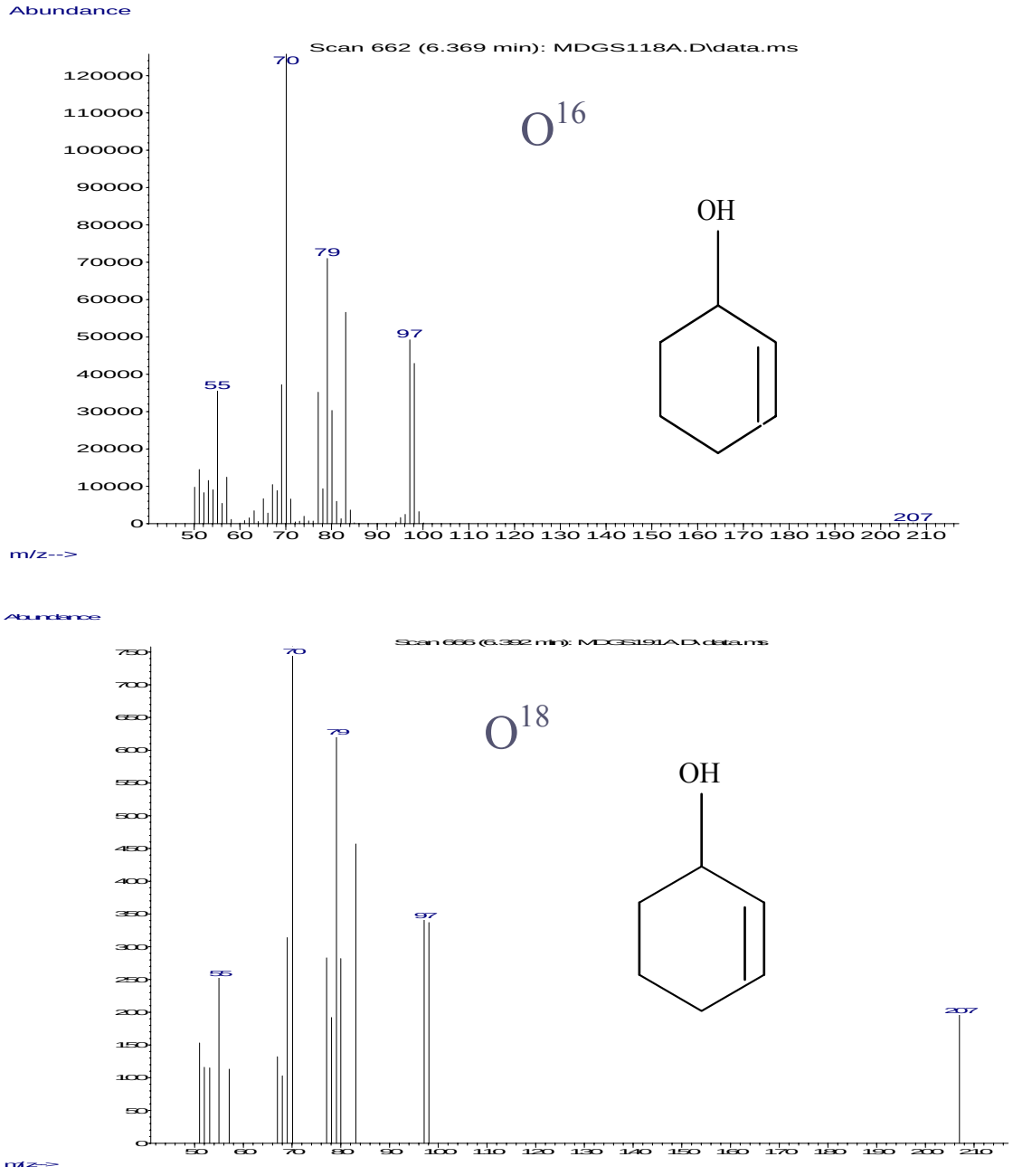

Figure 4. 9. Mass Spectra profile when using nanoparticles in 10% H_2O^{18} showing ~ 0% ^{18}O incorporation into alcohol. Top O^{16} profile, bottom O^{18} profile.

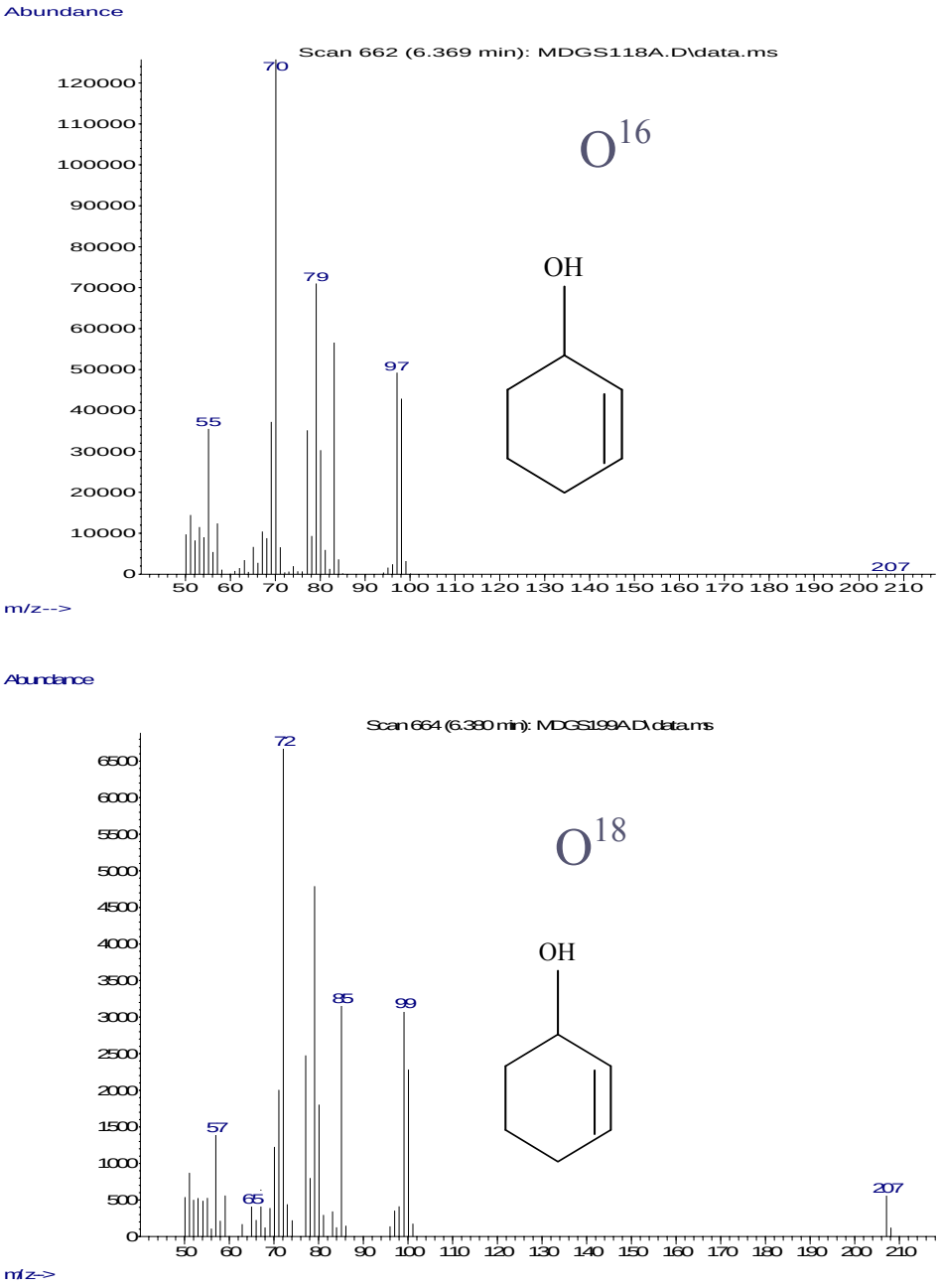

Figure 4. 10. Mass Spectra profile when using nanoparticles in H_2O with 97% ^{18}O added showing ~ 95% ^{18}O incorporation into alcohol.
Top O^{16} profile, bottom O^{18} profile.

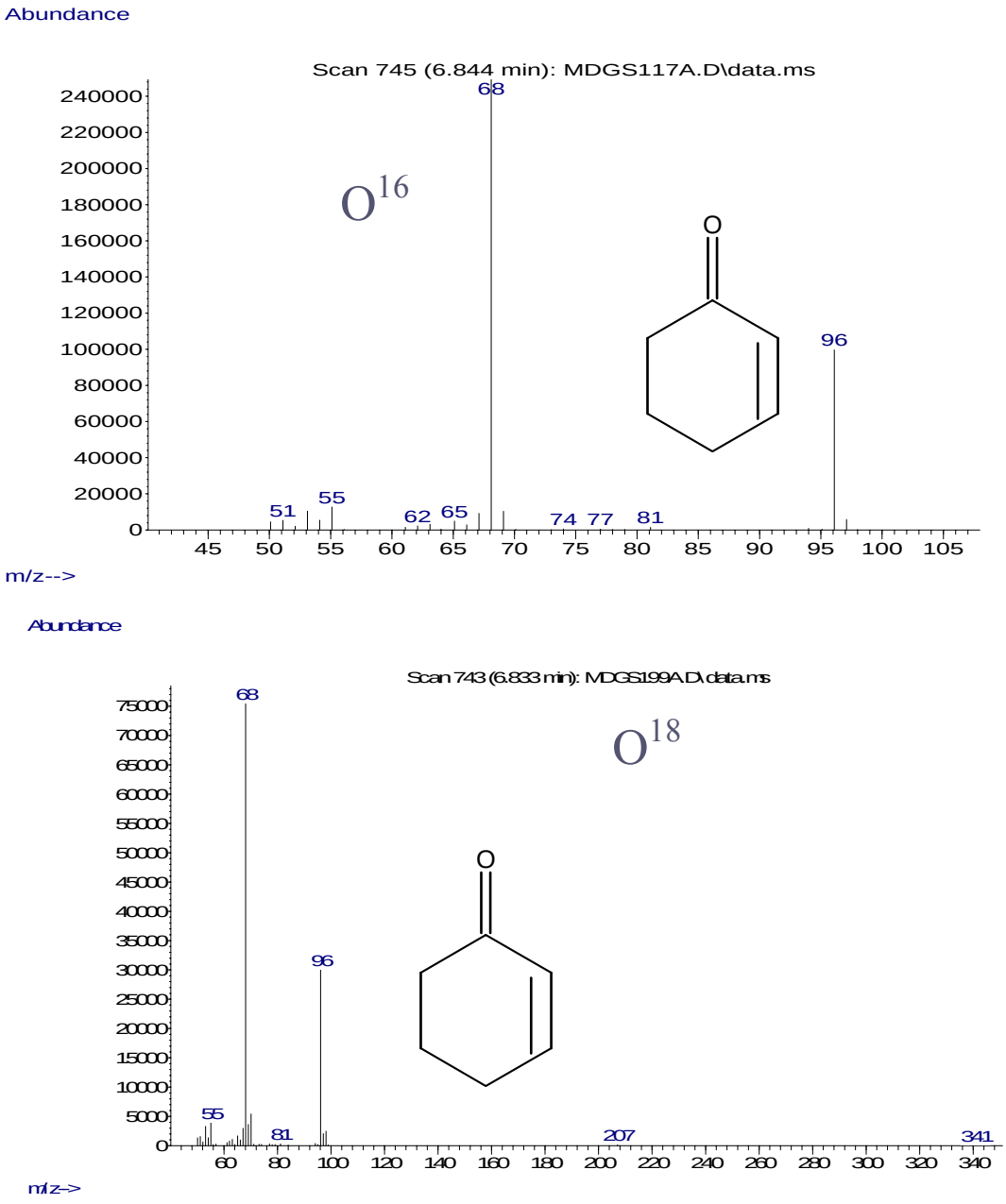

Figure 4. 11. Mass Spectra profile when using nanoparticles in H_2O with 97% ^{18}O added showing ~ 10% ^{18}O incorporation into ketone.
Top O^{16} profile, bottom O^{18} profile.

4. 6. Appendix

The standard response of GC area for each component in 2 mL CH_2Cl_2 total volume is reported below in Table 4.4:

Table 4. 4 The standard response of GC area for each component

Compounds	Response factor	Ratio to toluene	Volume used	Corrected area	Moles injected
Cyclohexene	1.30	1.76	20 μL	4040215	7.52×10^{-10}
Toluene	2.29	1	20 μL	6782091	7.17×10^{-10}
Cyclohexene oxide	1.00	2.29	20 μL	3109662	7.54×10^{-10}
2-cyclohexene 1-ol	1.21	1.90	20 μL	3877485	7.77×10^{-10}
2-cyclohexene 1-one	1.86	1.86	20 μL	4014942	7.88×10^{-10}

So we use a response factor of 1.90 for the combined products when we calculate our TON for reactions. The TON for each reaction was calculated based on the corrected area for each peak using the internal standard (toluene) and the response factor obtained in GC-MS.

E.g. *For H_2O_2 reaction:*

The 2.6 mL reaction mixture volume was extracted once with 2.8 mL dichloromethane and the layers were allowed to separate. The water fraction and some of the organic fraction was removed to leave a total volume of 2 mL (this assures the same volume for every reaction assay).

To this volume reaction is added 20 μL toluene. 4μL of the extract was diluted into 1 mL dichloromethane and then 2 μL of this solution was injected into GC-MS.

Area toluene = 12549151

Area products (total) = 225029 (alcohol) + 330657 (ketone) = 555686

Moles toluene injected in GC = 7.17×10^{-10} moles

Moles product calculated based on toluene moles, corrected area and response factor:

(Area products/Area toluene = moles products/moles toluene) x response factor

Moles products injected in GC = 6.10×10^{-11} moles

Where response factor to toluene = 1.90

Thus 6.10×10^{-11} moles products are in the 2 μL injected

Or 3.05×10^{-11} moles products are in 1 μL

So 3.05×10^{-8} moles products are in 1 mL

7.62×10^{-6} moles products from the 4 μL taken from the extract reaction solution

2.13×10^{-5} moles products in the 2.8 ml reaction solution

TON = moles products/ moles porphyrin = $2.13 \times 10^{-5} / 1.25 \times 10^{-7} = 170$

For O_2 reaction:

The 2.6 mL reaction mixture volume was extracted once with 8 mL dichloromethane and the layers were allowed to separate. The water fraction and some of the organic fraction was removed to leave a total volume of 6 mL (this assures the same volume for every reaction assay). To this volume reaction is added 20 μL toluene. 4μL of the extract was diluted into 1 mL dichloromethane and then 2 μL of this solution is injected into GC-MS.

Area toluene = 4606305

Area products (total) = 781031 (alcohol) + 2398134 (ketone) = 3179165

Moles toluene injected in GC = 2.9 $x10^{-10}$ moles

Moles product calculated based on toluene moles, corrected area and response factor:

(Area products/Area toluene = moles products/moles toluene) x response factor

Moles products injected in GC = 3.79 x 10^{-10} moles

Where response factor to toluene = 1.90

Thus 3.79 x 10^{-10} moles products are in the 2 μL injected

Or 1.89 x 10^{-10} moles products are in 1 μL

So 1.89 x 10^{-7} moles products are in 1 mL

4.74 $x10^{-5}$ moles products from the 4 μL taken from the extract reaction solution

3.79 x 10^{-4} moles products in the 8 ml reaction solution

TON = moles products/ moles porphyrin = 3.79 x 10^{-4} / 1.25 x 10^{-7} = 3037

References:

1. Stephenson, N. A.; Bell, A. T., *Inorg. Chem.* **2006,** 45, (14), 5591-5599.
2. Groves, J. T.; Nemo, T. E., *J. Am. Chem. Soc.* **1979,** 101, (105), 5786-5791.
3. Groves, J. T.; Nemo, T. E.; Meyers, R. S., *J. Am. Chem. Soc.* **1979,** 101, 1032.
4. Groves, J. T.; Haushalter, R. C.; Makamura, M.; Nemo, T. E.; Evans, B. J., *J. Am. Chem. Soc.* **1981,** 103, 2884-2886.
5. Groves, J.; Viski, P., *J. Org. Chem.* **1990,** 55, 3628.
6. Groves, J. T., *Proc. Natl. Acad. Sci., USA* **2003,** 100 (7), 3569-3574.
7. Groves, J. T., *Journal of Inorganic Biochemistry* **2006,** 100, 434-447.
8. Ortiz de Montellano, P. R., 2nd. ed.; Plenum Press: New York, **1995**.
9. Schenning, A. P. H. J.; Hubert, D. H. W.; Feiters, M. C.; Nolte, R. J. M., *Langmuir* **1996,** 12, (6), 1572-1577.
10. Mayer, J. M., Meunier, B., Ed. Imperial College Press: **2000**; pp 1-43.
11. Newcomb, M.; Hollenberg, P. F.; Coon, M. J., *Archives of Biochemistry and Biophysics* **2003,** 409, (1), 72-79.
12. Chandrasena, R. E. P.; Vatsis, K. P.; Coon, M. J.; Hollenberg, P. F.; *J. Am. Chem. Soc.* **2004,** 126, 115-126.
13. Meunier, B.; de Visser, S. P.; Shaik, S., *Chem. Rev.* **2004,** 104, 3947-3980.
14. Silaghi-Dumitrescu, R., *Journal of Biological Inorganic Chemistry* **2004,** 9, (4), 471-476.
15. Schmidt, J. A. R.; Mahadevan, V.; Getzler, Y. D. Y. L.; Coates, G. W., *Org. Lett.* **2004,** 6, (3), 373-376.

16. Mansuy, D.; Mahy, J. P.; Dureault, A.; Bedi, G.; Battioni, P., *Journal of the Chemical Society-Chemical Communications* **1984**, (17), 1161-1163.

17. Groves, J. T.; Watanabe, Y., *Inorg. Chem.* **1986,** 25, 4808-4810.

18. Barloy, L.; Battioni, P.; Mansuy, D., *Chem. Comm.* **1990**, 1365-1367.

19. Wang, C. Q.; Shalyaev, K. V.; Bonchio, M.; Carofiglio, T.; Groves, J. T., *Inorg. Chem.* **2006,** 45, (12), 4769-4782.

20. Merlau, M. L.; Cho, S. H.; Sun, S. S.; Nguyen, S. T.; Hupp, J. T., *Inorg. Chem.* **2005,** 44, (15), 5523-5529.

21. Suslick, K. S., *In the Porphyrin Handbook*, Kadish, K. M.; Smith, K. M.; Guilard, R., Eds. Academic Press: New York, **2000**; Vol.4, pp 41-63.

22. Simonneaux, G.; Le Maux, P.; Ferrand, Y.; Rault-Berthelot, J., *Coordination Chemistry Reviews* **2006,** 250, (17-18), 2212-2221.

23. Ungashe, S. B.; Groves, J. T., *Adv. Inorg. Biochem.* **1994,** 9, 317-351.

24. Ellis, P. E.; Lyons, J. E., *Catalysis Let.* **1989,** 3, 389-397.

25. Lyons, J. E.; Ellis, P. E., *Catalysis Let.* **1991,** 8, 45-51.

26. Bartoli, J. F.; Brigaud, O.; Battioni, P.; Mansuy, D., *J. Chem. Commun.* **1991**, 440-442.

27. Grinstaff, M. W.; Hill, M. G.; Labinger, J. A.; Gray, H. B., *Science* **1994,** 264, (5163), 1311-1313.

28. Grinstaff, M. W.; Hill, M. G.; Birnbaum, E. R.; Schaefer, W. P.; Labinger, J. A.; Gray, H. B., *Inorg. Chem.* **1995,** 34, 4896-4902.

29. Doro, F. G.; Smith, J. R. L.; Ferreira, A. G.; Assis, M. D., *Journal of Molecular Catalysis a-Chemical* **2000,** 164, (1-2), 97-108.

30. Traylor, T. G.; Kim, C.; Fann, W. P.; Perrin, C. L., *Tetrahedron* **1998,** 54, 7977-7986.

31. Traylor, T. G.; Xu, F., *J. Am. Chem. Soc.* **1990,** 112, 178-186.

32. Moore, K. T.; Horvath, I. T.; Therien, M. J., *Inorg. Chem.* **2000,** 39, (15), 3125-3139.

33. Nam, W.; Han, H. J.; Oh, S.-Y.; Lee, Y. J.; Choi, M.-H.; Han, S.-Y.; Kim, C.; Woo, S. K.; Shin, W., *J. Am. Chem. Soc.* **2000,** 122, 8677-8684.

34. Stephenson, N. A.; Bell, A. T., *J. Am. Chem. Soc.* **2005,** 127, (24), 8635-8643.

35. Stephenson, N. A.; Bell, A. T., *Inorg. Chem.* **2006,** 45, (6), 2758-2766.

36. Battioni, P.; Renaud, J. P.; Bartoli, J. F.; Reinaartiles, M.; Fort, M.; Mansuy, D., *J. Am. Chem. Soc.* **1988,** 110, (25), 8462-8470.

37. Higuchi, T.; Shimada, K.; Maruyama, N.; Hirobe, M., *J. Am. Chem. Soc.* **1993,** 115, (16), 7551-7552.

38. Traylor, T. G.; Popovitz-Biro, R., *J. Am. Chem. Soc.* **1988,** 110, (1), 239-243.

39. Yamaguchi, K.; Watanabe, Y.; Morishima, I., *J. Am. Chem. Soc.* **1993,** 115, (10), 4058-4065.

40. Rosenthal, J.; Pistorio, B. J.; Chng, L. L.; Nocera, D. G., *J. Org. Chem.* **2005,** 70, (5), 1885-1888.

41. Evans, S.; Lindsay, J. R., *J. Chem. Soc., Perkin Trans. 2* **2001**, 174 - 180.

42. Tolman, C. A.; Herron, N., *J. Am. Chem. Soc.* **1987** 109, 2837-2839.

43. Bedioui, F., *Coordination Chemistry Reviews* **1995,** 144, 39-68.

44. Battioni, P.; Lallier, J.-P.; Barloy, L.; Mansuy, D., *Chem. Commun.* **1989**, 1149-1151.

45. Lee, S. J.; Hupp, J. T., *Coordination Chemistry Reviews* **2006,** 250, 1710-1723.

46. Merlau, M. L.; Mejia, M. d. P.; Nguyen, S. T.; Hupp, J. T., *Angew. Chem. Int. Ed.* **2001,** 40, (22), 4239-4242.

47. Drain, C. M.; Chen., X., *In Encyclopedia of Nanoscience & Nanotechnology*, Nalwa, H. S., Ed. American Scientific Press: New York, **2004**; Vol. 9, pp 593-616.

48. Drain, C. M.; Smeureanu, G.; Batteas, J.; Patel, S., *In Dekker Encyclopedia of Nanoscience and Nanotechnology*, Schwartz, J. A.; Contescu, C. I.; Putyera, K., Eds. Marcel Dekker, Inc.: New York, **2004**; Vol. 5, pp 3481-3502.

49. Drain, C. M.; Bazzan, G.; Milic, T.; Vinodu, M.; Goeltz, J. C., *Israel J. Chem.* **2005,** 45, 255-269.

50. Drain, C. M.; Goldberg, I.; Sylvain, I.; Falber, A., *Topics in Current Chemistry* **2005,** 245, 55–88.

51. Gong, X.; Milic, T.; Xu, C.; Batteas, J. D.; Drain, C. M., *J. Am. Chem. Soc.* **2002,** 124, (48), 14290-14291.

52. Drain, C. M.; Smeureanu, G.; Patel, S.; Gong, X.; Garno, J.; Arijeloye, J., *New J. Chem.* **2006,** 30, 1834-1843.

53. Limberg, C., *Angew. Chem. Int. Ed.* **2003,** 42, 5932 - 5954.

54. Patzelt, H.; Woggon, W. D., *Helv. Chim. Acta* **1992,** 75, 523.

55. Lee, A. L.; Nam, W., *J. Am. Chem. Soc.* **1997,** 119, 1916-1922.

56. Mansuy, D., *Coordination Chemistry Reviews* **1993,** 125, (1-2), 129-141.

57. Drain, C. M.; Gentemann, S.; Roberts, J. A.; Nelson, N. Y.; Medforth, C. J.; Jia, S.; Simpson, M. C.; Smith, K. M.; Fajer, J.; Shelnutt, J. A.; Holten, D., *J. Am. Chem. Soc.* **1998,** 120, (15), 3781-3791.

58. Drain, C. M.; Kirmaier, C.; Medforth, C. J.; Nurco, D. J.; Smith, K. M.; Holten, D., *J. Phys. Chem.* **1996,** 100, (29), 11984-11993.

59. Retsek, J. L.; Drain, C. M.; Kirmaier, C.; Nurco, D. J.; Medforth, C. J.; Smith, K. M.; Sazanovich, I. V.; Chirvony, V. S.; Fajer, J.; Holten., D., *J. Am. Chem. Soc.* **2003,** 125, 9787-9800.

60. Garno, J. C.; Xu, C.; Bazzan, G.; Batteas, J. D.; Drain, C. M., Schubert, U. S.; Newcome, G. R.; Manners, I., Eds. American Chemical Society: Washington, DC., **2006**; Vol. 928, pp 168-183.

61. Drain, C. M.; Gong, X., *Chem. Commun.* **1997**, 2117-2118.

BIBLIOGRAPHY

Research outline

1. Chambron, J.-C.; Heitz, V.; Sauvage, J.-P., *In The Porphyrin Handbook*, Kadish, K. M.; Smith, K. M.; Guilard, R., Eds. Academic Press: New York, **2000**; Vol. 6, 1-42.
2. Lehn, J.-M., *Pure Appl. Chem.* **1994,** 66, (10/11), 1961-1966.
3. Belanger, S.; Hupp, J. T., *Angew. Chem., Int .Ed.* **1999,** 38, 2222 - 2224.
4. Drain, C. M.; Nifiatis, F.; Vasenko, A.; Batteas, J., *Angew. Chem., Int. Ed* **1998,** 37, 2344-2347.
5. Kosal, M. E.; Chou, J.-H.; Nalwa, H. S.; Rakow, N. A.; Suslick, K. S., Academic Press: New York, **2000**; Vol. 6, p 43-131.
6. Lehn, J.-M., *Angew. Chem. Int. Ed. Engl.* **1990,** 29, 1304-1319.
7. Drain, C. M., *Proc. Natl. Acad. Sci., USA* **2002,** 99, 5178.
8. Drain, C. M.; Batteas, J. D.; Flynn, G. W.; Milic, T.; Chi, N.; Yablon, D. G.; Sommers, H., *Proc. Natl. Acad. Sci., USA* **2002,** 99, 6498-6502.
9. Milic, T. N.; Chi, N.; Yablon, D. G.; Flynn, G. W.; Batteas, J. D.; Drain, C. M., *Angew. Chem. Int. Ed.* **2002,** 41, (12), 2117-2119.
10. Drain, C. M.; Mauzerall, D. C., *Biophysic. Journal.* **1992,** 63, 1544-1555.
11. Drain, C. M.; Mauzerall D. C, *Biochemistry and Bioenergetics.* **1990,** 24, 263-268.
12. Drain, C. M.; Christensen, B.; Mauzerall, D.C., *Proc. Natl. Acad. Sci., USA* **1989,** 86, 6959-6962.

13. Drain, C. M.; Hupp, J. T.; Suslick, K. S.; Wasielewski, M. R.; Chen, X., *Journal of Porphyrins and Phthalocyanines* **2002,** 6, (4), 243-258.

14. Ogawa, K.; Zhang, T.; Yoshihara, K.; Kobuke, Y., *J. Am. Chem. Soc.* **2002,** 124, 23.

15. Alivisatos, A. P.; Barbara, P. F.; Castleman, A. W.; Chang, J.; Dixon, D. A.; Klein, M. L.; McLendon, G. L.; Miller, J. S.; Ratner, M. A.; Rossky, P. J.; Stupp, S. I.; Thompson, M. E., *Adv. Mater.* **1998,** 10, (16), 1297-1336.

16. Epstein, A. J., *MRS Bulletin* **2000**, Vol.25, 11, 33-40.

Chapter 1

1. Blankenship, R. E., *Molecular Mechanisms of Photosynthesis* **2002**.

2. Mauzerall, D. C., *Clinics Derm.* **1998,** 16, 195-201.

3. Jacoby, M., *Chem. Engineering News* **2004**, 29-32.

4. Brabec, C. J.; Sariciftci, N. S.; Hummelen, J. C., *Adv. Funct. Mater.* **2001,** 11, 15- 26.

5. Shaheen, S. E.; Brabec, C. J.; Sariciftci, N. S.; Padinger, F.; Fromherz, T.; Hummelen, J. C., *Appl. Phys .Lett.* **2001,** 78, 841-843.

6. Hoppe, H.; Sariciftci, N. S., *J. Mater. Res.* **2004,** 19, 1924-1945.

7. Linke-Schaetzel, M.; Bhise, A. D.; Gliemann, H.; Koch, T.; Schimmel, T.; Balaban, T. S., *Thin Solid Films* **2004,** 451-452, 16-21

8. van Grondelle, R.; Dekker, J. P.; Gillbro, T.; Sundstrom, V., *Biochim. Biophys. Acta* **1994,** 1187, 1-65.

9. Andrizhiyevskaya, E. G.; Frolov, D.; van Grondelle, R.; Dekker, J. P.,

Biochim.Biophys. Acta **2004**.

10. Bahatyrova, S.; Frese, R. N.; Siebert, C. A.; Olsen, J. D.; van der Werf, K.; van Grondelle, R.; Niederman, R. A.; Bullough, P. A.; Otto, C.; Hunter, C. N., *Nature* 2004**,** 430, 1058-1062.
11. Brookfield, R. L.; Ellul, H.; Harriman, A.; Porter, G., *J. Chem. Soc.* **1986,** 82, 219-233.
12. Davila, J.; Harriman, A.; Milgrom, L. R., *Chem. Phys. Lett.* **1987,** 136, 427-430.
13. Gust, D.; Moore, T. A.; Moore, A. L.; Gao, F.; Luttrull, D.; DeGraziano, J. M.; Ma, X. C.; Makings, L. R.; Lee, S. -J.; Trier, T. T.; Bittersmann, E.; Seely, G. R.; Woodward, S.; Bensasson, R. V.; Rougée, M.; De Schryver, F. C.; Van der Auweraer, M., *J. Am. Chem. Soc.* **1991,** 113, 3638-3649.
14. Gensch, T.; Hofkens, J.; Herrmann, A.; Tsuda, K.; Verheijen, W.; Vosch, T.; Christ, T.; Basché, T.; Müllen, K.; De Schryver, F. C., *Angew. Chem. Int. Ed.* **1999,** 38, 3752-3756.
15. Hofkens, J.; Maus, M.; Gensch, T.; Vosch, T.; Cotlet, M.; Köhn, F.; Herrmann, A.; Müllen, K.; De Schryver, F., *J. Am. Chem. Soc.* **2000,** 122, 9278-9288.
16. Adronov, A.; Fréchet, J. M., *J. Chem. Commun.* **2000**, 1701-1710.
17. Fleischer, E. B.; Shachter, A. M., *Inorg. Chem.* **1991,** 30, 3763-3769.
18. Drain, C. M.; Lehn, J.-M., *Chem. Commun.* **1994**, 2313-2315.
19. Drain, C. M.; Bazzan, G.; Milić, T.; Vinodu, M.; Goeltz, J. C., *Israel J. Chem* **2005,** 45, 255-269.
20. Balaban, T. S.; Eichhöfer, A.; Prische, M. J.; Lehn, J.-M., *Helv. Chim. Acta*

2006, 89, 333-351

21. Blankenship, R. E.; Olson, J. M.; Miller, M., *Kluwer Academic Publishers: Dordrecht, The Netherlands,* **1995**, 399-435.

22. Blankenship, R. E.; Brune, D. C.; Wittmershaus, B. P., *Kluwer Academic Publishers: Dordrecht, The Netherlands,* **1998**, 32-46.

23. Frigaard, N. U.; Bryant, D. A., *Microbiol. Monogr. Springer-Verlag: Berlin* **2006**.

24. Balaban, T. S.; Holzwarth, A. R.; Schaffner, K.; Boender, G.-J.; de Groot, H. J. M., *Biochemistry* **1995,** 34, 15259-15266.

25. Balaban, T. S.; Tamiaki, H.; Holzwarth, A. R.; Würthner, F., *Ed. Topics Curr. Chem. Springer Verlag: Heidelberg* **2005**.

26. Balaban, T. S., *Encyclopedia of Nanoscience and Nanotechnology* **2004,** 4, 505- 559.

27. Harvey, P. D., *In The Porphyrin Handbook,* **2003,** 18, 63-250.

28. Drain, C.; Fischer, R.; Nolen, E.; Lehn, J., *Chem. Commun.* **1993**, 243-245.

29. Drain, C.; Russel, K.; Lehn, J.-M., *Chem. Commun.* **1996**, 337-338.

30. Drain, C. M.; Goldberg, I.; Sylvain, I.; Falber, A., *Top Curr Chem* **2005,** 245, 55- 88.

31. Shi, X.; Barkigia, K. M.; Fajer, J.; Drain, C. M., *J. Org. Chem.* **2001,** 66, 6513-6522.

32. Fouquey, C.; Lehn, J.-M.; Levelut, A.-M., *Adv. Mater* **1990,** 2, 254-257.

33. Gulik-Krzywicki, T.; Fouquey, C.; Lehn, J.-M., *Proc. Natl. Acad. Sci .USA* **1993,** 90, 163-167.

34. Berl, V.; Schmutz, M.; Krische, M. J.; Khoury, R.G.; Lehn, J.-M.,*Chem. Eur.J* **2002,** 8, 1227-1244.

35. Lehn, J.-M., *Supramolecular Chemistry. Concepts and Perspectives* **1995**.

36. Drain, C. M.; Shi, X.; Milić, T.; Nifiatis, F., *Chem. Commun.* **2004**, 287-288.

37. Gong, X.; Milić, T.; Xu, C.; Batteas, J. D.; Drain, C. M., *J. Am. Chem. Soc.* **2002,** 124, 14290- 14291.

Chapter 2

1. Alivisatos, A. P.; Barbara, P. F.; Castleman, A. W.; Chang, J.; Dixon, D. A.; Klein, M. L.; McLendon, G. L.; Miller, J. S.; Ratner, M. A.; Rossky, P. J.; Stupp, S. I.; Thompson, M. E., *Adv. Mater.* **1998,** 10, (16), 1297–1336.

2. Tour, J. M., *Acc. Chem. Res.* **2000,** 33, (11), 791–804.

3. Lent, C. S., *Science* **2000,** 88, 1597-1599.

4. Fox, M. A., *Acc. Chem. Res.* **1999,** 32, (3), 201-207.

5. Ellenbogen, J. C.; Love, J. C., *Proc. IEEE* **2000,** 88, (3), 386-426.

6. Mauzerall, D. C., *Clin. Dermatol.* **1998,** 16, 195-201.

7. Adler, A. D.; Longo, F. R.; Shergalis, W., *J. Am. Chem. Soc.* **1964,** 86, (15), 3145-3149.

8. Lindsey, J. S., *Eds. Academic Press: New York* **2000,** 1, 45-118.

9. Drain, C. M.; Gong, X., *Chem. Commun* **1997**, 2117-2118.

10. Chou, J.-H.; Kosal, M. E.; Nalwa, H. S.; Rakow, N. A.; Suslick, K. S., *Eds. Academic Press: New York* **2000,** 6, 43-131.

11. Drain, C. M.; Hupp, J. T.; Suslick, K. S.; Wasielewski, M. R.; Chen, X., *J.*

Porphy. Phthalocyanines **2002,** 6, (4), 241-256.

12. Chambron, J.-C.; Heitz, V.; Sauvage, J.-P., *Eds. Academic Press: New York* **2000,** 6, 1-42.
13. Valkova, L.; Borovkov, N.; Kopranenkov, V.; Pisani, M.; Bossi, M.; Rustichelli, F., *Mater. Sci. Eng.* **2002,** 22, (2), 167–170.
14. Valkova, L.; Borovkov, N.; Maccioni, E.; Pisani, M.; Rustichelli, F.; Erokhin, V.; Patternolli, C.; Nicolini, C., *Colloids Surf. A Physicochem. Eng. Asp* **2002,** 198-200, 891- 896.
15. Lange, S. J.; Nie, H.; Stern, C. L.; Barrett, A. G. M.; Hoffman, B. M., *Inorg. Chem.* **1998,** 37, (25), 6435–6443.
16. Engelkamp, H.; Middelbeek, S.; Nolte, R. J. M., *Science* **1999,** 284, (5415), 785–788.
17. Burrell, A. K.; Wasielewski, M. R., *J. Porphy. Phthalocyanines* **2000,** 4, (5), 401- 406.
18. Fabbrizzi, L.; Licchelli, M.; Pallavicini, P., *Acc. Chem. Res.* **1999,** 32, (10), 846– 853.
19. Wagner, R. W.; Lindsey, J. S.; Seth, J.; Palaniappan, V.; Bocian, D. F., *J. Am. Chem. Soc.* **1996,** 118, (16), 3996–3997.
20. Mines, G. A.; Tzeng, B. C.; Stevenson, K. J.; Li, J.; Hupp, J. T., *Angew. Chem, Int. Ed. Engl.* **2002,** 41, (1), 154-157.
21. Rakow, N. A.; Suslick, K. S., *Nature* **2000,** 406, 710-713.
22. Andrew, R.; Seiji, S., *Coord. Chem. Rev.* **2000,** 205, (1), 157-199.
23. Sun, S.-S.; Lees, A. J., *Coord. Chem. Rev.* **2002,** 230, (1-2), 170–191.

24. Wosnick, J. H.; Swager, T. M., *Chem. Biol.* **2000,** 4, (6), 715-720.

25. Diskin-Posner, Y.; Dahal, S.; Goldberg, I., *Angew. Chem., Int. Ed. Engl.* **2000,** 39, (7), 1288–1292.

26. Diskin-Posner, Y.; Patra, G. K.; Goldberg, I., *Eur. J. Inorg. Chem.* **2001,** 10, (2515-2523).

27. Goldberg, I., *Cryst. Eng. Commun.* **2002,** 4, 109-116.

28. Kumar, R. K.; Diskin-Posner, Y.; Goldberg, I., *J. Incl. Phenom. Macrocycl. Chem.* **2000,** 37, 219-230.

29. Lu, X.; Jin, J.; Kang, J.; Lv, B.; Liu, H.; Geng, Z., *Mater. Chem. Phys.* **2003,** 77, (3), 952–957.

30. Ikeda, A.; Ayabe, M.; Shinkai, S.; Sakamoto, S.; Yamaguchi, K., *Org. Lett.* **2000,** 2, (23), 3707–3710.

31. Johnston, M. R.; Latter, M. J.; Warrener, R. N., *Org. Lett.* **2002,** 4, (13), 2165-2168.

32. Lehn, J.-M., *Proc. Natl. Acad. Sci.U. S. A* **2002,** 99, (8), 4763–4768.

33. Lehn, J.-M., *Angew. Chem., Int. Ed. Engl.* **1990,** 29, 1304-1319.

34. Lehn, J.-M., *Pure Appl. Chem.* **1994,** 66, (10/11), 1961–1966.

35. Lawrence, D. S.; Jiang, T.; Levett, M., *Chem. Rev* **1995,** 95, (6), 2229–2260.

36. Moulton, B.; Zaworotko, M. J., *Chem. Rev.* **2001,** 101, (6), 1629–1658.

37. Nguyen, S. T.; Gin, D. L.; Hupp, J. T.; Zhang, X., *Proc. Natl. Acad. Sci. U.S.A* **2001,** 98, (21), 11849–11850.

38. Tabellion, F. M.; Seidel, S. R.; Arif, A. M.; Stang, P. J., *J. Am. Chem. Soc.* **2001,**123, (31), 7740–7741.

39. Whitesides, G. M.; Simanek, E. E.; Mathias, J. P.; Seto, C. T.; Chin, D. N.; Mammen, M.; Gordon, D. M., *Acc. Chem. Res.* **1995,** 28, (1), 37–44.

40. Aakeroy, C. B.; Seddon, K. R., *Chem. Soc. Rev.* **1993**, 397–407.

41. Desiraju, G. R., *Acc. Chem. Res.* **2002,** 35, (7), 565–573.

42. Drain, C. M., *Proc. Natl. Acad. Sci. U. S. A.* **2002,** 99, 5178-5182.

43. Drain, C. M.; Batteas, J. D.; Flynn, G. W.; Milic, T.; Chi, N.; Yablon, D. G.; Sommers, H., *Proc. Natl. Acad. Sci.U.S.A.* **2002,** 99, 6498–6502.

44. Milic, T. N.; Chi, N.; Yablon, D. G.; Flynn, G. W.; Batteas, J. D.; Drain, C.M *Angew.Chem., Int. Ed. Engl.* **2002,** 41, 2117–2119.

45. Ishida, A.; Majima, T., *Chem. Commun.* **1999**, 1299-1300.

46. Kong, D.-S.; Wan, L.-J.; Han, M.-J.; Pan, G.-B.; Lei, S.-B.; Bai, C.-L.; Chen, S.- H., *Electrochim. Acta* **2002,** 48, (4), 303–309.

47. Imae, T.; Niwa, T.; Zhang, Z., *J. Nanosci. Nanotechnol.* **2002,** 2, (1), 37–40.

48. Oberg, K.; Eliasson, B., *Mater. Lett* **2001,** 49, (3-4), 147–153.

49. Sarno, D. M.; Grosfeld, D.; Jiang, B.; Afriyie, J. O.; Matienzo, L. J.; Jones, W. E., Jr, *Langmuir* **2000,** 16, (15), 6191–6199.

50. Drain, C. M.; Shi, X.; Milic, T.; Nifiatis, F., *Chem. Commun.* **2001**, 287–288.

51. Gong, X.; Milic, T.; Xu, C.; Batteas, J. D.; Drain, C. M., *J. Am. Chem. Soc.* **2002,** 124, (48), 14290–14291.

52. Kwok, K. S.; Ellenbogen, J. C., *Moletronics: Mater.Today* **2002,** 5, (2), 28–37.

53. Merlau, M. L.; Mejia, M. D. P.; Nguyen, S. T.; Hupp, J. T., *Angew. Chem. Int. Ed. Engl* **2001,** 40, (22), 4239–4242.

54. Borovkov, V. V.; Lintuluoto, J. M.; Sugeta, H.; Fujiki, M.; Arakawa, R.;

Inoue, Y., *J. Am. Chem. Soc.* **2002,** 124, (12), 2993–3006.

55. Ogawa, K.; Zhang, T.; Yoshihara, K.; Kobuke, Y., *J. Am. Chem. Soc.* **2002,** 124, (1), 22–23.

56. Aratani, N.; Osuka, A.; Kim, Y. H.; Jeong, D. H.; Kim, D., *Angew. Chem., Int. Ed. Engl.* **2000,** 39, (8), 1458–1462.

57. Aratani, N.; Osuka, A., *Org. Lett.* **2001,** 3, (26), 4214–4216.

58. Ambroise, A.; Wagner, R. W.; Rao, P. D.; Riggs, J. A.; Hascoat, P.; Diers, J. R.; Seth, J.; Lammi, R. K.; Bocian, D. F.; Holten, D.; Lindsey, J. S., *Chem. Mater.* **2001,** 13, (3), 1023–1034.

59. Benites, M. D. R.; Johnson, T. E.; Weghorn, S.; Yu, L.; Rao, P. D.; Diers, J. R.; Yang, S. I.; Kirmaier, C.; Bocian, D. F.; Holten, D.; Lindsey, J. S., *J. Mater.Chem.* **2002,** 12, (1), 65–80.

60. Drain, C. M.; Christensen, B.; Mauzerall, D., *Proc. Natl. Acad. Sci. U. S. A.* **1989,** 86, 6959–6962.

61. Drain, C. M.; Mauzerall, D., *Bioelectrochem.Bioenerg.* **1990,** 24, 263–266.

62. Drain, C. M.; Fischer, R.; Nolen, E.; Lehn, J. M., *Chem. Commun.* **1993**, 243–245.

63. Drain, C. M.; Lehn, J. M., *Chem. Commun.* **1994**, 2313–2315.

64. Araki, K.; Wagner, M. J.; Wrighton, M. S., *Langmuir* **1996,** 12, (22), 5393–5398.

65. Guldi, D. M.; Pellarini, F.; Prato, M.; Granito, C.; Troisi, L., *Nano Lett* **2002,** 2, (9), 965–968.

66. Qian, D.-J.; Nakamura, C.; Miyake, J., *Chem.Commun.* **2001**, 2312–2313.

67. Imahori, H.; Arimura, M.; Hanada, T.; Nishimura, Y.; Yamazaki, I.; Sakata, Y.; Fukuzumi, S., *J. Am. Chem. Soc.* **2001,** 123, (2), 335–336.

68. Nishimura, N.; Ooi, M.; Shimazu, K.; Fujii, H.; Uosaki, K., *J. Electroanal.Chem.* **1999,** 473, (1-2), 75–84.

69. Imahori, H.; Hasobe, T.; Yamada, H.; Nishimura, Y.; Yamazaki, I.; Fukuzumi, S., *Langmuir* **2001,** 38, (9), 1257–1261.

70. Ashkenasy, G.; Kalyuzhny, G.; Libman, J.; Rubinstein, I.; Shanzer, A., *Angew. Chem., Int. Ed.Engl.* **1999,** 38, (9), 1257–1261.

71. Foubert, P.; Vanoppen, P.; Martin, M.; Gensch, T.; Hofkens, J.; Helser, A.; Seeger, A.; Taylor, R. M.; Rowan, A. E.; Nolte, R. J. M.; Schryver, F. C. D., *Nanotechnology* **2000,** 11, (1), 16–23.

72. Latterini, L.; Blossey, R.; Hofkens, J.; Vanoppen, P.; De Schryver, F. C.; Rowan, A. E.; Nolte, R. J. M., *Langmuir* **1999,** 15, (10), 3582–3588.

73. Collings, P. J., *Liquid Crystals; Princeton University Press: Princeton, NJ,* **1990**.

74. Simon, J.; Bassoul, P.; Leznoff, C. C.; Lever, A. B. P., *Phthalocyanines: Properties and Applications; VCH: New York,* **1989,** 2.

75. Donnio, B.; Bruce, D. W., *In Structure and Bonding; Springer-Verlag: Berlin* **1999,** 95, 193-247.

76. Monobe, H.; Miyagawa, Y.; Mima, S.; Sugino, T.; Uchida, K.; Shimizu, Y., *Thin Solid Films* **2001,** 393, 217-224.

77. Shimizu, Y.; Matsuno, J.; Miya, M.; Nagata, A., *Chem. Commun.* **1994**, 2411-2412.

78. Patel, B. R.; Suslick, K. S., *J. Am. Chem. Soc.* **1998,** 120, 11802-11803.

79. Van Nostrum, C. F.; Nolte, R. J. M., *Chem. Commun.* **1996**, 2385- 2392.

80. Kugimiya, S.; Takemura, M., *Tetrahedron Lett.* **1990,** 31, 3157-3160.

81. Liu, C.-Y.; Pan, H.-L.; Fox, M. A.; Bard, A. J., *Science* **1993,** 261, 897-899.

82. Adams, D. M.; Kerimo, J.; Liu, C.-Y.; Bard, A. J.; Barbara, P. F., *J. Phys. Chem. B* **2000,** 104, 6728-6736.

83. Kimura, M.; Saito, Y.; Ohta, K.; Hanabusa, K.; Shirai, H.; Kobayashi, N., *J. Am. Chem. Soc.* **2002,** 124, 5274-5275.

84. Burrows, H. D.; Gonsalves, A. M. R.; Leitao, M. L. P.; Miguel, M. d. G.; Pereira, M. M., *Supramol. Sci.* **1997,** 4, 241-246.

85. Zhang, Z.; Yoshida, N.; Imae, T.; Xue, Q.; Bai, M.; Jiang, J.; Liu, Z., *J. Colloid Interface Sci.* **2001,** 243, 382-387.

86. Lei, S. B.; Wang, C.; Yin, S. X.; Wang, H. N.; Xi, F.; Liu, H. W.; Xu, B.; Wan, L. J.; Bai, C. L., *J. Phys. Chem. B* **2001,** 105, 10838-10841.

87. Ohshiro, T.; Ito, T.; Buhlmann, P.; Umezawa, Y., *Anal. Chem.* **2001,** 73, 878-883.

88. Qui, X.; Wang, C.; Zeng, Q.; Xu, B.; Yin, S.; Wang, H.; Xu, S.; Bai, C., *J. Am. Chem. Soc.* **2000,** 122, 5550-5556.

89. Drain, C. M.; Mauzerall, D. C., *Biophys. J.* **1992,** 63, 1556-1563.

90. Drain, C. M.; Mauzerall, D. C., *Biophys. J.* **1992,** 63, 1544-1555.

91. Holten, D.; Bocian, D. F.; Lindsey, J. S., *Acc. Chem. Res.* **2002,** 35, (1), 57–69.

92. Sharma, C. V. K.; Broker, G. A.; Szulczewski, G. J.; Rogers, R. D., *Chem. Commun.* **2000**, 1023–1024.

93. Zhang, Z.; Imae, T., *Nano Lett.* **2000,** 1, (5), 241–243.

94. Thomas, P. J.; Berovic, N.; Laitenberger, P.; Palmer, R. E.; Bampos, N.; Sanders, J. K. M., *Chem. Phys. Lett.* **1998,** 294, (1-3), 229–232.

Chapter 3

1. Drain, C. M.; Goldberg, I.; Sylvain, I.; Falber, A., *Topics in Current Chemistry* **2005,** 245, 55–88.

2. Drain, C. M.; Smeureanu, G.; Batteas, J.; Patel, S., *Dekker Encyclopedia of Nanoscience and Nanotechnology*, **2004,** 5, 3481-3502.

3. Drain, C. M.; Chen, X., *Encyclopedia of Nanoscience & Nanotechnology* **2004,** 9, 593-616.

4. Mauzerall, D. C., *Clin. Dermat.* **1998,** 16, 195-201.

5. Drain, C. M.; Bazzan, G.; Milic, T.; Vinodu, M.; Goeltz, J. C., *Israel J. Chem.* **2005,** 45, 255-269.

6. Drain, C. M.; Christensen, B.; Mauzerall, D. C., *Proc. Natl. Acad. Sci., USA* **1989,** 86, 6959-6962.

7. Drain, C. M.; Mauzerall, D., *Bioelectrochem. Bioenerg.* **1990,** 24, 263-266.

8. Drain, C. M.; Mauzerall, D. C., *Biophys. J.* **1992**, 1544-1555 .

9. Drain, C. M.; Mauzerall, D. C., *Biophys. J.* **1992,** 63, 1556-1563.

10. Drain, C. M.; Fischer, R.; Nolen, E.; Lehn, J. M., *Chem. Commun.* **1993**, 243-245.

11. Drain, C. M.; Gong, X., *Chem. Commun.* **1997**, 2117-2118.

12. Shi, X.; Barkigia, K. M.; Fajer, J.; Drain, C. M., *J. Org. Chem* **2001,** 66, 6513-6522.

13. Drain, C. M.; Shi, X.; Milic, T.; Nifiatis, F., *Chem. Commun.* **2001**, 287-288.

14. Drain, C. M.; Lehn, J.-M., *Chem. Commun.* **1994**, 2313-2315.

15. Drain, C. M.; Nifiatis, F.; Vasenko, A.; Batteas, J. D., *Angew. Chem. Int. Ed.* **1998,** 37, 2344-2347.

16. Drain, C. M., *Proc. Natl. Acad. Sci., USA* **2002,** 99, 5178-5182.

17. Kuramochi, Y.; Satake, A.; Kobuke, Y., *J. Am. Chem. Soc* **2004,** 126, 8668-8669.

18. Kobuke, Y., *J. Porph. Phthal.* **2004,** 8, 156-174.

19. Kobuke, Y.; Nagata, N., *Mol. Cryst. Liq. Cryst.* **2000,** 342, 51-56.

20. Gong, X.; Milic, T.; Xu, C.; Batteas, J. D.; Drain, C. M., *J. Am. Chem. Soc* **2002,** 124, 14290-14291.

21. Milic, T. N.; Chi, N.; Yablon, D. G.; Flynn, G. W.; Batteas, J. D.; Drain,C. M., *Angew. Chem., Int. Ed.* **2002,** 41, 2117-2119.

22. Drain, C. M.; Batteas, J. D.; Flynn, G. W.; Milic, T.; Chi, N.; Yablon, D. G.; Sommers, H., *Proc. Natl. Acad. Sci., USA* **2002,** 9, 6498-6502.

23. Lensen, M. C.; Takazawa, K.; Elemans, J.; Jeukens, C.; Christianen, P. C. M.; Maan, J. C.; Rowan, A. E.; Nolte, R. J. M., *Chem . Eur. J.* **2004,** 10, 831-839.

24. Elemans, J.; Rowan, A. E.; Nolte, R. J. M., *J. Mater. Chem.* **2003,** 13, 2661-2670.

25. Elemans, J.; Nolte, R. J. M.; Rowan, A. E., *J. Porph. Phthal.* **2003,** 7, 249-254.

26. Latterini, L.; Blossey, R.; Hofkens, J.; Vanoppen, P.; De Schryver, F. C.;

Rowan, A. E.; Nolte, R. J. M., *Langmuir* **1999,** 15, 3582-3588.

27. Foekema, J.; Schenning, A. P. H. J.; Vriezema, D. M.; G., B. B.; Norgaard, K.; Kroon, J. K. M.; Bjornholm, T.; Feiters, M.; A. Rowan, E.; Nolte, R. J. M., *J. Phys. Org. Chem.* **2001,** 14, 501-512.

28. Chen, X.; Hui, L.; Foster, D. A.; Drain, C. M., *Biochem* **2004,** 43, 10918-10929.

29. Xu, W.; Guo, H.; Akins, D. L., *J. Phys. Chem. B* **2001,** 105, 1543-1546.

30. Komatsu, T.; Tsuchida, E.; Böttcher, C.; Donner, D.; Messerschmidt, C.; Siggel, U.; StockerW. ; Rabe, J. P.; Fuhrhop, J.-H., *J. Am. Chem. Soc.* **1997,** 119, 11660-11665.

31. Shirakawa, M.; Kawano, S.-i.; Fujita, N.; Sada, K.; Shinkai, S., *J. Org. Chem.* **2003,** 68, 5037-5044.

32. Togashi, D. M.; Costa, S. M. B.; Sobral, A.; Gonsalves, A., *J. Phys. Chem. B* **2004,** 108, 11344-11356.

33. Terech, P.; Scherer, C.; Deme, B.; Ramasseul, P., *Langmuir* **2003,** 19, 10641-10647.

34. Milic, T.; Garno, J. C.; Smeureanu, G.; Batteas, J. D.; Drain, C. M., *Langmuir* **2004,** 20, 3974-3983.

35. Khalil, G.; Gouterman, M.; Ching, S.; Costin, C.; Coyle, L.; Gouin, S.; Green, E.; Sadilek, M.; Wan, R.; Yearyean, J.; Zelelow, B., *J. Porph. Phthal.* **2002,** 6, 135-145.

36. Zelelow B; Khalil G. E; Phelan G; Carlson B; Gouterman M; Callis J. B; Dalton L. R, *Sensors and Actuators, B: Chemical* **2003,** 96, 304-314.

37. Khalil, G. E.; Chang A. ; Gouterman, M.; Callis, J. B.; Dalton, L. R.; Turro, N. J.; Jockusch, S., *Review of Scientific Instruments* **2005,** 76, 1-8.

38. Chen, X.; Drain, C. M., *Drug Design Review - Online* **2004**, (1), 215-234.

39. Drain, C. M.; Smeureanu, G.; Patel, S.; Gong, X.; Garno, J.; Arijeloye, J., *New J. Chem.* **2006,** 30, (12), 1834-1843.

40. Takahashi, Y.; Kasai, H.; Nakanishi, H.; Suzuki, T. M., *Angew. Chem. Int. Ed* **2006,** 45, 913-916.

41. Nitschke, C.; O'Flaherty, S. M.; Kroll, M.; Blau, W. J., *J. Phys. Chem. B* **2004,** 108, 1287-1295.

42. Nitschke, C.; O'Flaherty, S. M.; Kroll, M.; Doyle, J. J.; Blau, W. J., *Chem. Phys. Lett.* **2004,** 383, 555-560.

43. Denisyuk, I. Y.; Kamanina, N. V., *Optics and Spectroscopy* **2004,** 96, 235-239.

44. Grinstaff, M. W.; Hill, M. G.; Labinger, J. A.; Gray, H. B., *Science* **1994,** 264, 1311-1313.

45. Selke, M.; Sisemore, M. F.; Valentine, J. S., *J. Am. Chem. Soc* **1996,** 118, 2008- 2012.

46. Ikeue, T.; Ohgo, Y.; Saitoh, T.; Yamaguchi, T.; Nakamura, M., *Inorg. Chem.* **2001,** 40, 3423-3434.

47. Mauzerall, D.; Greenbaum, N. L., *Biochim. Biophys. Acta* **1989,** 974, 119-140.

48. Kasha, M.; Rawls, H. R.; El-Bayoum, M. A., *Pure Appl. Chem.* **1965,** 11, 371-381.

49. Sun, S.-S.; Lees, A. J., *Coord. Chem. Rev.* **2002,** 230, 170-191.

50. Udal'tsov A. V. ; Kazarin L. A. ; A., S. A., *J. Mol. Struct* **2001,** 562, 227-239.

51. Okada, S.; Segawa, H., *J. Am. Chem. Soc.* **2003,** 125, 2792-2796.

52. Akins, D. L.; Ozcelik, S.; Zhu, H. R.; Guo, C., *J. Phys. Chem. B* **1996,** 100, 14390-14396.

53. Akins, D. L.; Zhu, H. R.; Guo, C., *J. Phys. Chem. B* **1996,** 100, 5420-5425.

54. Drain, C. M.; Hupp, J. T.; Suslick, K. S.; WasielewskiM. R. ; Chen, X., *J. Porph. Phthal.* **2002,** 6, 241-256.

55. Hasobe, T.; Imahori, H.; Fukuzumi, S.; Kamat, P. V., *J. Mater. Chem.* **2003,** 13, 2515-2520.

56. Konan, N.; Cerny, R.; Favet, J.; Berton, M.; Gurny, R.; Allemann, E., *Eur. J. Pharmaceutics and Biopharmaceutics* **2003,** 55, 115-124.

57. van der Boom, T.; Hayes, R. T.; Zhao, Y.; Bushard, P. J.; Weiss, E. A.; Wasielewski, M. R., *J. Am. Chem. Soc.* **2002,** 124, 9582-9590.

58. Nazeeruddin, K.; Hunphry-Baker, R.; Officer, D. L.; Campbell, W. M.; Burrell, A. K.; Graetzel, M., *Langmuir* **2004,** 20, 6514-6517.

59. Ahrens, J.; Sinks, L. E.; Rybtchinski, B.; Liu, W. H.; Jones, B. A.; Giaimo, J. M.;Gusev, A. V.; Goshe, A. J.; Tiede, D. M.; Wasielewski, M. R., *J. Am. Chem. Soc.* **2004,** 126, 8284-8294.

Chapter 4

1. Stephenson, N. A.; Bell, A. T., *Inorg. Chem.* **2006,** 45, (14), 5591-5599.

2. Groves, J. T.; Nemo, T. E., *J. Am. Chem. Soc.* **1979,** 101, (105), 5786-5791.

3. Groves, J. T.; Nemo, T. E.; Meyers, R. S., *J. Am. Chem. Soc.* **1979,** 101, 1032.

4. Groves, J. T.; Haushalter, R. C.; Makamura, M.; Nemo, T. E.; Evans, B. J., *J. Am. Chem. Soc.* **1981,** 103, 2884-2886.

5. Groves, J.; Viski, P., *J. Org. Chem.* **1990,** 55, 3628.

6. Groves, J. T., *Proc. Natl. Acad. Sci., USA* **2003,** 100 (7), 3569-3574.

7. Groves, J. T., *Journal of Inorganic Biochemistry* **2006,** 100, 434-447.

8. Ortiz de Montellano, P. R., 2nd. ed.; Plenum Press: New York, **1995**.

9. Schenning, A. P. H. J.; Hubert, D. H. W.; Feiters, M. C.; Nolte, R. J. M., *Langmuir* **1996,** 12, (6), 1572-1577.

10. Mayer, J. M., Meunier, B., Ed. Imperial College Press: **2000**; pp 1-43.

11. Newcomb, M.; Hollenberg, P. F.; Coon, M. J., *Archives of Biochemistry and Biophysics* **2003,** 409, (1), 72-79.

12. Chandrasena, R. E. P.; Vatsis, K. P.; Coon, M. J.; Hollenberg, P. F.; *J. Am. Chem. Soc.* **2004,** 126, 115-126.

13. Meunier, B.; de Visser, S. P.; Shaik, S., *Chem. Rev.* **2004,** 104, 3947-3980.

14. Silaghi-Dumitrescu, R., *Journal of Biological Inorganic Chemistry* **2004,** 9, (4), 471-476.

15. Schmidt, J. A. R.; Mahadevan, V.; Getzler, Y. D. Y. L.; Coates, G. W., *Org. Lett.* **2004,** 6, (3), 373-376.

16. Mansuy, D.; Mahy, J. P.; Dureault, A.; Bedi, G.; Battioni, P., *Journal of the Chemical Society-Chemical Communications* **1984**, (17), 1161-1163.

17. Groves, J. T.; Watanabe, Y., *Inorg. Chem.* **1986,** 25, 4808-4810.

18. Barloy, L.; Battioni, P.; Mansuy, D., *Chem. Comm.* **1990**, 1365-1367.

19. Wang, C. Q.; Shalyaev, K. V.; Bonchio, M.; Carofiglio, T.; Groves, J. T., *Inorg. Chem.* **2006,** 45, (12), 4769-4782.

20. Merlau, M. L.; Cho, S. H.; Sun, S. S.; Nguyen, S. T.; Hupp, J. T., *Inorg. Chem.* **2005,** 44, (15), 5523-5529.

21. Suslick, K. S., *In the Porphyrin Handbook*, Kadish, K. M.; Smith, K. M.; Guilard, R., Eds. Academic Press: New York, **2000**; Vol.4, pp 41-63.

22. Simonneaux, G.; Le Maux, P.; Ferrand, Y.; Rault-Berthelot, J., *Coordination Chemistry Reviews* **2006,** 250, (17-18), 2212-2221.

23. Ungashe, S. B.; Groves, J. T., *Adv. Inorg. Biochem.* **1994,** 9, 317-351.

24. Ellis, P. E.; Lyons, J. E., *Catalysis Let.* **1989,** 3, 389-397.

25. Lyons, J. E.; Ellis, P. E., *Catalysis Let.* **1991,** 8, 45-51.

26. Bartoli, J. F.; Brigaud, O.; Battioni, P.; Mansuy, D., *J. Chem. Commun.* **1991**, 440-442.

27. Grinstaff, M. W.; Hill, M. G.; Labinger, J. A.; Gray, H. B., *Science* **1994,** 264, (5163), 1311-1313.

28. Grinstaff, M. W.; Hill, M. G.; Birnbaum, E. R.; Schaefer, W. P.; Labinger, J. A.; Gray, H. B., *Inorg. Chem.* **1995,** 34, 4896-4902.

29. Doro, F. G.; Smith, J. R. L.; Ferreira, A. G.; Assis, M. D., *Journal of Molecular Catalysis a-Chemical* **2000,** 164, (1-2), 97-108.

30. Traylor, T. G.; Kim, C.; Fann, W. P.; Perrin, C. L., *Tetrahedron* **1998,** 54, 7977-7986.

31. Traylor, T. G.; Xu, F., *J. Am. Chem. Soc.* **1990,** 112, 178-186.

32. Moore, K. T.; Horvath, I. T.; Therien, M. J., *Inorg. Chem.* **2000,** 39, (15), 3125-3139.

33. Nam, W.; Han, H. J.; Oh, S.-Y.; Lee, Y. J.; Choi, M.-H.; Han, S.-Y.; Kim, C.; Woo, S. K.; Shin, W., *J. Am. Chem. Soc.* **2000,** 122, 8677-8684.

34. Stephenson, N. A.; Bell, A. T., *J. Am. Chem. Soc.* **2005,** 127, (24), 8635-8643.

35. Stephenson, N. A.; Bell, A. T., *Inorg. Chem.* **2006,** 45, (6), 2758-2766.

36. Battioni, P.; Renaud, J. P.; Bartoli, J. F.; Reinaartiles, M.; Fort, M.; Mansuy, D., *J. Am. Chem. Soc.* **1988,** 110, (25), 8462-8470.

37. Higuchi, T.; Shimada, K.; Maruyama, N.; Hirobe, M., *J. Am. Chem. Soc.* **1993,** 115, (16), 7551-7552.

38. Traylor, T. G.; Popovitz-Biro, R., *J. Am. Chem. Soc.* **1988,** 110, (1), 239-243.

39. Yamaguchi, K.; Watanabe, Y.; Morishima, I., *J. Am. Chem. Soc.* **1993,** 115, (10), 4058-4065.

40. Rosenthal, J.; Pistorio, B. J.; Chng, L. L.; Nocera, D. G., *J. Org. Chem.* **2005,** 70, (5), 1885-1888.

41. Evans, S.; Lindsay, J. R., *J. Chem. Soc., Perkin Trans. 2* **2001**, 174 - 180.

42. Tolman, C. A.; Herron, N., *J. Am. Chem. Soc.* **1987** 109, 2837-2839.

43. Bedioui, F., *Coordination Chemistry Reviews* **1995,** 144, 39-68.

44. Battioni, P.; Lallier, J.-P.; Barloy, L.; Mansuy, D., *Chem. Commun.* **1989**, 1149-1151.

45. Lee, S. J.; Hupp, J. T., *Coordination Chemistry Reviews* **2006,** 250, 1710-1723.

46. Merlau, M. L.; Mejia, M. d. P.; Nguyen, S. T.; Hupp, J. T., *Angew. Chem. Int. Ed.* **2001,** 40, (22), 4239-4242.

47. Drain, C. M.; Chen., X., *In Encyclopedia of Nanoscience & Nanotechnology*, Nalwa, H. S., Ed. American Scientific Press: New York, **2004**; Vol. 9, pp 593-616.

48. Drain, C. M.; Smeureanu, G.; Batteas, J.; Patel, S., *In Dekker Encyclopedia of Nanoscience and Nanotechnology*, Schwartz, J. A.; Contescu, C. I.; Putyera, K., Eds. Marcel Dekker, Inc.: New York, **2004**; Vol. 5, pp 3481-3502.

49. Drain, C. M.; Bazzan, G.; Milic, T.; Vinodu, M.; Goeltz, J. C., *Israel J. Chem.* **2005,** 45, 255-269.

50. Drain, C. M.; Goldberg, I.; Sylvain, I.; Falber, A., *Topics in Current Chemistry* **2005,** 245, 55–88.

51. Gong, X.; Milic, T.; Xu, C.; Batteas, J. D.; Drain, C. M., *J. Am. Chem. Soc.* **2002,** 124, (48), 14290-14291.

52. Drain, C. M.; Smeureanu, G.; Patel, S.; Gong, X.; Garno, J.; Arijeloye, J., *New J. Chem.* **2006,** 30, 1834-1843.

53. Limberg, C., *Angew. Chem. Int. Ed.* **2003,** 42, 5932 - 5954.

54. Patzelt, H.; Woggon, W. D., *Helv. Chim. Acta* **1992,** 75, 523.

55. Lee, A. L.; Nam, W., *J. Am. Chem. Soc.* **1997,** 119, 1916-1922.

56. Mansuy, D., *Coordination Chemistry Reviews* **1993,** 125, (1-2), 129-141.

57. Drain, C. M.; Gentemann, S.; Roberts, J. A.; Nelson, N. Y.; Medforth, C. J.; Jia, S.; Simpson, M. C.; Smith, K. M.; Fajer, J.; Shelnutt, J. A.; Holten, D., *J. Am. Chem. Soc.* **1998,** 120, (15), 3781-3791.

58. Drain, C. M.; Kirmaier, C.; Medforth, C. J.; Nurco, D. J.; Smith, K. M.; Holten, D., *J. Phys. Chem.* **1996,** 100, (29), 11984-11993.

59. Retsek, J. L.; Drain, C. M.; Kirmaier, C.; Nurco, D. J.; Medforth, C. J.; Smith, K. M.; Sazanovich, I. V.; Chirvony, V. S.; Fajer, J.; Holten., D., *J. Am. Chem. Soc.* **2003,** 125, 9787-9800.

60. Garno, J. C.; Xu, C.; Bazzan, G.; Batteas, J. D.; Drain, C. M., Schubert, U. S.; Newcome, G. R.; Manners, I., Eds. American Chemical Society: Washington, DC., **2006**; Vol. 928, pp 168-183.

61. Drain, C. M.; Gong, X., *Chem. Commun.* **1997**, 2117-2118.